UNIVERSITÉ DE STRASBOURG

ÉCOLE DOCTORALE de Physique et Chimie-Physique

Unité de recherche de BioMatériaux et BioIngénierie

Inserm UMR-S 1121

THÈSE présentée par :

Scavello Francesco

soutenue le: **03 Mai 2017**

pour obtenir le grade de: **Docteur de l'université de Strasbourg**

Discipline/Spécialité: Physique et Chimie-Physique/Biochimie

Cateslytine et Chromofungine, deux peptides dérivés de la Chromogranine A qui sont de nouveaux acteurs des systèmes immunitaire et cardiaque

THÈSE dirigée par:

M. Tommaso ANGELONE	Professeur, université de la Calabria
M. Francis SCHNEIDER	Professeur, université de Strasbourg
Mme Marie-Hélène. METZ-BOUTIGUE	Directeur de recherche, université de Strasbourg

RAPPORTEURS:

M. Youssef ANOUAR	Directeur de recherche, université de Rouen
M. Pasquale PAGLIARO	Professeur, université de Turin

AUTRES MEMBRES DU JURY:

Mme Claudia PENNA	Professeur, université de Turin
M. Burkhard BECHINGER	Professeur, université de Strasbourg

University of Calabria-Italy
Inserm U1121University of Strasbourg-France

Thesis
Co-tutorship between University of Calabria, Doctorate in "Life Sciences" and University of Strasbourg, Doctorate in "Physics and Physical Chemistry"

Discipline: Physiology (BIO/09) and Biochemistry (BIO/10)

Title

Cateslytin and Chromofungin, two CgA derived peptides: actors of the immune and cardiac systems

Dr. Francesco Scavello

Coordinator of the Doctorate in Life Sciences
Prof. Marcello Canonaco

Tutor
Prof. Tommaso Angelone

co-Tutor
Dr. Marie-Hélène Metz-Boutigue

Prof. Francis Schneider

This study was supported by "Vinci Project 2014"- Università Italo-Francese (project number C2_72)

INDEX

Abbreviations

5HD: 5-hydroxydecanoate
A. brassicola: Alternaria brassicola
A. fumigates: Aspergillus fumigatus
A: Alanine
aa: Amino acids
AKT: *Protein*-chinasi B
AMP: Antimicrobial peptide
AP: aortic pressure
AR: Adrenergic receptors
ARC: Activity-regulated cytoskeleton-associated *protein*
b: Bovine
BNP: B-type natriuretic peptide
C. tropicalis: Candida tropicalis
C. albicans: Candida albicans
C. neoformans: Candida neoformans
CA: Catecholamine
CaM: Calmodulin
CFU: Colony forming unit
CgA: Chromogranin A
cGMP: Cyclic guanosine monophosphate
Chr: Chromofungin
CNS: Central nervous system
COX-2: Cyclooxygenase-2
CP: Coronary Pressure
CPE: Carboxypeptidase E
Ctl: Cateslytin
Cts: Catestatin
CTSL: Cysteine protease cathepsin L
D*: DOPA-K-DOPA-K-DOPA
D*T*Ctl: DOPA-K-DOPA-K-DOPA-TLRGGE-RSMRLSFRARGYGFR
D: Dextrorotation
DOPA: Levo-3,4-dihydroxyphenylalanine
DPC: Dodecylphophatidylcholine
E. coli: Escherichia coli
E/S: Enzyme/Substrate
E: Glutamic acid
EIA: Enzyme Immunoassay
ELISA: Enzyme-linked immunosorbent assay
eNOS: Endothelial nitric oxide synthase
ERK: Extracellular signal regulated kinase
ET-1: Endothelin-1
F. culmorum: Fusarium culmorum
F. oxysporum: Fusarium oxysporum
G: Glycine
GSK-3β: Glycogen synthase kinase-3β
h: Human

HPLC: High-performance liquid chromatography
HR: Heart Rate
HTR: Half Time Relaxation
I/R: Ischemia/Reperfusion
IL-1β: Interleukin-1β
IL-6: Interleukin-6
iNOS: Inducible nitric oxide synthase
$iPLA_2$: Calcium-independent phospholipase A2
ISO: Isoproterenol
K: Lysine
KH: Krebs-Henseleit solution
L: Leucine
L: Levorotation
LDH: Lactic-dehydrogenase
L-NIO: N(5)-(1-imino-3-butenyl)-l-ornithine
LV: Left ventricle
LVEDP: Left ventricular end-diastolic pressure
LVP: Left Ventricular Pressure
M. luteus: Micrococcus luteus
MALDI-TOF: Matrix Assisted Laser Desorption-Time Of Flight
MH: Mueller-Hinton
MHB: Mueller-Hinton Broth
MIC: Minimal inhibitory concentration
miRNA-21: mircoRNA-21
MitoKATP channel: Mitochondrial adenosine triphosphate-dependent potassium
MRSA: Methicillin-resistant *Staphylococcus aureus*
MSSA: Methicillin sensitive *Staphylococcus aureus*
N. crassa: Neurospora crassa
N. haematococca: Nectria haematococca
$NaIO_4$: Sodium Periodate
NO: nitric oxide
OD: Optical density
ODQ: [1H-[1,2,4]oxadiazolo[4,3- a]quinoxalin-1-one]
P: Proline
PBS: Phosphate-buffered saline
PC: Prohormone convertases
PCR: Polymerase chain reaction
PD: PD98059
PI3K: Phosphoinositide 3-kinase
PKC: Protein-chinasi C
PKG: Protein-chinasi G
PMN: Polymorphonuclear neutrophil
PostC: Postconditioning
PTP: Prohormone thiol protease
PVE: Prosthetic valve endocarditis
PVL: Panton-Valentine leucocidin
R: Arginine
RISK: Reperfusion Injury Salvage Kinases

ROS: Reactive oxygen species
RPP: Rate Pressure Product
S. aureus: *Staphylococcus aureus*
S. cerevisiae: Saccharomyces cerevisiae
S: Serine
SAFE: Survivor Activating Factor Enhancement
SDS: Sodium dodecyl sulfate
SDS-Page: Sodium dodecyl sulfate polyacrylamide gel electrophoresis
sGC: Soluble guanylate cyclase
STA: Serine-Threonine-Alanine
T*: TLRGGE
T*Ctl: TLRGGE-RSMRLSFRARGYGFR
TFA: Trifluoroacetic acid
TFE: Trifuoroethanol
TMB: 3,3′,5,5′-tetramethylbenzidine
TNF-α: Tumor necrosis factor α
Vs-I: Vasostatin I
WT: Wortmannin

Université de Calabre-Italie
Inserm U1121Université de Strasbourg-France

Titre de la thèse

Cateslytine et Chromofungine, deux peptides dérivés de la Chromogranine A qui sont de nouveaux acteurs des systèmes immunitaire et cardiaque

Auteur
Dr. Francesco Scavello

Résumé français

La Chromogranine A (CgA) est une des protéines de la famille des granines. Elle est présente dans un très grand nombre de cellules nerveuses, neuro-endocrines, immunitaires et des cellules de la peau. La chromogranine A est une pro-hormone stockée dans les granules de sécrétion et elle subit une maturation protéolytique conduisant à la formation d'un très grand nombre de peptides dérivés. De plus, la CgA possède de nombreuses modifications post-traductionnelles (phosphorylation, O-glycosylation) qui confèrent une très grande variabilité aux fragments dérivés et aux activités biologiques correspondantes. La CgA est un marqueur plasmatique de désordres physiologiques (cancers, maladies cardio-vasculaires et maladies neurodégénératives).

Plusieurs peptides naturellement générés par clivage protéolytique possèdent des activités biologiques qui participent au retour à l'homéostasie après la réaction au stress. Ces peptides agissent au niveau du système cardio-vasculaire (inhibition de la vasoconstriction, effet inotropique), de la régulation hormonale (inhibition de la libération d'insuline), et possèdent des propriétés anti-microbiennes.

La Vasostatine-I, qui correspond au peptide CgA_{1-76} et qui est généré par le clivage après la paire de résidus basiques en position 77 et 78 du domaine N-terminal de la CgA, puis par l'action de la carboxypeptidase (Metz-Boutigue et al., 1993), agit comme un modulateur de la performance cardiaque chez les mammifères avec un effet anti-adrénergique et agissant avec un inotropisme et un lusitropisme négatifs sur le cœur de rats (Cerra et al., 2006; Cerra et al, 2008; Gallo et al., 2007).

Dans le cas de coeurs de rats perfusés selon la méthode de Langendorff dans les conditions basales, la Vasostatine-I cause une réduction dose-dependante de la pression ventriculaire gauche (LVP) et de (RPP), qui correspond au produit de LVP par la vitesse du cœur HR LVP x (HR) (Cerra et al., 2006). L'implication de la voie de signalisation NO-cGMP-

PKG dans l'effet inotropique négatif de la Vasostatine-I (Cerra et al., 2008; Tota et al., 2014) suggère la possibilité d'une protection contre l'extension d'un infractus du myocarde. En effet, l'administration à faible dose de Vasostatine-I avant l'ischémie-reperfusion (I/R) réduit la taille de l'infractus (Cappello et al., 2007).

En parallèle, la Catestatine ($CgA_{344–364}$) (Cts) induit un inotropisme négatif et un lusitropisme impliquant les récepteurs β_3-adrenergiques (β_3-AR), mais montrant une forte affinité pour β_2-AR (Angelone et al., 2012). Ces effets sont médiés par les mécanismes impliquant la voie β_2-ARs-Gi/oProtein-eNOS-NO-cGMP-PKG (Angelone et al., 2012). Par ailleurs, Cts-induit l'activation de phosphodiesterases de type 2 et l'augmentation de la S-nitrosylation du phospholamban et de la β-arrestin, suggérant un mécanisme supplémentaire pour la modulation du calcium intra-cellulaire et la péponse and β-adrenergique (Angelone et al., 2012). Plusieurs études ont aussi montré que Cts agit comme un puissant inhibiteur de ISO (Angelone et al., 2008, 2012). Dans le cas de coeurs isolés de rats Cts administrée en reperfusion (Cts-Post), diminue la taille de l'infractus, limite la contraction et améliore la fonction systolique post-ischémique (Penna et al., 2010). Cts réduit aussi, mais à un degré moindre, la taille de l'infractus lorsqu'il est administré comme agent de pre-conditionnement. De plus, seul Cts-Post augmente significativement la LVP post-ischémique (Penna et al., 2010). Ainsi, Cts apparaît plus protecteur en tant qu'agent PostC que comme agent de pré-conditionnement. Cts est aussi capable d'induire la cardio protection pendant la phase de reperfusion précoce dans les coeurs isolés, ou si elle est administrée pendant l'ischémie dans des cellules isolées par un mécanisme de pro-survie avec une cascade de signalisation intrinsèque qui implique les voies de Reperfusion Injury Salvage Kinases (RISKs), de Survivor Activating Factor

Enhancement (SAFE), PI3K ou un grand spectre de PKC, PKCε mitoK_{ATP} canaux et l' expression de ROS (Penna et al., 2010, 2014; Perrelli et al., 2013).

Vasostatin-I et Catestatine ont été caractérisés en tant que nouveaux peptides antimicrobiens et agents de défense de l'hôte durant les infections. Ils agissent à des concentrations de l'ordre du micromolaire contre les bactéries, champignons, levures et ne sont pas toxiques vis-à vis des cellules de l'hôte. Ils sont détectés dans les fluides biologiques impliqués dans les mécanismes de défense (sérum, salive) et dans les sécrétions de neutrophiles stimulés (Lugardon et al., 2000; Briolat et al., 2005; Helle et al., 2007). De plus, lorsque les polymorphonucléaires (PMNs) qui sont les premières cellules présentes sur les sites infectieux sont stimulés par des agents bactériens tels que la leucocidine de panton valentine (PVL) ils produisent et sécrètent dans le milieu extra-cellulaire les formes complètes et dégradées de la CgA dont la Vasostatine-I et la Catestatine (Lugardon et al., 2000, Briolat et al., 2005, Zhang et al., 2009).

La vasostatine I bovine possède une activité antimicrobienne contre les bactéries à Gram positif (*Micrococcus luteus et Bacillus megaterium*) avec une CMI dans la gamme 0.1-1 µM, Les champignons filamenteux (*Neurospora crassa, Aspergillus fumigatus, Alternaria brassicola, Nectria haematococca, Fusarium culmorum, Fusarium oxysporum*) avec une CMI de 0.5-3 µM et contre les levures (*Saccharomyces cerevisiae, Candida albicans*) avec une CMI de 2 µM. Cependant, la Vasostatine-I est incapable d'inhiber la croissance d'*Escherichia coli* et *Staphylococcus aureus* (Lugardon et al., 2000).

La catestatine possède des activités antimicrobiennes à des concentrations de l'ordre du micromolaire contre des bactéries à Gram négatif et positif, des champignons et levures. Les 2 variants P370L et G364S possèdent des activités antimicrobiennes contre *M. luteus*

avec une CMI de 2 et 1 µM repectivement et contre *E. coli* avec une CMI de 20 and 10 µM, respectivement (Briolat et al., 2005).

Ainsi, la Chromofungine (Chr: CgA_{47-66}) et la Cateslytine (Ctl: $CgA_{344–358}$) possèdent des propriétés antimicrobiennes (bactéries, champignons et levures). La Chr est un fragment du peptide naturel Vasostatine-I (1-76) et la Ctl correspond au domaine actif de la Catestatine ($CgA_{344–364}$). En plus de leur action directe sur les microorganismes ces peptides activent les neutrophiles et Ctl possède des propriétés anti-inflammatoires.

Staphylococcus aureus est un pathogène très virulent qui provoque un très grand nombre de graves infections cliniques et il représente une des causes principales des infections nosocomiales. Cette bactérie a un fort impact de morbidité et mortalité en milieu communautaire et hospitalier. En effet *S. aureus* est la première cause d'infections en milieu chirurgical et représente le pathogène Gram-positif le plus fréquent dans les cas de sepsis.

Dans le domaine des pathologies cardio-vasculaires, *S. aureus* provoque la destruction du tissu endocardiaque après implantation de valve cardiaque. Ce pathogène est remarquable par sa capacité à résister aux antibiotiques administrés et à répandre des clones résistants ce qui aggrave les cas d'infection liés au *S. aureus*. En 2013, Aslam et al., (Aslam et al., 2013) ont montré que Ctl est actif contre *S. aureus* et résistant à la dégradation par les protéases de *S. aureus*.

La présente thèse s'articule autour de 3 axes:

1- L'analyse dans le système de Langendorff des effets de Chr sur des coeurs de rats dans les conditions basales et pathologiques.

2- L'analyse des propriétés antimicrobiennes d'un peptide synthétique dérivé de Ctl qui sera utilisé pour recouvrir des valves cardiaques pour combattre les infections contre *S. aureus*.
3- L'étude *in vivo* sur des rats infectés par *S. aureus* de l'activité antibactérienne et cardio-protective de Ctl.

La première partie de l'étude a été réalisée en utilisant la technique de Langendorff sur coeurs isolés et perfusés, un test ELISA et la PCR en temps réel. Nous avons montré que'en conditions basales, des doses croissantes de Chr (11–165 nM) induisent un effet inotropique négatif sans changement de la pression coronarienne.

En particulier en exposant des préparations de perfusats cardiaques de rats selon la technique de Langendorff à des concentrations croissantes de Chr (1–165 nM) pendant 10 min, nous avons montré que le peptide induit une diminution de la contractilité et la la relaxation myocardiaque. Pour une concentration de 11 nM, les effets inotropique négatif (LVP et $+(LVdP/dt)_{max}$) et lusitropique ($(LVdP/dt)_{max}$ et augmentant T/−t) sont significatifs et sans influence sur CP et HR.

Dans le cas des mammifères, l'acide nitrique (NO) est fortement impliqué dans chaque battement du cœur et dans la modulation de la fonction cardiaque à moyen et long terme (Casadei and Sears, 2003). Pour évaluer si les effets cardiaques produits par Chr impliquent la production de NO, l'inotropisme négatif et le lusitropisme ont été analysés en présence d'inhibiteurs spécifiques de la signalisation NO. L'exposition au peptide induit une diminution de LVP, $+(LVdP/dt)_{max}$ et $-(LVdP/dt)_{max}$ qui est supprimée par un co-traitement par WT, un inhibiteur spécifique de PI3K ou L-NIO, un inhibiteur sélectif de eNOS, ou ODQ, un inhibiteur spécifique de CG, ou KT5823, un inhibiteur spécifique de PKG. A l'aide d'un test ELISA l'augmentation des niveaux de cGMP a été observée

dans des extraits cardiaques après exposition à la Chr (65 nM). Ainsi nous avons montré que l'activation de la voie de signalisation AKT/eNOS/cGMP/PKG est responsable de cet effet de Chr.

L'hypothèse selon laquelle Chr induise la cardioprotection a été recherchée en comparant les effets induits par la procedure I/R manoeuvres avec ceux produits par le peptide administré après I/R (PostC). Les fonctions systolique et diastolique ont été analysées. Bien qu'en conditions normales Chr ne change pas HR, les coeurs soumis au protocole I/R ont été modulés pour éviter les influences chronotropiques. La fonction systolique est représentée par le niveau de l'activité inotropique (i.e., LVP) (Angelone et al., 2013). Les cœurs soumis au protocole I/R ont présenté une valeur de LVP limitée; avec à la fin de la reperfusion une valeur de LVP de 11±1.7 mm Hg (la ligne de base correspond à 87.75±9.3 mmHg). Chr améliore très sensiblement la LVP pendant la reperfusion avec une valeur de LVP de 51±4 mm Hg (la ligne de base correspond à 87.75±9.3 mm Hg), à la fin de la reperfusion, qui correspond au retour à une performance ~73% par rapport au contrôle. La fonction diastolique est représentée par le niveau de contraction (i.e., LVEDP 4 mmHg ou plus au-dessus de la ligne de base). I/R induit nettement une augmentation de LVEDP (de 7.1±0.7 mmHg à 38±10 mmHg à la fin de la reperfusion). Pendant la reperfusion, Chr empêche le développement des contractions; ainsi, à la fin de la reperfusion LVEDP est à 5±0.5 mmHg. La taille totale de l'infarctus est exprimée comme un pourcentage de LVP. La mesure de la taille des infarctus indique la valeur 65±5% dans le protocole I/R et de 35±3% dans le cœur perfusé avec Chr. Le relargage de LDH dans le groupe I/R group est évalué à 1320±170 U/g (unités per g of d'extrait de coeur) et il est significativement réduit après reperfusion avec Chr (820±140 U/g).

L'effet d'amélioration de la valeur post-ischémique de LVP est supprimé quand les coeurs sont traités simultanément par l'inhibiteur de PI3K (WT), ou de CG (ODQ), ERK1/2 (PD), ou les canaux mitoKATP (5HD).

Par ailleurs, la cardioprotection induit aussi une augmentation du niveau intracardiaque de cGMP. Pour vérifier le rôle de miRNA-21 dans la protection induite par Chr, nous avons mesuré le niveau dans les cas de rats en situation I/R et PostC-Chr. Les résultats montrent qu'en situation de PostC-Chr, les niveaux de miRNA-21 sont statistiquement augmentés dans les groups I/R et Sham group, tandis que les niveaux d'I/R n'étaient pas significativement différents comparés à ceux du groupe Sham.

En conclusion, nous avons aussi montré que Chr agit comme un agent de post-conditionnement contre les effets négatifs de l'ischémie/reperfusion en réduisant la taille de l'infarctus et le niveau de LDH. Les responsables de cette cardio-protection impliquent les cascades de signalisation PI3K, RISK, MitoKATP et miRNA-21.

L'ensemble de ces résultats suggère que Chr affecte directement la performance du travail du coeur, protège contre les blessures du myocarde par ischémie/reperfusion, par l'activation de kinases (Filice et al., 2015).

En conclusion, Chr peut être proposé comme un nouveau modulateur physiologique neuroendocrine capable de prévenir des dysfonctionnements cardiaques. Son potentiel clinique méritera d'être approfondi par de nouvelles recherches.

Dans la seconde partie de la thèse, 2 nouveaux peptides synthétiques contenant Ctl (RSMRLSFRARGYGFR) ont été designés:

D*T*Ctl (DOPA-K-DOPA-K-DOPA-TLRGGE-RSMRLSFRARGYGFR),

T*Ctl (TLRGGE-RSMRLSFRARGYGFR) with D*: DOPA-K-DOPA-K-DOPA and T*: TLRGGE.

Cette étude comprend une première partie d'expériences réalisées en solution. Elle est basée sur les propriétés adhésives de la séquence DOPA-K-DOPA-K-DOPA et sur l'aptitude de l'endoprotéase Glu-C pour cliver après la séquence TLRGGE.

La stratégie expérimentale utilisée pour analyser la dynamique de l'interaction entre D*T*Ctl et *S. aureus* est composée de: (1) la caractérisation de l'activité antimicrobienne de D*T*Ctl contre des souches MSSA et MRSA, (2) l'étude analytique de la protéolyse de D*T*Ctl par la protéase Glu-C de *S. aureus* V8 et (3) le rôle des conditions oxydatives pour les propriétés antibactériennes de D*T*bCtl contre *S. aureus*.

En utilisant des techniques de biochimie, protéomique (séquençage, spectrométrie de masse) et microbiologie, nous avons montré que la dégradation par la protése Glu-C de T*Ctl et D*T*Ctl génère la Ctl active.

Afin de définir les conditions expérimentales pour la digection enzymatique nous avons traité 12.5 µg de T*Ctl (L) avec 3.5 µg de la protéase Glu-C dans 50 mM de Tris-HCl à pH 8.2 pendant 8 h à 37°C. Après digestion, les peptides resultant ont été purifies en utilisant l'HPLC de phase inverse. Trois pics élués 18.0 min, 19.9 min et 21.9 min ont été purifiés et analysés par analyse MALDI-TOF. Ils ont été identifiés comme correspondant à la séquence ARGYGFR (826.457 Da) pour le pic 1, TLRGG (501.067 Da) pour le pic 2 et SMRLSFR (1052.655 Da) pour le pic 3. Le fragment TLRGG résulte de la perte du résidu E C-terminal pendant l'analyse par MALDI-TOF. L'identification du fragment RSMRLSFR démontre le clivage entre E et R. A partir de ces résultats nous pouvons conclure que l'enzyme agit au site attendu (E-R), mais qu'un clivage supplémentaire (R-

A) est caractérisé au milieu de la séquence Ctl (L), empêchant la libération de la séquence complète de Ctl (L).

Pour prévenir ce clivage secondaire on a étudié le clivage par la protéase Glu-C de l'isoforme le plus T*Ctl (D). Après séparation par HPLC, 2 pics élués à 24.4 and 24.6 min, respectivement ont été identifiés. L'analyse par MALDI-TOF indique que le pic 1 correspond à bCtl (D) (1860.08 Da), et le pic 2 à un mélange avec T*Ctl (2473.48 Da). La mesure de l'absorbance à 214 nm indique la libération de l'isoforme Ctl (D) (50-60%) du peptide complet T*Ctl (D).

La digestion par la protéase Glu-C de D*T*Ctl est réalisée pendant 4 h, 6 h, et 18 h. Les peptides résultant ont été purifiés en utilisant un système chromatographique par HPLC et on a obtenu le même profil chromatographique pour les 3 temps d'incubation avec la protéase : 9 pics élués respectivement 18.2 min, 18.8 min, 20.0 min, 21.0 min, 21.5 min, 22.0 min, 23.2 min, 24.3 min, and 25.2 min, ont été identifiés par MALDI-TOF.

Le pic 1 (826.42 Da) correspond à D* (812 Da) avec l'addition de 1'oxydation. Le pic 2 (1425.76 Da) correspond à D*T*. Le pic 3 a été caractérisé comme un mélange complexe de D*T* (1426.03 Da et 1449.99 Da avec l'addition d'un ion sodium et plusieurs formes oxydées de D* (861.31 Da, 877.24 Da, 893.25 Da, 909.21 Da). Le pic 4 correspond à D*TL avec addition d'une oxydation et un ion sodium (1068.60 Da). Le pic 5 minoritaire n'a pas été identifié et le pic 6 correspond à un mélange de D*TL avec l'addition d'un ion sodium (1052.63 Da) et D*TL avec l'addition d'une oxydation et d'un ion sodium (1068.52 Da). Le pic 7 correspond à Ctl avec addition d'une oxydation (1875.97 Da) et le pic 8 correspond à Ctl avec addition d'un ion sodium (1881.36 Da). La séquence complète D*T*Ctl avec une oxydation (3282.83 Da) est éluée dans le pic 9. En tenant compte des $A_{214\ nm}$ respectives nous avons évalué une libération de 90% de Ctl à partir de D*T*Ctl. Ce résultat suggère que D*T*Ctl est plus accessible à l'enzyme Glu-C que T*Ctl.

Puis l'analyse prédictive de la structure secondaire suggère la présence d'un domaine en hélice α pour D*T*Ctl. Le groupement D* semble stabiliser la structure secondaire et faciliter le clivage par la protése Glu-C pour libérer le peptide Ctl actif. Ainsi, l'addition du groupe Dopa améliore la stabilité de Ctl et permet une meilleure accessibilité du site de clivage attendu. Nous avons analysé les prédictions de structures secondaires (logiciel GOR) et établi que D*T*Ctl possède une hélice α centrale (10 aa: RSMRLSFRAR, i.e. 38.46% de la sequence complete par GOR) et 9 aa: RSMRLSFRA, i.e. 34.62% de la séquence complète par PHD) tandis que T*Ctl possède une α hélice (8 aa: MRLSFRA, i.e. 38.10% de la séquence complète par GOR). Pour la forme D du peptide T*Ctl il semble possible que la structure secondaire soit la même que pour la forme L, mais la forme D résiste à la dégradation protéolytique.

Le groupement D* stabiliserait la structure secondaire du peptide D*T*Ctl et faciliterait le clivage exclusif qui produit le peptide Ctl actif.

Par la suite nous avons testé l'activité antibactérienne de D*T*Ctl contre la souche de *S. aureus* capable de produire la protéase Glu-C. Après action de l'enzyme pendant 6 h et 18 h, les produits de la digestion de D*T*bCtl (75 μM) (MIC) après 18 h ont tué *S. aureus* V8 à 99±5%, et à 96±2% après 6h. En conclusion, après digestion de D*T*Ctl, les produits de digestion sont capables de lyser *S. aureus* V8.

De plus, on a examiné si D*T*Ctl était capable d'un effet direct sur *S. aureus* (MSSA et MRSA). Ctl est un AMP cationique avec une charge globale (+5) et la séquence D*T*Ctl possède 2 charges positives additionnelles correspondant aux 2 résidus K de la partie D*. Ainsi, la présence du résidu E dans la séquence T*, et la charge globale de +6 peuvent faciliter l'interaction du peptide avec les charges négatives des phospholipides à la membrane bactérienne. On a testé les activités antimicrobiennes du peptide D*T*Ctl (5

µM to 100 µM) contre différentes souches de *S. aureus* incluant des souches sensibles (MSSA) et résistantes (MRSA). Après incubation avec 50 µM de D*T*Ctl, nous avons obtenu un fort effet antibactérien pour les souches MSSA (25923 et 49775) avec 88±1% and 94±2% tandis que pour les souches MRSA nous avons obtenu seulement 32±5% et 15±3% d'inhibition. Cependant à une concentration D*T*Ctl de 70 µM on a observé une inhibition 96±1% et 100±1% pour MSSA et de 90±5% pour MRSA et 100±1% pour la souche produisant V8.

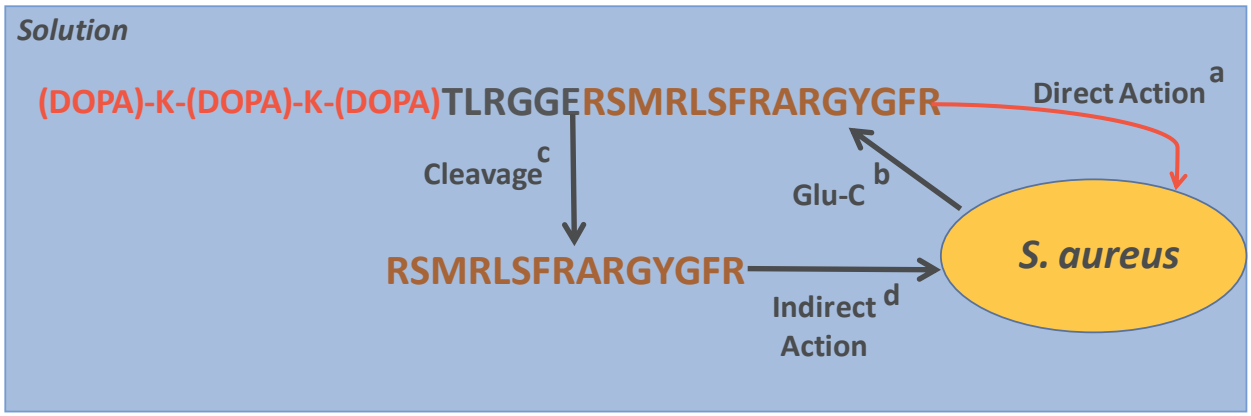

*Mécanisme d'action de D*T*Ctl contre S. aureus*

Afin de recouvrir le biomatériau par le peptide D*T*Ctl il est nécessaire de procéder à une étape d'oxydation (Ponzio et al., 2014). Ce processus d'oxydation va activer le groupement DOPA pour permettre sa liaison au matériau. Pour pouvoir intégrer le peptide dans un revêtement de matériau il est nécessaire de procéder à une oxydation par $NaIO_4$. Après cette étape on a recherché la production du peptide actif Ctl et analysé l'activité antibactérienne.

L'étude protéomique a clairement montré par spectrométrie de masse la formation de polymères qui gênent le clivage par la protéase Glu-C et la formation de Ctl. En préambule nous avons montré une activité antibactérienne contre *S. aureus* pour le peptide D*T*Ctl

avec une CMI de 75 µM. Cependant après oxydation on observe la formation d'aggrégats qui gênent le clivage nécessaire à la formation de Ctl.

La réaction d'oxydation de D*T*bCtl (3.3 mg) a été réalisée en utilisant du périodate de sodium ($NaIO_4$; 1.1mg). Après une rapide incubation pendant 1 min dans 50 mM Tris-HCl, on a procédé à l'analyse par HPLC et MALDI TOF. Dans le cas du matériel non oxydé on observe l'élution d'un seul pic à 44 min. Par contre dans le cas du matériel oxydé 3 pics sont identifiés) correspondant à une forme monomérique avec 1 oxydation et 1 ion sodium (3308.91 Da) et une forme dimérique de D*T*Ctl (L) (avec addition de 2 oxydations; 6567.91 Da). Le pic 2 correspond au mélange de D*T*Ctl (L) (avec addition d'1 oxydation; 3282.63 Da), une forme dimérique de D*T*Ctl (L) (avec addition d'1 ion sodium; 6559.52 Da), une forme trimérique de D*T*Ctl (L) (avec addition d'1 ion sodium; 9871.27 Da) et une forme tétramérique de D*T*Ctl (L) (avec addition d'1 oxydation; 13136.29). Le Pic 3 correspond au mélange de D*T*Ctl (L) (avec addition d'1 oxydation; 3281.10 Da), une forme dimérique de D*T*Ctl (L) (avec addition de 2 oxydations et 1 ion sodium; 6588.43 Da), et une forme trimérique de D*T*Ctl (L) (avec addition de 3 oxydations; 9844.57 Da).

Ensuite, nous avons incubé la forme oxydée de D*T*Ctl avec l'endoprotéase Glu-C et analysé les fragments générés par HPLC. Aucun fragment n'a été détecté, ce qui suggère que l'aggrégation du matériel résultant du processus d'oxydation gêne la réaction enzymatique. Nous avons aussi testé l'action antibactérienne de D*T*Ctl (L) contre *S.aureus* 25923 (ATCC) (MSSA), *S. aureus* 49775 (ATCC) (MSSA), *S. aureus* S1 (MRSA) et *S. aureus* V8. En contrôle on a vérifié que l'agent oxydant ne possède pas des propriétés antimicrobiennes. Les formes aggrégées de D*T*Ctl (L) oxydée sont incapables d'avoir une action antibactérienne totale à une concentration inférieure à

200µM. Ainsi, à une concentration de 70 µM pour les souches 25923 (MSSA), 49775 (MSSA) et V8 on obtient pour le matériel oxydé des activités inhibitrices de 38±4%, 5±2% and 6±2%, et pas d'inhibition pour la souche S1 (MRSA). Au contraire à 70 µM D*T*Ctl (L) non oxydé inhibe les différentes souches testées.

La forme oxydée de D*T*Ctl est aussi analysée par nano HPLC en présence de milieu Muller-Hinton Broth (MHB) et du surnageant de *S. aureus* 25923. Lorsque la forme oxydée de D*T*Ctl est mise en présence du surnageant on observe que le pic de D*T*Ctl disparaît. Cependant, si on rajoute un agent réducteur tel que le β-mercaptoethanol, de faibles quantités des formes normales de D*T*Ctl sont retrouvées et les formes aggrégées majoritaires sont éluées à 4 min. Un résultat similaire est obtenu après incubation de la forme oxydée de D*T*Ctl dans le milieu MHB. L'ensemble de ce travail fait l'objet d'un manuscrit en cours de rédaction.

Dans la troisième partie de cette thèse nous avons évalué l'activité antibactérienne *in vivo* de Ctl ainsi que la protection cardiaque qui serait apportée par Ctl sur un modèle de rats infectés par *S. aureus*. Au niveau systémique et cardiaque nous avons cherché à identifier les cibles moléculaires de l'inflammation qui seraient visées par l'administration de Ctl. Ces expériences ont été réalisées par l'utilisation des techniques de Western blot, ELISA et analyses microbiologiques au niveau du coeur et du plasma.

Dans cette étude on a examiné l'activité antibactérienne de la Ctl bovine contre *S. aureus* dans un modèle de rat infecté (Knuefermann et al., 2004). Dans les études *in vitro* Ctl se montre plus actif contre les différentes souches de *S. aureus* que les autres peptides dérivés de la CgA. Il agit avec une CMI de 37–45 µg/mL (21 µM) (Aslam et al., 2013). Les effets de *S. aureus* ont été comparés avec ceux du tampon de transport dans le cas de rats traités par voie intra-péritonéale par *S. aureus* seul (contrôle négatif), *S. aureus* plus Ctl (1.5 mg/kg) et Ctl seul (1.5 mg/kg) (Rabbi et al., 2014). Le contrôle positif correspond à des

rats traités avec *S. aureus* plus Penicilline-Streptomycine (35,000 units/Kg de Pénicilline aqueuse plus 18 mg/Kg de Streptomycine) (Sigma-Aldrich Produktions GmbH, Steinheim, Germany) (Steigbigel et al., 1975). Pour chaque animal 0,5 mL de plasma a été deposé dans une boîte de Petri en présence d'agar dans MHB et la croissance des bactéries a été observée après 24h d'incubation à 37°C. En parallèle, 50 µL de plasma de rats (infectés ou non) est incubé avec 50 µL de milieu MHB et incubé pendant 24 h à 37°C dans une plaque à 96 puits (Sarstedt AG and Co., Nümbrecht, Germany). De plus, les cœurs de chaque groupe de rats sont analysés pour l'évaluation des fonctions cardiaques. Nous observons dans le plasma une forte diminution de la croissance bactérienne. A une concentration de 1.5 mg/Kg Ctl est capable de combattre *S. aureus* en induisant *in vivo* un effet antibactérien dans les extraits cardiaques et les plasmas. Une analyse quantitative de l'activité antibactérienne est obtenue par addition de milieu MHB frais avant incubation de plasma ou extraits de coeur 24 h at 37 °C. L'analyse spectrophotométrique à 620 nm indique un pourcentage de croissance bactérienne évalué à 95±1% dans le plasma de rats traités en présence de *S. aureus*. Au contraire, dans le groupe ayant reçu l'administration conjointe de *S. aureus*+Ctl nous observons une croissance bactérienne de 9±1%, tandis que dans le groupe traité exclusivement par Ctl nous n'observons pas de croissance bactérienne. De façon similaire on observe une croissance bactérienne de 87±8% dans les coeurs de rats traités par *S. aureus*, de 9±7% dans les cœurs de rats traités par *S. aureus*+Ctl et une croissance de 10±8% pour les rats traités uniquement par Ctl.

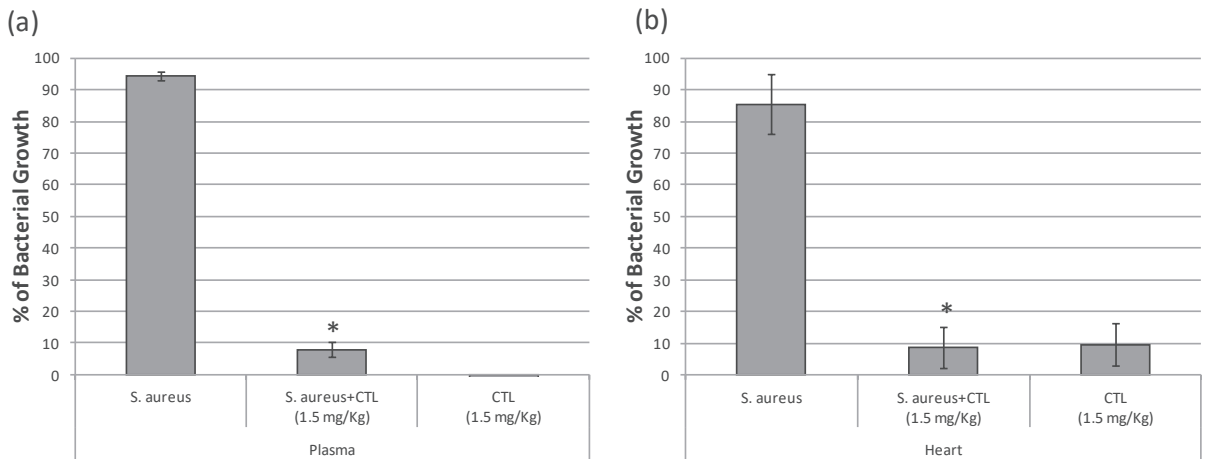

Croissance bactérienne de S. aureus mesurée au niveau (a) plasmatique et (b) cardiaque sur des rats infectés par S. aureus et traités par Ctl.

En tenant compte de l'action anti-inflammatoire et de la modulation de l'inflammation intestinale par Ctl dans les cas de colite (Rabbi et al., 2014) on a cherché à évaluer dans chaque groupe l'état de l'inflammation systémique en controlant dans le plasma les concentrations TNF-α et IL-1β, deux cytokines pro-inflammatoires majoritaires (Knuefermann et al., 2004). La LDH plasmatique a aussi été évaluée en tant qu'index de détérioration (Cofiell et al., 2015). Dans le groupe contrôle (Solution Saline), LDH plasmatique est évaluée à 121±69 UI/L. Le traitement par *S. aureus* induit une augmentation significative de LDH de 1041±66 UI/L, tandis que le co-traitement *S. aureus* plus Ctl montre une réduction significative avec une valeur de (555±200 UI/L). Dans le groupe traité par Ctl seul, la quantité de LDH est évaluée à 425±132 UI/L. En ce qui concerne TNF-α, dans le groupe contrôle (solution saline), la concentration plasmatique est de 7.8±3.2 pg/mL. Le traitement avec *S. aureus* induit une augmentation significative avec une valeur de (55.6±17.9 pg/mL), tandis que le traitement simultané par *S. aureus* plus Ctl montre une réduction signficative avec une valeur de 10.4±3.4 pg/mL. Dans le groupe traité par Ctl seule, la concentration de TNF-α plasmatique est de 9.8±7.1

pg/mL. La même tendance est observée pour IL-1β dans le groupe contrôle (Solution Saline), avec une concentration plasmatique de 11.8±3.4 pg/mL et le traitement par *S. aureus* induit une augmentation significative IL-1β avec une valeur mesurée de 121.5±32.3 pg/mL, tandis que le co-traitement par *S. aureus* plus Ctl montre une réduction significative de IL-1β (32.4±19.5 pg/mL). Dans le groupe traité avec Ctl seul, la concentration d'IL-1β plasmatique est de 20.4±10.5 pg/mL.

En conclusion, ces résultats démontrent que chez le rat une administration de Ctl (1.5 mg/Kg) pendant l'infection par *S. aureus* réduit l'infection systémique, la production de cytokines pro-inflammatoires (TNF-α, IL-1β) ainsi que la production de LDH.

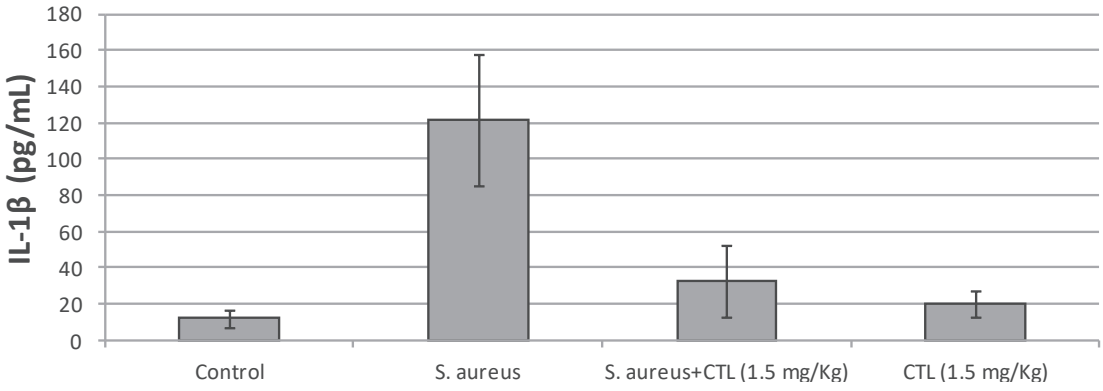

Concentration de IL-1β dans le plasma de rats infectés par S. aureus

Pendant une maladie cardiaque les médiateurs majeurs de l'inflammation sont iNOS et COX-2 (Aoki and Narumiya, 2012). Pour vérifier l'implication de ces médiateurs inflammatoires dans les pathologies cardiaques induites par *S. aureus*, on a réalisé des Western blot pour évaluer la présence de iNOS et COX-2 dans les extraits cardiaques des différents groupes de rats (Contrôle, *S. aureus* seul, *S. aureus* plus Ctl et Ctl seul). Les expériences de Western blot réalisées sur les extraits cardiaques montrent que le

traitement par Ctl induit une diminution des marqueurs pro-inflammatoires tels qu'iNOS et COX-2.

Ces premiers résultats réalisés *in vivo* montrent que le traitement par Ctl de rats infectés par *S. aureus* combat l'infection et assure une protection du myocarde.

Dans le but de réaliser des études cliniques, nous rechercherons le plus peptit peptide dérivé de Ctl assurant l'ensemble des propriétés recherchées.

Dans cette thèse nous avons démontré que Chr (CgA_{47-66}) agit directement sur la performance sur le coeur isolé de rat et le coeur perfusé selon le procedé Langendorff par des effets dose-dépendant, inotropique négatif et lusitropique impliquant la cascade de signalisation AKT/NOS/cGMP/PKG. Chr protège aussi contre l'agression resultant du procédé I/R, en agissant comme un agent de post-conditionnement par l'activation de RISK et des canaux mito KATP. Sur le cœur de rat isolé et soumis au modèle de Langendorff, nous observons que Chr induit un effet inotropique négatif et lusitropique à partir d'une concentration de 11 nM. En l'absence de stimulation Chr réduit significativement LVP, et $+(LVdP/dt)_{max}$ (index d'inotropisme) et $(LVdP/dt)_{max}$ et T/−t (index de lusitropisme), sans affecter HR and CP. Ces effets ont été obtenus à des concentrations de Chr proches de la concentration physiologique de la CgA qui en est le précurseur (Helle et al., 2007). Les effets négatifs d'inotropisme et lusitropisme induits par l'administration de Chr (~40%) sont à rapprocher de la cardiodépression induite sur le cœur de rat par la vasostatine recombinante (hrVs-I) (~20%) qui inclut la séquence Chr (Cerra et al., 2006). Par ailleurs il a été rapporté que le fragment CgA_{1-64} (séquence de rat) provoque une vasodilatation coronarienne (Cerra et al., 2008). Cet effet est contraire à l'augmentation de l'activité coronarienne induite par hrVs-I sur le cœur de rat (Cerra et

al., 2006). Dans le présent travail nous avons trouvé que Chr ne change pas la réactivité coronarienne du rat bien que Vs-I et Chr induisent des effets similaires sur la contractilité et la relaxation du myocarde. Les séquences qui sont différentes peuvent jouer un rôle dans les différences observées au niveau des réponses coronariennes. En fait les effets induits par Chr impliquent la voie de signalisation AKT/NOS-NO/cGMP.

Les résultats obtenus ont permis d'étendre à la Chr les propriétés de cardio-protection des autres fragments de la CgA tels que Vs-I et Cts (Cappello et al., 2007). Ceci peut inciter à analyser le potentiel de ce peptide comme comme agent pharmacologique PostC. Suivant des mécanismes de pre- et post conditionement de nombreuses substances protègent le coeur en activant des voies de signalisation PI3K/Akt, PKC et ERK1/2, qui peuvent cibler GSK-3β, un substrat de nombreuses kinases de survie telles que RISK chez les rongeurs (Hausenloy et al., 2004; Penna at al., 2008) et implique l'ouverture de canaux de KATP (Penna et al. 2007, 2008). Dans notre cas nous observons que cette cascade est activée dans les coeurs exposés à Chr au cours de la reperfusion précoce. En fait, l'inhibition des kinases PI3K and ERK1/2 s'oppose à la performance systolique induite par Chr.

Ainsi, la cardioprotection induite par Chr s'accompagne d'une augmentation de l'expression de miRNA-21 (Zhang, 2008). Les miRNAs sont impliqués dans la physiopathologie cardiaque et leur expression dérégulée est liée au développement de pathologies cardio-vasculaires (Da Costa Martins et al., 2012). En particulier, il a été démontré que la surexpression de miRNA-21 réduit la taille de l'infractus et que cela est associé avec l'inhibition de gènes pro-apoptotiques et l'augmentation de gènes anti-apoptotiques (Dong et al., 2009; Cheng et al., 2009).

Pour la prevention de l'infection sur les biomatériaux tells que les valves cardiaques artificielles, nous avons utilisé un peptide synthétique couple à un groupement Levo-3,4-dihydroxyphenylalanine (DOPA) pour couvrir de manière non-spécifique toutes les sortes de biomatériaux (Lynge et al., 2011; Ponzio et al., 2014). La méthode de utilisée pour le dépôt de polydopamine est basée sur l'utilisation d'oxydants is based on the use of oxidants, (Bernsmann et al., 2011), sodium periodate and peroxodisulfate (Wei et al., 2010). Lorsque la dopamine est oxydée par l'oxygène de l'air et commence à polymériser des molécules amphiphiles vont s'organiser pour migrer à l'interface air/eau pour former un film (Ponzio et al., 2014).

Les limites de cette méthodes concernent la formation d'aggrégats qui réduisent forttement l'activité antibactérienne. Ainsi, des études complémentaires sont nécessaires pour developer différentes strategies qui permettent de diminuer la formation d'aggrégats en maintenant l'activité antibactérienne dans les biomatériaux. Jusqu'à présent, le problème de l'aggrégation de D*T*Ctl après oxidation n'est pas résolu et il est crucial de trouver une nouvelle méthode pour réduire ou bloquer la formation d'aggrégats de D*T*Ctl (L) aggregates à la surface.

Dans notre travail nous avons montré que *in vitro,* le peptide synthétique D*T*Ctl (L) possède une activité antibactérienne contre différentes souches de *S. aureus*. En presence de Glu-C, une endoprotease spécifique de *S. aureus,* le peptide D*T*Ctl (L) peut être clivé pour libérer bCtl.

D*T*Ctl (L) est moins actif que Ctl (L). Pour Ctl la valeur de la CMI est autour de 20 µM (Aslam et al., 2013), tandis que D*T*Ctl en solution la CMI est de l'ordre de 75 µM contre différentes souches de *S. aureus.* Ce résultat n'est pas cohérent avec l'addition de 2 charges supplémentaires sur le groupement DOPA.

En fait au cours de cette étude il a été montré que dans les conditions oxydantes le peptide perd son activité antibactérienne par la formation d'aggrégats. L'addition du groupement DOPA à la séquence Ctl (L) conduit à une plus grande stabilité du peptide au cours de la digestion par la protéase Glu-C. En effet la digestion par Glu-C de Ctl (L) génère le clivage sur 2 sites qui produit des fragments sans activité antimicrobienne. La présence du groupement DOPA dans D*T*Ctl (L) induit une modification de la structure secondaire avec la formation d'une hélice alpha plus longue dans la partie médiane de Ctl (L). Cette modification améliore la stabilité du peptide permettant le clivage au site de clivage spécifique de la protease.

En conclusion, nous avons montré que le peptide synthétique (D*T*Ctl) peut induire la lyse des bactéries sur les biomatériaux au cours de la première phase de l'infection par S. aureusfor the biomaterials et la libération de l'endoprotéase Glu-C. L'enyme est alors capable de libérer la forme active Ctl (L). Le clivage se produit après 4h d'incubation et à 18h le rendement de clivage de D*T*Ctl (L) est dans la gamme 85-95%.

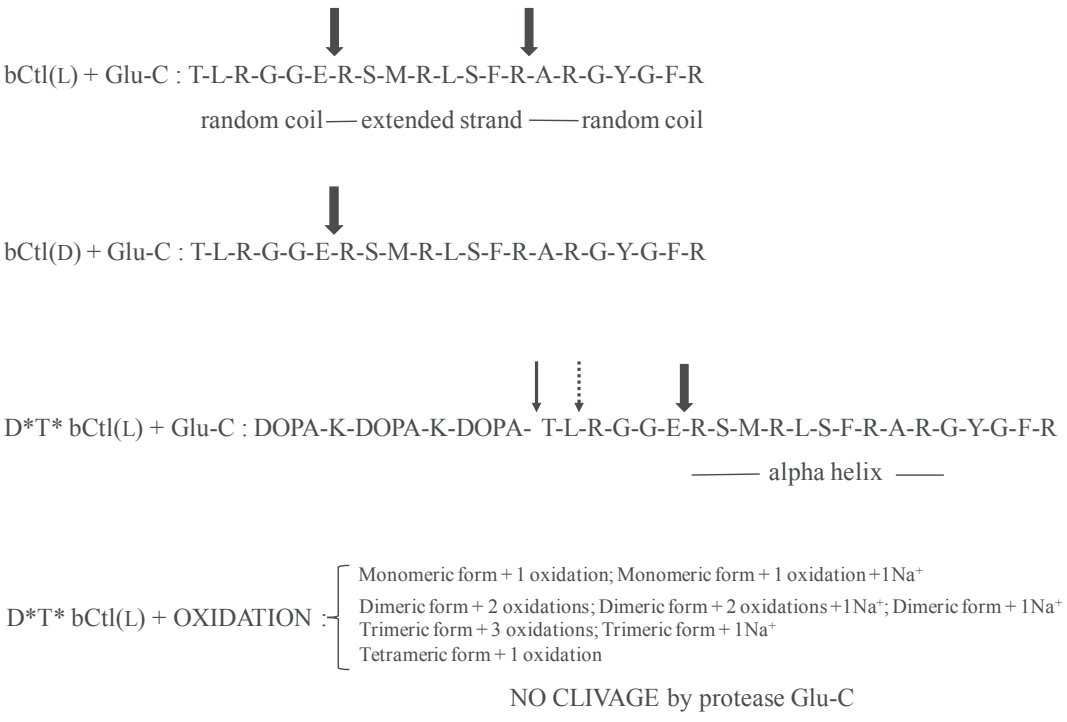

Représentation schématique des résultats obtenus par digestion du peptide dérivée de Ctl par la protéase Glu-C de S. aureus V8.

Les infections nosocomiales sont souvent causées by la colonisation d'un biofilmdur les implants médicaux. De nombreuses stratégies pour éviter les infections liées à la formation de biofilm ont été proposées pour éviter la formation du biofilm (Ribeiro et al., 2016). Différentes stratégies peuvent être appliquées. Par exemple, il s'agit d'agents qui bloquent l'adhesion cellulaire aux implants médicaux ou qui inhibent la production de la matrice extra-cellulaire. Dans ce même contexte les molecules qui peuvent induire la déstabilisation et la rupture des biofilms sont recherchés. Les PAMs cationiques en plus de leurs actions antimicrobiennes directes sont capables de posséder plusieurs de ces effets (Melvin et al., 2016).

Sur la base de nos résultats, le D*T*Ctl est un PAM cationique capable d'empêcher la formation du biofilm et de produire sa déstabilisation. Quand *S. aureus* interagit avec le matériau recouvert par D*T*Ctl, ce peptide est capable de tuer la bactérie dans un premier temps par un mécanisme de lyse. De plus, comme un résultat de cette première étape, on observe une augmentation de la production de l'endoprotéase Glu-C (Ribeiro et al., 2016) et par la suite le clivage de D*T*bCtl par l'endoprotéase Glu-C pour générer la forme active de Ctl. L'ensemble des 2 étapes fournit au peptide D*T*Ctl, une activité antibactérienne exponentielle contre *S. aureus*.

S. aureus est aussi capable de resister aux antibiotiques et de developer plusieurs mécanismes de résistance, limitant ainsi les strategies thérapeutiques contre infections à *S. aureus* (Frieri et al., 2016). La diffusion de souches résistantes de *S. aureus* (MRSA) est devenue une des causes les plus importantes d'infections nosocomilaes (Frieri et al., 2016; Klein et al., 2007; Moran et al., 2006). Ce constat ainsi que la résistance aux

antibiotiques conventionnels ont fait de la Vancomycine le prmeir choix pour le traitement des infections à *S. aureus* (Holubar et al., 2016). Dans ce contexte l'intérêt pour les PAMs naturels est en nette augmentation (Riberio et al., 2016).

Dans le dernier chapitre de ma thèse par une étude *in vivo* nous avons montré que Ctl est capable de combattre les infections à *S. aureus* chez le rat. Le traitement par Ctl (1.5 mg/Kg) pendant une infection à *S. aureus* montre une inhibition totale de la croissance bactérienne au nivau plamsmatique et cardiaque. Pourla première fois le traitement in vivo par Ctl montre les mêmes effets antibactériens contre *S. aureus* que les antibiotiques conventionnels. Dans le domaine de l'inflammation, l'augmentation de l'expression de TNF-α et de IL-1 β est spécifique du sepsis expérimental et représente l'index principal de l'infection induite par des pathogènes (Knuefermann et al., 2004; Haziotet al., 1999, Haziot et al., 1999, Rabbi et al. 2014). Des résultats établissent une faible concentration de TNF-α and IL-1β dans le surnageant de macrophages isolés de la cavité péritonéale de souris orésentant une colite et traitées *in vivo* avec trois différents fragments de hCts ($hCgA_{352–372}$: SSMKLSFRARAYGFRGPGPQL; hCtl ($hCgA_{352–366}$: SSMKLSFRARAYGFR, et $hCgA_{360–372}$: ARAYGFRGPGPQL) (Rabbi et al., 2014). Avec nos résultats nous montrons que le traitement par bCtl (1.5 mg/Kg) de rats infectés par *S. aureus* réduit l'infection systémique avec une diminution des cytokines pro-inflammatoires TNF-α et IL-1β. Nous avons également montré une diminution de la concentration plasmatique de LDH (Cofiell et al., 2015) après traitement par bCtl.

Pendant l'infection, l'expression de cytokines dans le tissue cardiaque induit l'activation des voies de signalisation de l'inflammation mais aussi le recrutement des cellules de l'inflammation (Kumar et al., 1996; Cain et al., 1999; Aoki and Narumiya, 2012). Dans ces conditions,Under this condition, les médiateurs principaux de l'inflammation sont iNOS et COX-2 (Aoki and Narumiya, 2012). Les rôles des prostaglandins ont été verifiés

dans les pathologies cardio-vasculaires humaines, suggérant que la signalisation des prostaglandines peut être une cible thérapeutique prometteuse pour les maladies inflammatoires chroniques. Nous avons observé que dans le groupe de rats traités par *S. aureus* l'expression au niveau cardiaque de iNOS and COX-2 augmente, tandis que dans le groupe de rats traités aussi par Ctl nous observons une diminution de leur production. En conclusion, ces résultats montrent que le traitement par Ctl (1.5 mg/Kg) de rats infectés par *S. aureus* peut supprimer l'inflammation systémique et cardaique.

En conclusion, en utilisant 2 peptides de la CgA Chr et Ctl le travail de thèse présenté montre que:

1- Chr assure une protection cardiaque dans un modèle de coeur isolé utilisant l'ischémie/reperfusion
2- Dans le but d'élaborer un nouveau revêtement de valves cardiaques le peptide D*T*Ctl se révèle intéressant dans des conditions non oxydantes car (1) il présente une activité antimicrobienne contre *S. aureus*; (2) en présence de *S. aureus* il permet par clivage protéolytique de libérer le peptide Ctl actif. Afin de finaliser cette étude des expériences sont actuellement en cours à l'Inserm U1121 pour réussir le recouvrement de matériau sans l'étape d'oxydation.
3- Une première expérience réalisée *in vivo* a montré le rôle de Ctl pour combattre l'infection à *S. aureus* au niveau systémique et au niveau cardiaque, mais aussi assurer la protection du myocarde.

Summary

Chromogranin A (CgA) belongs to the granin family of uniquely acidic secretory that are ubiquitous in secretory cells of the nervous, endocrine, immune system. Numerous cleavage products of the granins have been identified, some of these peptides showed biological activities and are costored in secretory granules of different cells. Chromofungin (Chr: CgA_{47-66}) and Cateslytin (Ctl: $CgA_{344–358}$) are peptides that display antimicrobial activities and activate neutrophils, with important implications in inflammation and innate immunity. *Staphylococcus aureus* is an opportunistic pathogen and the leading cause of a wide range of severe clinical infections and one of the most important cause of hospital-acquired infections, in fact infections caused by this bacterium have classically an important impact in morbidity and mortality in the nosocomial and community scene. Furthermore, this pathogen is the primary cause of surgical site infections and the most frequently isolated pathogen in Gram-positive sepsis. In the specific field of cardiovascular disease *S. aureus* leading infective cause of destruction of endocardial tissue after implantation of prosthetic heart valve. This pathogen is also notorious for its ability to resist the available antibiotics and dissemination of various multidrug-resistant *S. aureus* clones that limit therapeutic options for a *S. aureus* infection. Aslam et al. in 2013 shown that Ctl is resistant to the degradation of *S. aureus* protease and is the most antibacterial CgA derived peptide against this bacterium. The aim of study was to evaluate the: 1) Effects of Chr on isolated and Langendorff perfused rat hearts in basal and pathological conditions; 2) In vitro antibacterial activity of a synthetic Cateslytin-derived peptide to cover artificial heart valves and prevent infection by *S. aureus*; 3) In vivo antibacterial activity of Ctl in rat infected with *S. aureus*.

The first part of the study was performed by using the isolated and Langendorff perfused rat hearts, Elisa assay and real-time PCR. We found that, under basal conditions, increasing doses (11–165 nM) of Chr induced negative inotropic effects without changing coronary pressure. The AKT/eNOS/cGMP/PKG pathway mediated this action. We also found that Chr acted as a postconditioning (PostC) agent against ischemia/reperfusion (I/R) damages, reducing infarct size and LDH level. Cardioprotection involved PI3K, RISK pathway, MitoKATPand miRNA-21. Therefore, we suggest that Chr directly affects heart performance, protects against I/R myocardial injuries through the activation of prosurvival kinases. Results may propose Chr as a new physiological neuroendocrinemodulator able to prevent heart dysfunctions, also encouraging the clarification of its clinical potential.

In the second part of the study, two new synthetic peptides containing Ctl (RSMRLSFRARGYGFR) were designed: D*T*Ctl (DOPA-K-DOPA-K-DOPA-TLRGGE-RSMRLSFRARGYGFR), T*Ctl (TLRGGE-RSMRLSFRARGYGFR) with D*: DOPA-K-DOPA-K-DOPA and T*: TLRGGE. This study is based on the observation of the adhesive properties of the DOPA-K-DOPA-K-DOPA sequence and on the ability of *S. aureus* endoprotease Glu-C to cleave the TLRGGE sequence. Firstly, using techniques of biochemistry, proteomics (sequencing, mass spectrometry) and microbiology we shown that the digestion by the Glu-C protease of T*Ctl and D*T*Ctl is able to release active Ctl. The prediction analisys of the secondary structure suggested the presence of an alpha helix domain in the case of D*T*Ctl with respect to T*Ctl. The D* group stabilized the secondary structure and facilitated the cleavage by Glu-C to the release of the active peptide Ctl. Subsequently, the effect of the oxidation by $NaIO_4$ of D*T*Ctl on the release of Ctl and the antibacterial activity was analized. Proteomic

analysis showed the formation of polymers inhibiting the action of Glu-C and the release of Ctl. We also shown that D*T*Ctl had a MIC value around 75 μM against different strains of *S. aureus*. This data shown that D*T*Ctl had a direct action against the bacteria without Glu-C cleavage. However, in oxidizing conditions the formation of aggregates of D*T*Ctl reduced the antibacterial action of this synthetic peptide.

In the last part of this thesis, we evaluated the *in vivo* antibacterial activity of Ctl and whether and to which extent Ctl elicit cardioprotection in rat infected with *S. aureus*, as a model of infection with this bacterium. Identification of specific molecular targets of tissue and systemic inflammation and damage were analysed by Western blotting, ELISA and microbiological analysis in cardiac homogenates and plasma. A strong reduction of plasma bacterial growth, TNF-α, IL-1β and LDH plasma levels was observed in infected rat treated with Ctl. Western blotting analysis of cardiac extracts showed that Ctl treatment is accompanied by reduction of expression of pro-inflammatory markers, such as iNOS and COX-2. These preliminary data suggest that *in vivo* Ctl treatment is able to counteract the deleterious effects of *S. aureus*, and elicits myocardial protection.

Introduction

1. *Cardiac physiology and pathophysiology*

The heart, during its role of pump, is subjected to interaction with various molecules such as the endogenous hormones (Burley et al., 2007). Many of these factors, such as atrial natriuretic peptide (ANP) or brain natriuretic peptide (BNP), are able to (1) reduce contractility or relaxation, (2) improve the pump property, such as Urocortin, Serpinin (Sarzani et al., 2017; Díaz and Smani, 2013, Tota et al., 2014) and (3) induce vasoactive effects on coronary vessels (Nichols and Epstein, 2009).

In pathophysiological conditions such as heart failure, damage consequent to sepsis and myocardial infarction the pump function of the heart can be altered (Minucci et al., 2011; Suzuki et al., 2017) and several hormones may protect the heart against these alterations (Hausenloy et al., 2004 and 2016). In particular, several evidences reported that many hormones are able to protect the heart against the ischemia/reperfusion (I/R) damage (Burley et al., 2007). The most critical point in I/R damage is the time of reperfusion, because in this period the reoxygenation alters redox states that are implicated as the primary causes of oxidative stress and tissue damage in ischemic heart disease (Jeroudi et al., 1994). This deleterious phenomenon induces mitochondrial dysfunction, ROS generation, additional Ca^{2+} influx, lower concentration of ATP and apoptosis activation (Hausenloy et al., 2016). The powerful mechanisms for protecting the myocardium against this damage are ischemic preconditioning and postconditioning, in which transient non-lethal phases of myocardial ischemia (repeated respectively before and after the global ischemia) confer protection against the myocardial infarction (Hausenloy et al., 2004, 2005 and 2016). Recently several data showed that pharmacological administration before or after ischemia can also induce cardioprotection, and this approach represents a new therapeutic strategy against myocardial infarction (Hausenloy et al., 2004 and 2016).

In pre- and post-conditioning process the activation of several pro-survival kinases, during the time of reperfusion, confer powerful cardioprotection against myocardial I/R injury (Hausenloy et al., 2004 and 2005).

Sepsis is a systemic state of infection that induces severe organ dysfunctions related to a massive infection of host tissues. Several clinical studies estimated that patients associated with sepsis often die from cardiovascular complications (Suzuki et al., 2017). In fact, it has been reported that during sepsis, the consequences of the heart ischemia and reperfusion injury are more evident (Bar-Or et al., 2015); in fact, the infarct size is exacerbated by the local inflammation with a production of pro-inflammatory cytokines (Suzuki et al., 2017). The septic shock can induce destruction of myofilaments and degradation of contractile apparatus mediated by increased matrix metalloproteinase activity (Rudiger and Singer, 2007). These structural alterations of cardiac tissue, during a septic event, can induce hemodynamic disorders characterized by a reduced ejection fraction and enlarged end-diastolic volume index that lead to cardiac dysfunction during the early stages of sepsis (Calvin et al., 1981; Packer et al., 1984). The heart valves are most commonly affected by pathogen, but the infection may also occur in other structural areas of the heart including septal defects, patent ductus arteriosus or on the mural endocardium (Yusuf et al., 2012). The infection of cardiac valves occurs in four steps. In a first part, the microorganisms induce a valvular endothelial damage, after this process the pathogens form a platelet-fibrin thrombus. This platelet-thrombus plaque develops a surface that allows a major adherence of bacteria. Only then, the local bacterial proliferation with hematogenous seeding and consequent biofilm formation can occur (Frontera and Gradon, 2000). The most common microorganism associated with infective endocarditis is the Gram-positive *Staphylococcus aureus* (Yusuf et al., 2012). The mortality rate associated with *S. aureus* prosthetic valve endocarditis is high, and patients

with this complication are haemodynamically unstable and develop heart failure or valvular dysfunction (Attaran et al., 2012).

2. *Chromogranin A*

Chromogranin A (CgA) belongs to the granin family of uniquely acidic glyco-phospho proteins that are ubiquitous in secretory cells of the nervous, endocrine, immune system (Helle, 2004). This protein was the first granin to be characterized as co-stored and co-released with the catecholamine hormones from the bovine adrenal medulla (Banks and Helle, 1965). After this identification, CgA was also observed in the granules of many other cells such as cardiomyocytes (Glattard et al., 2006; Pieroni et al., 2007), keratinocytes (Corti and Ferrero, 2012), and neutrophils (Lugardon et al., 2000; Briolat et al., 2005). This protein displays important intracellular functions such as granule maturation, trafficking and exocytotic mechanisms (Helle and Aunis, 2000). Human and bovine CgA contain 439 and 431 amino acid residues, respectively. Mature human and bovine CgA have approximately 49 kDa molecular weight and contain post-translational modifications sites such as phosphorylations and glycosylations sites (Zhang et al., 1997; Strub et al., 1997; Gadroy et al., 1998; Bauer et al., 1999) and a large number of acidic residues (Metz-Boutigue et al., 1993a; Gadroy et al., 1998).

Bovine protein ($bCgA_{1–431}$) is shorter than human ($hCgA_{1–439}$) and rat ($rCgA_{1–448}$) proteins (Iacangelo et al.,1988). However, the N- and C-terminal domains, i.e. $CgA_{1–76}$ and $CgA_{316–431}$, are highly conserved sequences in mammals (Yanaihara et al., 1998; Benedum et al., 1986). The hypothesis that CgA may serve as a prohormone for shorter fragments with regulatory properties has been reported (Benedum et al., 1986; Eiden, 1987).

In fact, through proteolytic processing, often in a tissue-specific manner, CgA generates various smaller biologically active fragments that participate in peptide hormone regulation of physiological systems in health and disease conditions (Angelone and Tota, 2012).

2.1 Prohormone Chromogranin A and its derived peptides

Numerous pairs of basic amino acids, present in the sequence of CgA, indicate potential sites for cleavage by the prohormone convertases (PC1/3 and PC2), prohormone thiol proteases (PTP), and carboxypeptidase E (CPE) that occur as co-stored components of neurosecretory granules (Seidah and Chretien, 1999; Metz-Boutigue et al., 1993a). Numerous cleavage products of the granins have been identified, some of which show biological activities and are co-stored in secretory granules of different cells (Helle, 2004). The intracellular processing of CgA was shown for the first time in chromaffin cells whose secretory vesicles contain proteolytic enzymes. Among them, the neuroendocrine-specific carboxypeptidase E/H that removes basic residues from neuropeptides intermediates, the prohormone convertases (PC1/2; Seidah and Chretien, 1999), and the Lys/Arg aminopeptidases (Seidah and Chretien, 1999).

In the bovine chromaffin granules the proteolytic processing of CgA occurs at 13 sites, 5 of them at the N-terminal side, 2 in the middle and the rest at the C-terminal end. These sites are located at residues 3–4, 64–65, 76–77, 78–79, 115–116, 247–248, 291–292, 315–316, 331–332, 350–351, 353–354, 358–359, 386–387, and 403–429 (Wohlfarter et al., 1989; Metz-Boutigue et al., 1993b; Koshimizu et al., 2011) (**Figure 1**).

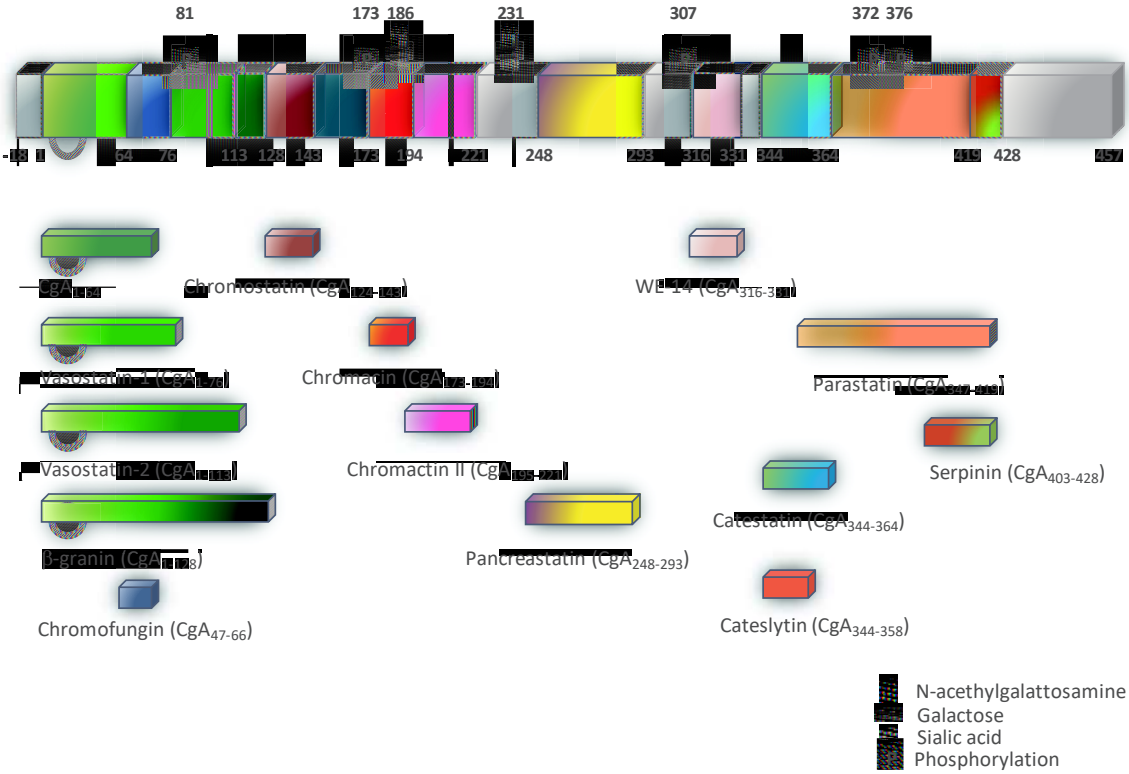

Figure 1: Schematic illustration of biologically active Chromogranin A (CgA)-derived peptides originating from the stress-activated, diffuse neuroendocrine system (from Angelone and Tota, 2012).

3. *Modulation of cardiac function and cardioprotection of Chromogranin A-derived peptides, Vasostatin and Catestatin*

Several studies have shown the presence of CgA in secretory granules of rat atrial myoendocrine cells and in human ventricular myocardium (Steiner et al., 1990; Pieroni et al., 2007). Colocalization of CgA and atrial natriuretic peptides in rat heart cardiomyocytes (Steiner et al., 1990) and in human ventricular cardiomyocytes has been shown and circulating levels of CgA are correlated with BNP (Pieroni et al., 2007). CgA has also been detected in rat Purkinje fiber cells of the conducting system, and in both rat atrium and ventricle (Weiergraber et al., 2000). Pasqua and co-workers (2013) have shown

a direct demonstration of the intracardiac processing of CgA in response to hemodynamic and excitatory challenges with a clear evidence that the heart produces and processes vasostatin-containing peptides (Glattard et al., 2006; Pasqua et al., 2013). In the rat heart, the detected PC1/3, PC2 and carboxypeptidase H/E might be involved in the intracellular CgA maturation process (Zheng et al., 1994; Muth et al., 2004). Some of these fragments may also result from extracellular processing, as reported for CgA in the adrenal gland (Metz-Boutigue et al., 1993). The presence of extracellular proteases both on cardiomyocyte cell membranes and in the extracellular matrix may indicate an extracellular processing (Glattard et al., 2006), as proposed for Angiotensin II (Jan Danser and Saris, 2002).

3.1 Vasostatin I and cardiovascular role

Vasostatin I (Vs-I) corresponds to the polypeptide $CgA_{1-76,}$ derived from the cleavage at the first pair of basic amino acid residues of the N-terminal domain of CgA (Metz-Boutigue et al., 1993a). The name of this peptide derives from its ability to maintain blood flow by reducing vascular contraction evoked in arterial and venous preparations by both high potassium and agonists such noradrenalin and endothelin (Aardal and Helle, 1992; Angeletti et al., 1994).

Several studies in literature have shown that Vs-I acts as as inotropic modulator of cardiac performance in mammals with an “anti-adrenergic” potential (Cerra et al., 2006; Cerra et al, 2008; Gallo et al., 2007). Also the human recombinant CgA_{1-78} exerts a negative inotropism and lusitropism on the rat heart (Cerra et al., 2006). This recombinant CgA-derived N-terminal peptide corresponds to the sequence of human Vs-I but also containing

the sequence of two residues (KK) at the C-terminus and three additional residues (STA) at the N-terminus, due to the molecular biology procedures (Corti et al., 1997).

On the Langendorff-perfused rat heart under basal conditions CgA_{1-78} causes a dose-dependent reduction of Left Ventricular Pressure (LVP) and Rate Pressure Product (RPP), obtained by LVPx Heart Rate (HR), thus, inducing a negative inotropism (Cerra et al., 2006). Since the negative inotropy is obtained without affecting neither HR nor Coronary Pressure (CP), the reduction of contractile performance, and consequently of cardiac work, is consistent with a direct myocardial influence of the peptide which is independent from coronary reactivity (Cerra et al., 2006).

Also the native rat CgA_{1-64} (from 33 nM) induces negative inotropism and lusitropism, and coronary dilation, counteracting the Isoproterenol (ISO) and Endothelin-1 (ET-1)-induced positive inotropic effects and ET-1-dependent coronary constriction in Langendorff perfused rat heart (Cerra et al., 2008). The CgA_{1-64} also depresses basal and ISO-induced contractility on rat papillary muscles, without affecting calcium transients on isolated ventricular cells (Cerra et al., 2008). In addition, structure-function analysis, using three modified peptides (i.e., $rCgA_{1–64}$ with S-S bridge, $rCgA_{1–64}$ without S-S bridge, and $rCgA_{1–64}$ oxidized), has revealed the key role of disulfide bridge in the cardiotropic action (Cerra et al., 2008).

Based on the ability of the domains CgA_{1-40} and CgA_{47-66} to interact and pass through the biological membrane (Maget-Dana et al., 2002; Zhang et al., 2009), the cardiac effects of human and rat Vs-I may be exerted by interacting with, or penetrating into, the cell membrane in a receptor independent-manner (Cerra et al. 2006). In line with this hypothesis, the inhibition of the ISO-mediated positive inotropism of both CgA_{1-64} and CgA_{1-78} in the rat heart may be explained *via* an allosteric modulation of the β-adrenergic receptor, independent from the ligand binding site *via* modulation of the downstream

intracellular signaling triggered by the activation of the β-adrenoceptor itself (Cerra et al., 2006, 2008).

The involvement of NO-cGMP-PKG pathway in the negative inotropic effect of CgA_{1-78} (Cerra et al., 2008; Tota et al., 2014) suggested the possibility that it exerts a protective effect against the extension of myocardial infarctions. Indeed, the administration of a low dose of CgA_{1-78} before Ischemia/Reperfusion (I/R) reduced the infarct size inducing a preconditioning-like effect (Cappello et al., 2007). This protective effect is suppressed by eNOS inhibition and 50% reduced by the blockade of adenosine A_1 receptors, indicating that at least two different pathways may be hypothesized as possible mediators of cardioprotection (**Figure 2**) (Cappello et al., 2007).

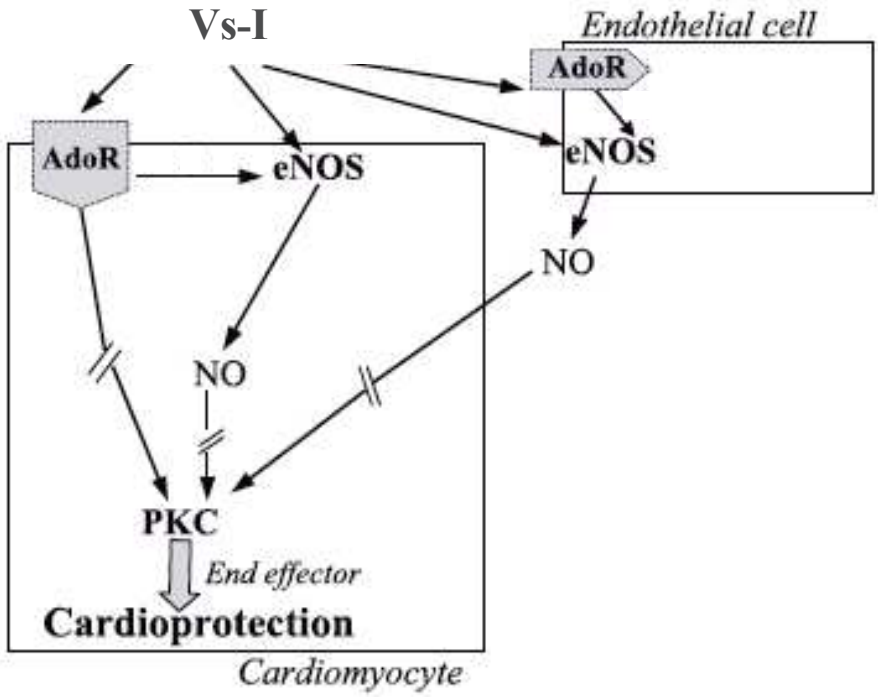

Figure 2: Diagram of mechanisms of Vs-I (CgA_{1-78})-induced cardioprotection (from Cappello et al., 2007).

3.2 Catestatin and cardiovascular role

Catestatin (Cts) ($CgA_{344–364}$) is a 21-residue long, cationic and hydrophobic peptide (Mahata et al., 1997) located at the N terminal end of parastatin (Fasciotto et al., 1993) and derives from intragranular and extragranular processing of the prohormone (Mahata et al., 1997; Preece et al., 2004; Parmer et al., 2000). Cts is a strong non-competitive inhibitor of nicotinic receptor-mediated catecholamine (CA) release (Mahata et al., 1997). Cts inhibits the calcium-dependent CA release as well as the acetylcholine-induced desensitization of the nicotinic receptor itself (Mahata et al., 1997). Furthermore, through interaction with histamine receptors, Cts exhibits vasorelaxant and antihypertensive characteristics (Kennedy et al., 1998). This antihypertensive profile is documented by a decrease of its plasma levels in patients with essential hypertension (O'Connor et al., 2002). Several studies have documented the direct myocardial and coronary effects of Cts and its mechanisms of action. The cardiosuppressive influence of Cts was evaluated on the isolated Langendorff-perfused rat heart under both basal and chemically stimulated conditions (Angelone et al., 2008). Cts induces negative inotropism and lusitropism also involving β_3-adrenergic receptors (β_3-AR), but showing a higher affinity for β_2-AR (Angelone et al., 2012). These effects were mediated by β_2-ARs-Gi/oProtein-eNOS-NO-cGMP-PKG mechanisms (Angelone et al., 2012). Furthermore, Cts-induced activation of phosphodiesterases type 2 and the increased S-nitrosylation of both phospholamban and β-arrestin, suggest an additional mechanism for intracellular calcium modulation and β-adrenergic responsiveness (Angelone et al., 2012). Several studies have also shown that Cts acts as potent inhibitors of ISO exerting different coronary vasoactivity (Angelone et al., 2008, 2012). In isolated rat hearts Cts, given at reperfusion (Cts-Post), decreases the infarct size, limits contracture and improves the post-ischemic systolic function (Penna et

al., 2010). Cts also reduces infarct size and post-ischemic contracture given as a pre-conditioning agent, but less than Cts-Post (Penna et al., 2010). Moreover, only Cts-Post significantly improves post-ischemic recovery of developed LVP. Therefore, Cts seems more protective as PostC agent than as a pre-conditioning agent (Penna et al., 2010). Cts is also able to induce cardioprotection during the early reperfusion phase in isolated hearts, or if added during a challenging ischemia in isolated cells by pro-survival intrinsic signaling cascades, which include the Reperfusion Injury Salvage Kinases (RISK) and Survivor Activating Factor Enhancement (SAFE) pathways (Penna et al., 2010, 2014; Perrelli et al., 2013). Several studies focused on cardioprotective pathways activated by Cts. Perrelli et al., (2013) in isolated Langendorff rat hearts have shown that inhibition of PI3K or a large spectrum of PKC, PKCε and mitoK$_{ATP}$ channels blockade or ROS scavengering abolished the infarct sparing effect of Cts (75nM, Cst-Post) (Perrelli et al., 2013) (**Figure 3**).

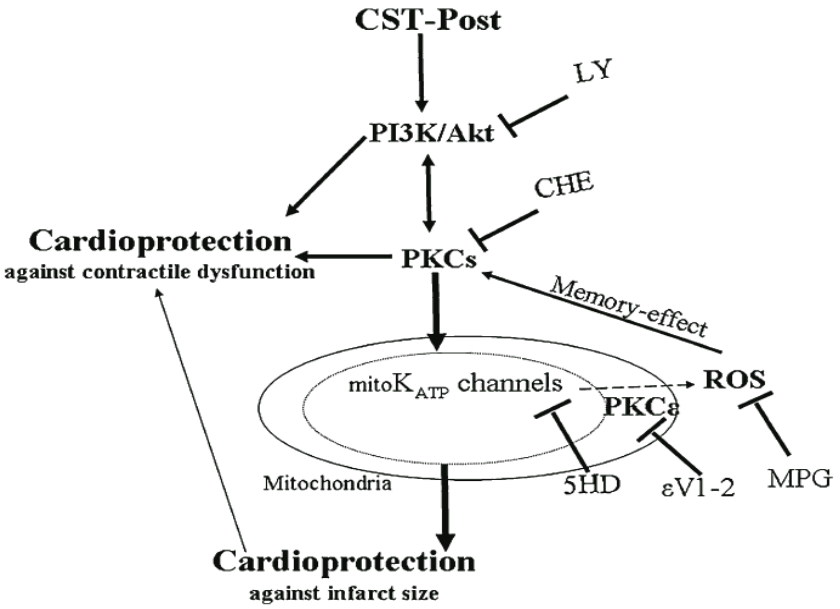

Figure 3: Diagram of mechanisms of Cts-induced cardioprotection (from Perrelli et al., 2013).

Notably, Cts can reverse the S-nitrosylation downregulation induced by I/R in spontaneously hypertensive rats (Penna et al., 2014). In fact, the S-nitrosylation of L-type calcium channel may limit calcium overload and may allow a better functional recovery of surviving cardiomyocytes (Sun et al., 2006; Murphy et al., 2012). Furthermore, Cts increases expression of pro-angiogenetic factors such as HIF-1α and eNOS after two-hour reperfusion (Penna et al., 2014). Cts triggers anti-apoptotic factors, such as ARC, and induces reduction of pro-apoptotic factors such as active Caspase 3 (Penna et al., 2014).

4. Chromofungin, the antifungal Chromogranin A (47–66)-derived peptide

In 2001, Lugardon et al. identified a natural CgA-derived peptide corresponding to the N-terminal Vs-I-derived sequence 47–66, and named Chromofungin (Chr) because of its antifungal activity (Lugardon et al., 2001). It is generated during infections after cleavage by *Staphylococcus aureus* endoprotease Glu-C (Aslam et al., 2012). Chr acts as an immediate protective shield against pathogens, in fact it displays antifungal activity at 2–15 μM against filamentous fungi (*N. crassa, A. fumigatus, A. brassicola, N. haematococca, F. culmorum, F. oxysporum*) and yeast cells (*C. albicans, C. tropicalis, C. neoformans*) (Lugardon et al., 2001). Furthermore, Chr is able to inhibit microbial cell metabolism (Lugardon et al., 2001; Aslam et al., 2012), and to penetrate the cell membrane, thus inducing extracellular calcium entry by a CaM-regulated $iPLA_2$ pathway (Zhang et al., 2009). The 3-D structure of Chr has revealed the amphipathic helical character of the sequence 53–56, whereas the segment 48–52 confers hydrophobic character (Lugardon 2001) (**Figure 4**).

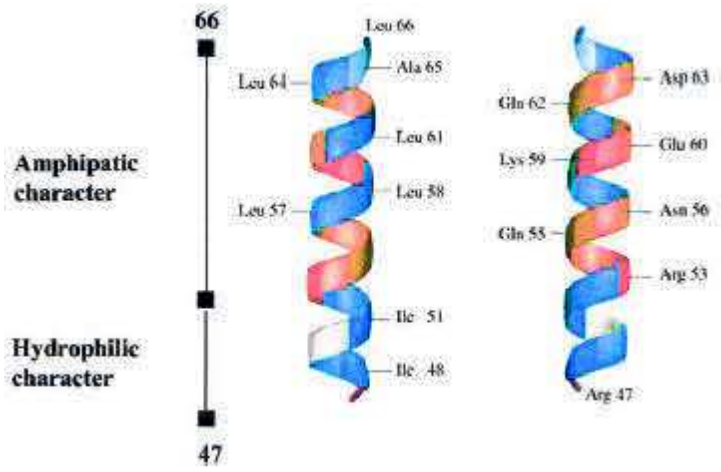

Figure 4: Three-dimensional representation of chromofungin (CgA_{47-66}) (from Lugardon et al., 2001).

Among all synthetic Vs-I derived peptides, Chr actually displays the highest antifungal activity on both fungi and yeast. The increase of the surface pressure in presence of ergosterol indicated a specificity for the fungal membranes (Lugardon et al., 2001). In addition, Chr induces membrane destabilization with the possible formation of holes (Lugardon et al., 2001). Interestingly, a cardioactive role is also suggested for Chr. As shown on the frog heart bioassay, a fragment corresponding to the Chr sequence, is found to depress myocardial contractility by eliciting a direct negative inotropic effect (Tota et al., 2003). These observations represent an intriguing starting point for investigating the heart sensitivity to Chr.

5. *Involvement of CgA and its derived peptides in immune system*

The innate immune system represents the primary defense in most living organisms. This system evolved as a set of very well organized events that protect the host from the invading pathogens such as bacteria, viruses, fungi, parasites and cancerous cells. Antimicrobial peptides (AMPs) are the unique component of the innate immune response that are highly conserved through evolutionary process (Ganz, 2003). AMPs are also called host defense peptides (Auvynet and Rosenstein, 2009). These are remarkably appreciable in their selection of target cells. These peptides are highly effective broad-spectrum antibiotics, which demonstrate their potential use as novel therapeutic agents. Antimicrobial peptides have been demonstrated to kill bacteria (including resistant strains), mycobacteria, enveloped viruses, fungi and even transformed or cancerous cells (Auvynet and Rosenstein, 2009). In addition, they also have the ability to enhance immunity by functioning as immunomodulators (Auvynet and Rosenstein, 2009). Antimicrobial peptides have two modes of action on microorganisms (Brogden, 2005). They can target cell membranes and permeabilize them according to several proposed mechanisms (Jenssen et al., 2006) or, alternatively, they act on intracellular targets to induce DNA binding, enzyme inhibition and cell wall synthesis inhibition. For numerous AMPs, the folded peptide adopts an amphipathic profile important for their microbial killing mechanism: the cationic character of AMPs induces an electrostatic attraction to the negatively-charged phospholipids of microbial membranes and their hydrophobicity aids the integration into the microbial cell membrane, leading to membrane disruption. Furthermore, the amphipathic structure also allows the peptides to be soluble both in aqueous environments and in lipid membranes (Yeaman and Yount, 2003).

Several Chromogranins-derived peptides have been characterized as new cationic antimicrobial peptides (Strub et al., 1996a, b; Metz-Boutigue et al., 1998; Lugardon et al., 2000; Briolat et al., 2005; Helle et al., 2007) and host defense agents derived from CgA during infections, were identified (Radek et al., 2008). The AMPs derived from CgA act at micromolar range against bacteria, fungi, yeasts and are non-toxic for mammalian cells. They are recovered in biological fluids involved in defense mechanisms (serum, saliva) and in secretion of stimulated human neutrophils (Lugardon et al., 2000; Briolat et al., 2005).

The CgA-derived peptides production and the molecular mechanism of the antimicrobial activities were characterized in several studies. In addition, when polymorphonuclear neutrophils (PMNs), known to accumulate at sites of infection, are stimulated by bacterial agents such as Panton-Valentine leucocidin (PVL), they produce and secrete complete and processed forms of CgA, such as Vs-I and Vs-II (Lugardon et al., 2000) and Cts (Briolat et al., 2005).

Others experiments have demonstrated the presence of Cts in infected skin (Radek et al., 2008). The potential relevance of Cts against skin pathogens was supported by the observation that CgA was expressed in keratinocytes. In human skin, CgA was found to be proteolytically processed to produce Cts (Radek et al., 2008). Interestingly, Cts expression in murine skin increases in response to injury and infection, providing potential for increased protection against infection (Radek et al., 2008). In fact, this peptide possesses antimicrobial activities at micromolar concentration against Gram-negative and Gram-positive bacteria, yeast, and fungi. (Briolat et al., 2005; Radek et al., 2008). The two human variants P370L and G364S display antibacterial activity against *M. luteus* with a minimal inhibitory concentration (MIC) of 2 and 1 μM, respectively, and against *E. coli* with a MIC of 20 and 10 μM, respectively (Briolat et al., 2005).

Cts acts against bacteria with a mechanism similar to that reported for Chr (Briolat et al., 2005). In fact, Cts is a cationic peptide with amphipathic structure such as Chr. This property allows to the hydrophobic domain to interact with the membrane while the cationic domain destabilizes and induces the pores formation (**Figure 5**).

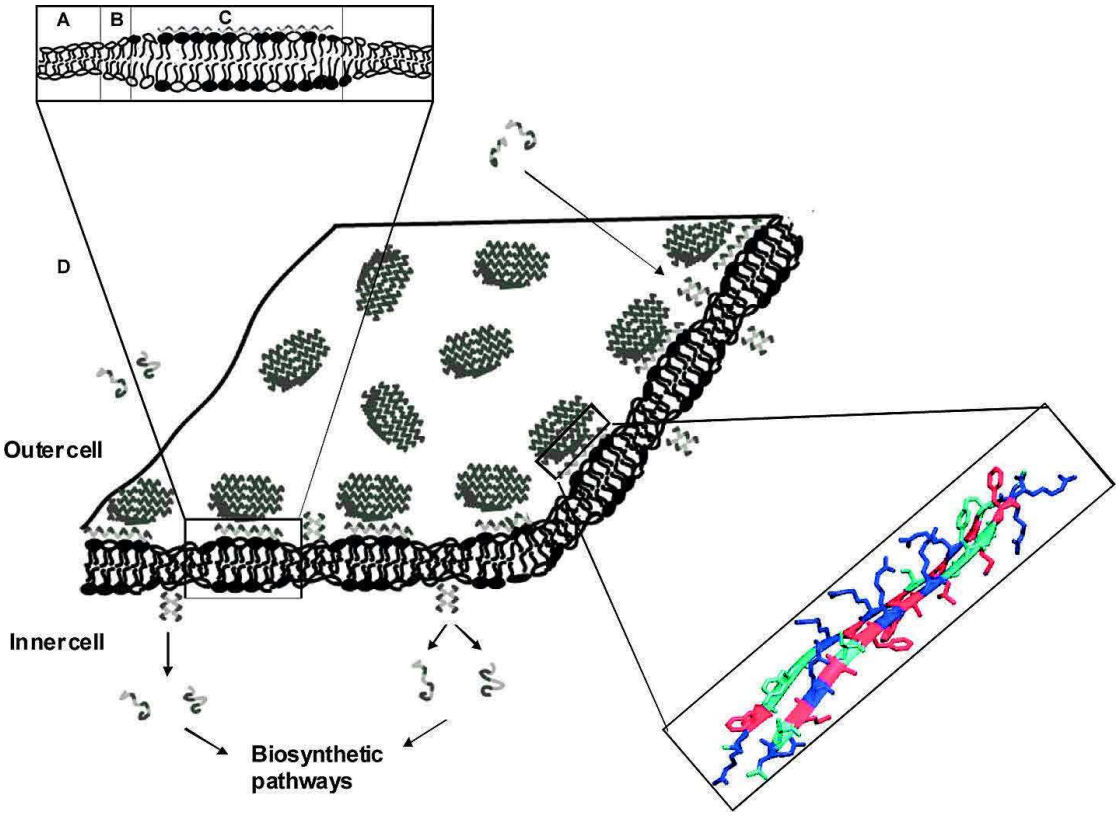

Figure 5: Model for interaction of Cateslytin (antimicrobial domain of Cts) with bacterial-like membrane domains (from Jean-François et al., 2008a).

Moreover, the outer leaflet of external bacterial membranes comprises a large amount of negatively charged peptides (whereas that of animals or plants is globally neutral), so the susceptibility of a microorganism to a particular AMP is mainly linked to its charge, hydrophobicity, and amphipathicity. Indeed, Cts adopts the α-helical structure when it interacts with negatively charged membranes and this interaction involves positively charged residues such as arginine. After this interaction the peptide induces a rigidity increase of the membrane regions where it interacts, as well as a thickening of these regions and formation of pores (Sugawara et al., 2010) (**Figure 6**).

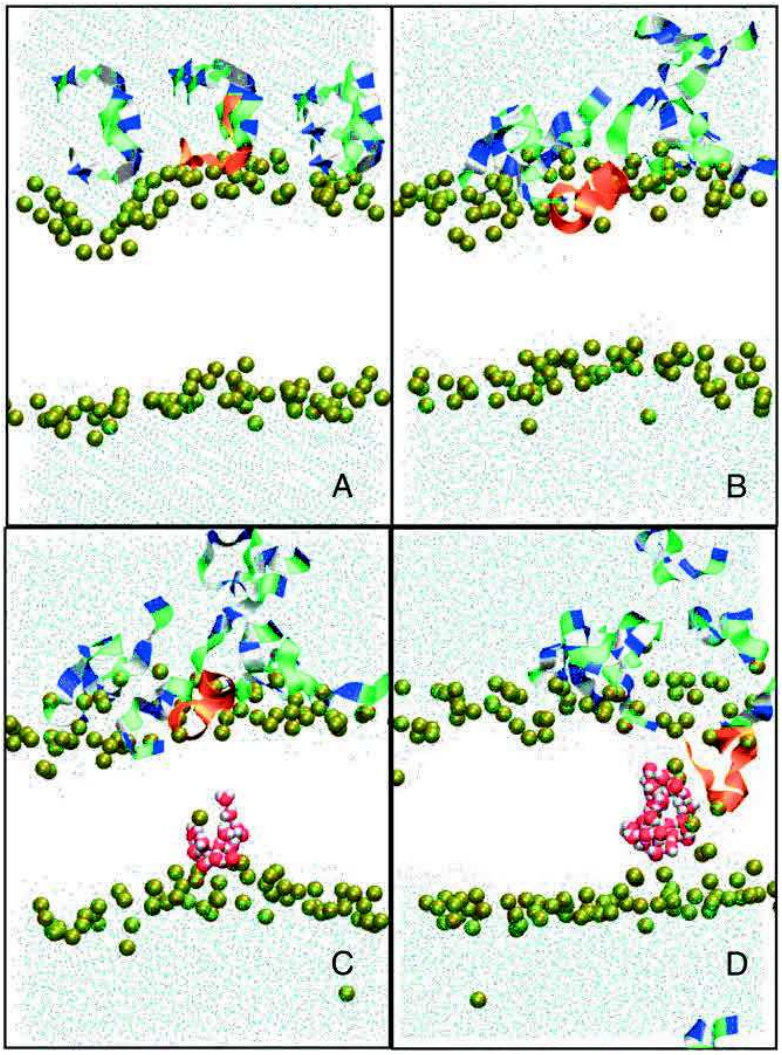

Figure 6: Molecular dynamics of pore formation induced in a 1,2-dimyristoyl-sn-glycero-3-phosphocholine bilayer (128 lipids, 6754 water molecules) by the presence of eight Cateslytins. (A) Starting conditions with the initial distribution of the peptides above the outer membrane leaflet; (B) the equilibrated bilayer and peptides on the outer membrane leaflet; and (C) the formation of a transient water defect. (D) Formation of a stable pore. The bilayer is only represented by the position of the interfacial phosphate groups (brown beads). Outside water molecules are in cyan, water molecules in the pore are in red. The peptides that do not contribute to the pore are represented as ribbons (residues: dark blue, basic; green, polar; and white, nonpolar). Peptide that inserts into the pore is in orange. (from Jean-François et al., 2008b).

However, the most active Cts peptide corresponds to the bovine sequence with higher number of residues with positive charges.

Literature data reported that bovine Vs-I, human recombinant Vs-I, and rat synthetic $CgA_{7–57}$ possess antimicrobial activities at micromolar concentration (Lugardon et al., 2000). Of note, bovine Vs-I displays antimicrobial activity against Gram-positive bacteria (*Micrococcus luteus and Bacillus megaterium*) with a MIC in the range 0.1-1 μM,

filamentous fungi (*Neurospora crassa, Aspergillus fumigatus, Alternaria brassicola, Nectria haematococca, Fusarium culmorum, Fusarium oxysporum*) with a MIC of 0.5-3 μM and yeast cells (*Saccharomyces cerevisiae, Candida albicans*) with a MIC of 2 μM. However, Vs-I is unable to inhibit the growth of *Escherichia coli* and *Staphylococcus aureus* (Lugardon et al., 2000).

Biochemical techniques, confocal microscopy, flow cytometry, calcium imaging, surface plasmon resonance, and proteomic analysis have shown the ability of Chr and Cts to stimulate exocytosis from PMNs by provoking a transient Ca^{2+} influx, independent of release from intracellular stores (Zhang et al., 2009).

For both peptides the mechanisms involve the calmodulin binding, the subsequent activation of the calcium-independent phospholipase A_2 for the opening of the store-operated channels to induce the secretion of numerous factors involved in innate immunity (Zhang et al., 2009; Aslam et al., 2012).

Stress and infection lead to two different pathways for stimulation of PMNs secretion, by release of CgA and CgA-derived peptides from the adrenal medulla, by PVL leucocidin stimulation and by *Staphylococcus aureus* infections (Aslam et al., 2012) (**Figure 7**). The negative feedback is induced by Cts on nicotinic cholinergic receptor of chromaffin. The infective route leads to activation of the putative Panton-Valentine leucocidin receptor coupled to opening of Ca^{2+} channels and a rise in intracellular Ca^{2+} that converges on docking of secretory granules and subsequent secretion of proteins of relevance for innate immunity (Zhang et al., 2009; Aslam et al., 2012) (**Figure 7**).

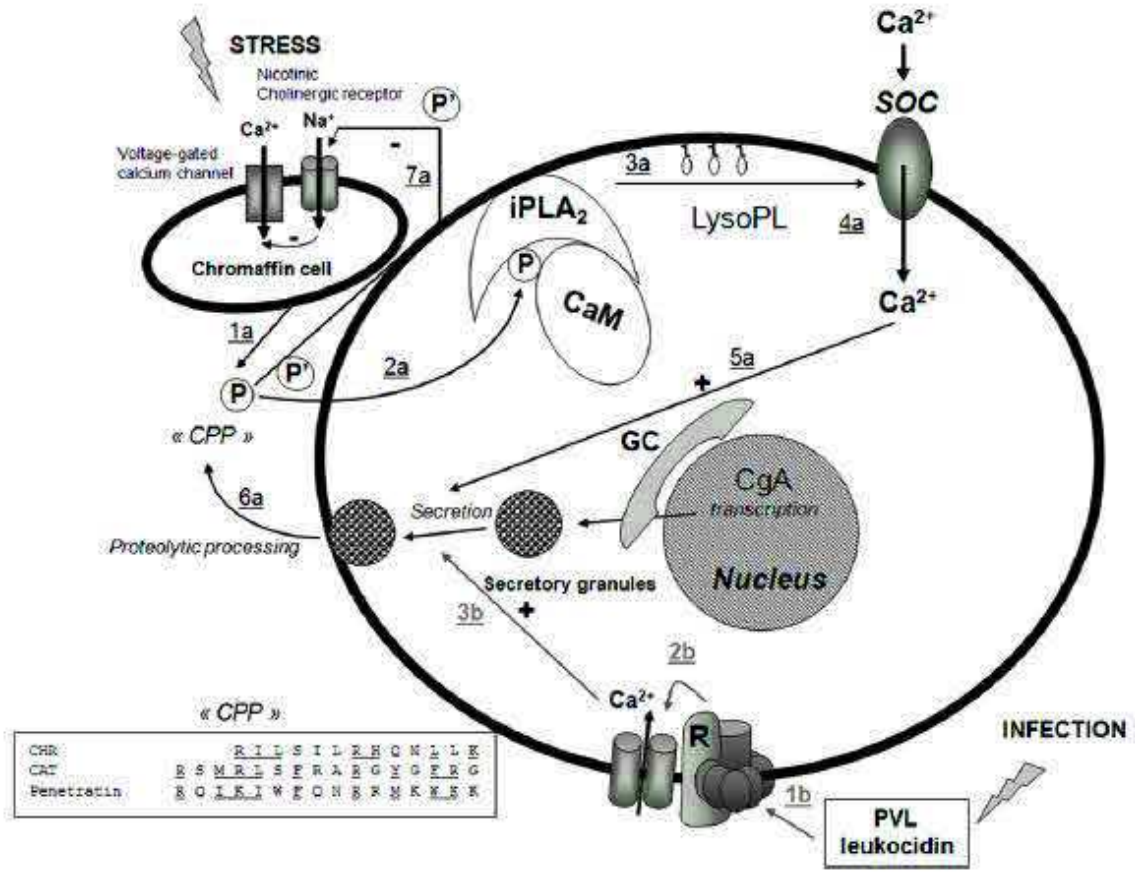

Figure 7: Model for the action of Chr and Cts on PMNs activation. Stress and infection lead to two different pathways for stimulation of PMN secretion, by release of CgA and CgA-derived peptides from the adrenal medulla, as indicated by 1a–6a (black), and by PVL leucocidin stimulation by *Staphylococcus aureus* infections, as indicated by 1b–3b (grey), respectively. Abbreviated symbols: P (Chr, Cts), P' (Cts), CPP (Cell Penetrating Peptide), CaM (calmodulin), $iPLA_2$ (calcium independent phospholipase A_2) LysoPL (lysophospholipids); GC (Golgi complex); PVL (Panton-Valentine leucocidin), R (receptor). The stress-stimulated pathway leads to penetration of P into the cytoplasm (2a), resulting in removal of inhibitory CaM, activation of $iPLA_2$ to produce LysoPL (3a) and activation of Ca^{2+} influx through SOC (4a), converging on activated docking of secretory granules (5a) and subsequent release of proteins of relevance for innate immunity (6a). The negative feedback induced by P' on nicotinic cholinergic receptor of chromaffin cell is also indicated (7a). The infective route leads to activation of the putative PVL receptor coupled to opening of Ca^{2+}-channels and a rise in intracellular Ca^{2+} (3b) that converges on docking of secretory granules and subsequent secretion of proteins of relevance for innate immunity (6a). Transcription of CgA in response to stress and infection is also indicated (from Zhang et al., 2009).

A well studied immunomodulatory activity of CgA-derived peptides is their ability to mediate monocyte chemotaxis (Shooshtarizadeh et al., 2010). It has been shown that human Cts is a potent chemotactic substance for monocytes, exhibiting its maximal effect at a concentration of 1 nM, comparable to the concentration of chemokines (Egger et al., 2008). Since the circulating concentration of Cts is around 2–3 nM (O'Connor et al.,

2002), the chemotactic effect of Cts is considered of physiological relevance. Additionally, lack of a chemotactic effect on neutrophils argues in favor of a specific chemotactic effect on monocytes (Egger et al., 2008).

In mouse model of experimental colitis, Cts has induced a reduction on colonic cytokine levels (Rabbi et al., 2014). Cts (1.5 mg/kg/day, 6 days, i.r.) has reduced IL-1β, IL-6 and TNF-α levels in colitic mice. This role was further studied by examining the ability of Cts to inhibit macrophages to produce pro-inflammatory cytokines by isolating macrophages from the peritoneal cavity of non-colitic or colitic mice treated or not *in vivo* and *in vitro* with the different peptides. These immune cells play an important role in the development of colitis, and recent data have demonstrated that these cells are the main producer of IL-1β, IL-6 and TNF-α (Rabbi et al., 2014). This study has shown that Cts regulates the macrophage pro-inflammatory cytokines release of monocytes and macrophages reducing inflammatory mechanism (Rabbi et al., 2014). These results can be explained by the fact the CgA or its derived peptides may have anti-inflammatory proprieties that need to be expressed not only during the acute phase but also during the remission phase to keep the inflammation under control *via* some anti-inflammatory mechanisms (Rabbi et al., 2014). These findings suggest that CgA or its derived peptides have an important role in the immune response to pathogens and in the development of inflammation, by regulating the infiltration of inflammatory cells and production of pro-inflammatory mediators.

5.1 Staphylococcus aureus and nosocomial infections

Staphylococcus aureus (*S. aureus)* is a dangerous gram positive bacterium which represents one of the most important cause of hospital-acquired infections. In particular, methicillin-resistant *Staphylococcus aureus* (MRSA) is the major nosocomial factor that induces illness and death linked to infections (Klein et al., 2007). During the last years, the number of isolated MSRA strains is increased in intensive care units (Klevens et al., 2006) as well as in outpatients (Sieradzki e al., 1999; Johnson et al., 2007), thus producing serious economic costs for public health (Klein et al., 2007).

Nosocomial infections are often caused by biofilm colonization of medical implants (Riberio et al., 2016) and several studies in hospitals have identified *S. aureus* colonization of intravascular catheters as a strong predictor of subsequent *S. aureus* bacteremia, even in the absence of clinical signs of systemic infection (Hetem et al., 2011). In this case, bacteremia is prevented by antibiotic therapy (within 24 hours after catheter removal) (Hetem et al., 2011). Untreated bacteremia can induce complications, such as endocarditis, septic thrombosis, tunnel infection, or metastatic seeding (Mermel et al., 2001).

It is clear that, possible solutions for this health problem include greater attention in hospital surveillance and identification of reporting requirements for *S. aureus* and MRSA infections (Klein et al., 2007). On the other hand, the development of agents or functionalized biomaterials against *S. aureus* could represent an alternative strategy (Riberio et al., 2016).

5.2 Staphylococcus aureus and prosthetic valve endocarditis

In the specific field of cardiovascular research several scientific data suggest that the mortality rate associated with *S. aureus* prosthetic valve endocarditis (PVE) is high. The patients with PVE induced by *S. aureus* show cardiac and central nervous system (CNS) complications, and in severe cases, death within 90 days of the diagnosis (John et al., 1998). Cardiac complications, but not CNS complications, are associated with increased mortality and valve replacement surgery during antibiotic therapy is associated with decreased mortality (John et al., 1998). (John et al., 1998).

For PVE, the most important point for surgical guidelines is to understand which patients with this post-operative pathology need valve replacement surgery. Attaran and collegues (2012) in their study compared the outcome and survival between surgically and non-surgically treated patients with prosthetic valve endocarditis. This study showed that in patients haemodynamically unstable and with cardiac complications, such as heart failure or valvular dysfunction, the valve replacement surgery should be performed as soon as possible (Attaran et al., 2012), and this approach is also in accordance with the guidelines of the American College of Cardiology and American Heart association. Furthermore, in PVE cases the presence of *S. aureus* is considered an urgent surgical indication in the treatment of prosthetic valve endocarditis (Attaran et al., 2012). In fact, *S. aureus* PVE is often induced by more resistent strains to antibiotic treatments compared to the other micro-organisms that can induce PVE (Attaran et al., 2012).

Even if in hospital practice the surgery intervention is appropriately performed in the majority of patients, more recently, Chu et al., 2015 reported that one quarter of patients with surgical indications do not undergo surgery intervention but they are treated with medical therapy alone during the initial hospitalization (Chu et al., 2015). However,

mortality risk in *S. aureus* PVE remains high even with antibiotics therapy or surgical interventions (John et al., 1998; Attaran et al., 2012; Chu et al., 2015).

These same complications are also present in pacemaker patients with Gram-positive occult bacteremia. Also in these cases, *S. aureus* represents one of the main pathogens associated with this clinical problem (Golzio et al., 2010).

6. *Antibacterial action of Cateslytin against Staphylococcus aureus*

Cateslytin (Ctl, $CgA_{344-358}$) is the biologically active fragment of Cts ($CgA_{344-364}$) which displays antimicrobial activity (Briolat et al., 2005). It is a positively charged (5+), arginine-rich peptide (bCgA, RSMRLSFRARGYGFR). The biosynthesis of Ctl results by the action of prohormone convertases PC1/2 present in the granular matrix of chromaffin cells (Aslam et al., 2013). The prohormone thiol protease (PTP) was also reported to be essential for Cts production ($bCgA_{344–364}$) by cleaving D-R and L-R (Lee et al., 2003). In addition, in chromaffin secretory vesicles, the cysteine protease cathepsin L (CTSL) (Biswas et al., 2009) generates Ctl by the additional cleavage of the R-G linkage of Cts (Aslam et a., 2013).

Of note, the sequences of Cts and Ctl are highly conserved during evolution and their arginine ratio is in modulating the interaction with negatively charges of the membranes of microorganism. For hCts, bCts, and bCtl the arginine ratios are 15%, 23%, and 33% respectively. High arginine ratio of bCtl supports a strong interaction with the negatively charged lipid bilayer as compared to the both Cts and Chr (Lugardon et al. 2001; Aslam et al., 2013).

Several studies have analyzed the structure/function relationship of Ctl. It possesses a random structure in powder, water, or Dodecylphophatidylcholine (DPC) micelles, but adopts a helical structure in Trifuoroethanol (TFE), and is structured in β-sheets to mimic a membrane environment (Jean-François et al., 2007, 2008a). In particular, Ctl is converted into antiparallel β-sheets that aggregate mainly flat at the surface of negatively charged bacterial membranes (Jean-François et al., 2008a). This structured interaction peptides-membrane confers major rigidy and thick to membrane domains enriched in negatively charged lipids (Jean-François et al., 2008a). The rigidity and thickness bring about phase boundary defects that ultimately lead to permeability induction and peptide crossing through bacterial membranes (Jean-François et al., 2008a). In fact, after the first binding Ctl is able to form pores with 1 nm diameter and 0.25 nS conductance. The structure in pore formation is close to a simulation of α-helical peptides. Indeed, the electrostatic forces play a crucial role in the process of pore formation (Jean-François et al., 2008b). Much less interaction is detected with neutral mammalian model membranes, as reflected by only minor percentages of β-sheets or helices in the peptide secondary structure. In fact, no membrane destruction was detected for mammalian model membranes.

Even if several CgA derived peptides display antimicrobial properties (Metz-Boutigue et al., 1998), data concerning killing of *S. aureus* is reported only for Ctl (Aslam et al., 2013). In fact, it is known that Vs-I (Lugardon et al., 2000), Chr (Lugardon et al., 2001), and Cts (Briolat et al., 2005; Aslam et al, 2013) are active against different bacterial strains at micromolar range, but not against *S. aureus*.

Many bacterial strains express a variety of proteases able to degrade, in specific and non-specific manner, many proteins involved in innate immunity (Potempa and Pike, 2009).

It has been suggested that several *S. aureus* proteases may degrade Cts to generate inactive peptides. For instance, several Metalloproteases (Sep A) (Lai et al., 2007) or leucine Aminopeptidase (LAP, pepZ) (Carroll et al., 2012), could cleave Cts in the sites S-F, G-F and L-S, respectively, that correspond to the proteolytic cleavage sites obtained by the incubation of Cts with different *S. aureus* strains (**Figure 8**). This proteolytic degradation could explain the observed low antibacterial activity of Cts (Aslam et al., 2013). Incubation with *S. aureus* supernatants has demonstrated that bovine and human Cts are similarly degraded to generate inactive fragments. For bovine and human Cts, the cleavage sites induced by the supernatants are different depending on bacterial strains.

On the contrary, Ctl resists to the degradation of *S. aureus* supernatant and maintains its activity against this gram-positive bacterium with a MIC value of 37–45 µg/mL (21 µM) (Aslam et al., 2013) (**Figure 8**).

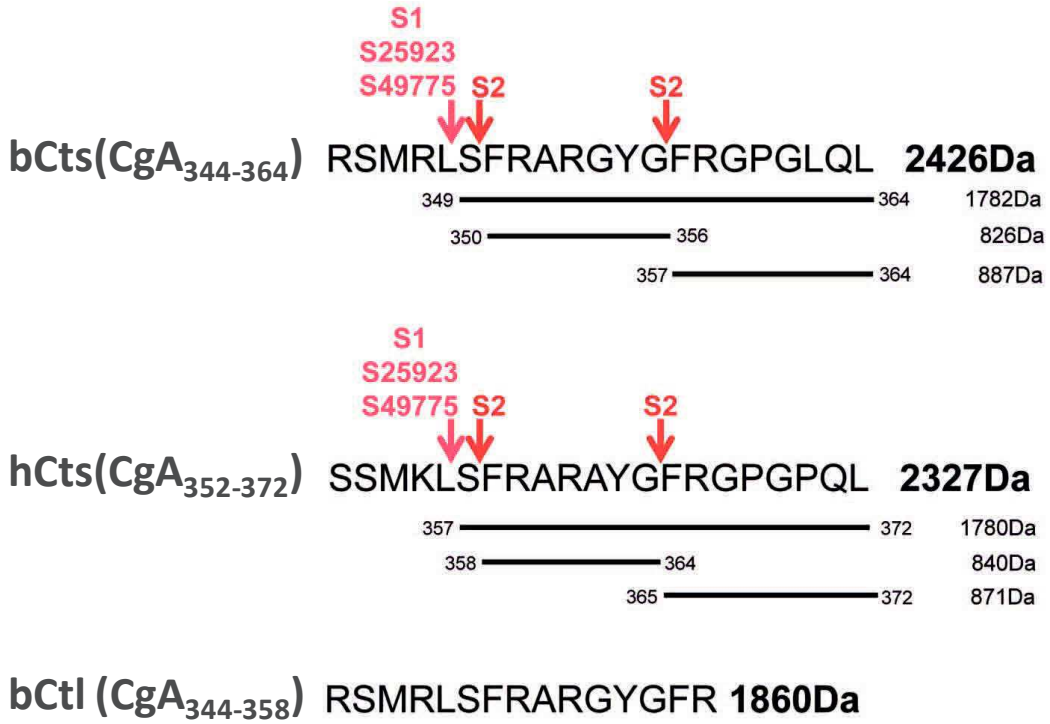

Figure 8: The proteolytic cleavage sites induced after treatment of bCts, hCts and bCtl with different *S. aureus* strains (ATCC25923, ATCC49775, S1 and S2) (from Aslam et al., 2013).

Another property that may explain the best action of Ctl against *S. aureus* concerns its secondary structure.

Both hCts and bCts adopt helical structures (residue 7 to residue 11) in the presence of high concentrations of DPC (Sugawara et al., 2010). In a similar way, Ctl adopts a β-sheet structure only on negatively charged membranes, whereas it is essentially unstructured in water (Jean-François et al., 2008a). These β-sheet formations give more stability to peptide respect to the helical formation (Jean-François et al., 2008a) as previously reported for Cts (Sugawara et al., 2010). In addition, in Ctl structure, the arginine and hydrophobic residues are in close proximity, thus creating a deep penetration of charged residues into the membrane (Ziegler et a., 2008). In fact, as previously described, the electrostatic interaction between positively charged arginine residues and negatively charged lipids appears to be responsible for binding of Ctl to the lipid bilayer, and at the same time, the aromatic residues stabilize the lipid-peptide interaction (Jean-François et al., 2008a, b; Aslam et al., 2013).

Furthermore, it is known that Ctl has antimicrobial activity against *Micrococcus luteus*, few yeasts and fungal strains, and it is not hemolytic for human erythrocytes (Briolat et al., 2005). Recently, a mechanism by which the peptides favor destabilization of bacterial membrane, allowing the antibiotics to rapidly penetrate inside bacterial cells to reaching their site of action, has been postulated (Aslam et al., 2013). These Authors have demonstrated that Ctl shows synergistic effects with antibiotics, such as Minocyclin or Voriconazole, and this co-treatment induces a reduction of the antibiotics concentration used and can potentiate their activities.

7. Aims of this thesis

Antimicrobial peptides are now viewed as multifunctional factors. Indeed, in addition to their antimicrobial activity, they also mediate inflammatory and immune responses. Furthermore, several antimicrobial peptides have been shown to exert either detrimental or beneficial effects on the cardiovascular system (Li, 2009). For example, PR-39 and LL-37, both belonging to Cathelicidin family, showed opposite effects: the first one inducing cardioprotective effects against I/R damage (Ikeda et al., 2001) while, LL-37 promoting atherogenesis and cardiovascular disease (Edfeldt et al., 2006). Among CgA-derived peptides, Vs-I and Cts, also show both antimicrobial activity and benefical cardiovascular effects (Helle et al., 2007; Angelone et al., 2012a).

Thus, on the basis of these previous data, a link between immune-derived CgA peptides and cardiovascular pathophysiology may be hypothesized.

The aim of this thesis was to evaluate the possible contribution of antimicrobial peptides Chr (Vs-I-derived fragment) and Ctl (Cts-derived fragment) in the cardiovascular pathophysiology and immune response.

The first part of the study was focused to evaluate the action of Chr in maintaining basal cardiac function and its putative role in cardioprotection. Furthermore, Tota and co-workers (2003) have shown the cardiac effects of Chr in an avascular model of the vertebrate myocardium. This peptide induced a depression of myocardial contractility by eliciting a direct negative inotropic effect isolated frog heart (*Rana esculenta*). The antimicrobial activity of Chr against fungi and yeast (Lugardon et al., 2001) is well recognised. In this thesis, for the first time, it has been evaluated:

- Whether Chr affects the basal cardiac performance and is able to protect the myocardium agains to I/R damage by using the rat heart as a prototypic mammalian heart. To corroborate the results on cardioprotection, the mechanism of action on RISK pathway activated during I/R has been evaluated.

In a second time, we have focused the attention on the ability of Ctl to prevent *S. aureus* infection in different pathological conditions. Aslam and co-workers (2013) have reported that Ctl represents the best CgA-derived AMP, and that it is able to resist to the degradation of *S. aureus* proteases and to kill this bacterium *in vitro*. It is known that *S. aureus* is the main pathogen which induces prosthetic valve endocarditis and this complication is associated with a high risk of mortality even with antibiotics therapy or surgical interventions (Attaran et al., 2012; Chu et al., 2015). Furthermore, MRSA strains, the major cause of nosocomial infections, are resistant to antibiotics therapy (Klein et al., 2007). Based on these premises here we aimed to evaluate:

- Whether Cts-derived peptide Ctl is able to coat surfaces and cover a biomaterial for medical and surgical applications to prevent *S. aureus* infection after implantation. For this purpose, it has been used a synthetic peptide composed of the following: a Levo-3,4-dihydroxyphenylalanine (DOPA) group, which covers in a nonspecific manner all the typologies of biomaterials (Lynge et al., 2011; Ponzio et al., 2014), and a specific sequence (TLRRGE) recognized by Glu-C endoprotease (produced and released by *S. aureus* during infection) (Drapeau, 1976, 1977), which allows the release of active Ctl (**Figure 9**).
- Whether Ctl is able to induce by *in vivo* treatment an antibacterial activity against *S. aureus* preventing infection by this pathogen in a rat model.

Materials and Methods

1. Isolated and perfused rat Langendorff heart

1.1 Animals

Male Wistar rats (Harlan Laboratories, Udine, Italy S.r.l.) weighting 250-350 g were housed three per cage in a ventilated cage rack system under standard conditions. Animals had food and water access *ad libitum*. The investigation conforms with the *Guide for the Care and Use of Laboratory Animals* published by US National Institutes of Health (NIH Publication No. 85-23, revised 1996) and to the Italian law (DL 116/92 and DL 26/14).

1.2 Isolated heart preparation

Rats were anaesthetized with ethyl carbamate (2 g/Kg rat, i.p.). The hearts were rapidly excised and transferred in ice-cold buffered Krebs-Henseleit solution (KHs). The aorta was immediately cannulated with a glass cannula and connected with the Langendorff apparatus to start perfusion at a constant flow-rate of 12 mL/min. To avoid fluid accumulation, the apex of the left ventricle (LV) was pierced. A water-filled latex balloon, connected to a BLPR gauge (WRI, Inc. USA), was inserted through the mitral valve into the LV to allow isovolumic contractions and to continuously record mechanical parameters. The balloon was progressively filled with water up to 80 µl to obtain an initial left ventricular end diastolic pressure of 5-8 mmHg (Javadov et al., 2000). Coronary pressure was recorded using another pressure transducer located just above the aorta. The perfusion solution consisted of a modified non re-circulating KHs containing 113 mM NaCl, 4.7 mM KCl, 25 mM $NaHCO_3$, 1.2 mM $MgSO_4$, 1.8 mM $CaCl_2$, 1.2 mM KH_2PO_4, 11 mM glucose, 1.1 mM mannitol, 5 mM Na-pyruvate. pH was adjusted to 7.4 with NaOH

(1 M) and the solution was equilibrated at 37°C by 95 % O_2 and 5% CO_2. All drug containing solutions were freshly prepared before the experiments. Haemodynamic parameters were assessed using a PowerLab data acquisition system and analysed using a Chart software (both purchased by ADInstruments, Basile, Italy).

2. Experimental protocols

2.1. Basal conditions

Cardiac performance was evaluated by analysing heart rate (HR, in beats/min), left ventricular pressure (LVP, in mmHg), which is an index of contractile activity, and the rate pressure product (RPP: HR x LVP, in 104 mmHg x beats/min), used as an index of cardiac work (Georget et al., 2003), $+(LVdp/dt)_{max}$, i.e. the maximal rate of left ventricular pressure contraction, Ttp, i.e. the time to peak tension of the isometric twitch, which indicates changes in relaxation, $-(LVdp/dt)_{max}$, i.e. the maximal rate of left ventricular pressure decline, HTR (Half Time Relaxation), and $+(LVdp/dt)_{max}/-(LVdp/dt)_{max}$, i.e. T/-t which indicates the ratio between maximal rates of contraction and relaxation (Vittone et al., 1994). The mean coronary pressure (CP, in mmHg) was calculated by averaging the coronary pressure during several cardiac cycles.

2.2. Drugs and chemicals

Chr (CgA_{47-76}) was synthesized at the INSERM U1121, Bio-materials and Bioengineering, Strasbourg, France, as described in Lugardon et al., 2001. It was dissolved in water before use. Selective eNOS inhibitor, N(5)-(1-imino-3-butenyl)-l-ornithine (L-NIO); soluble guanylate cyclase (sGC) inhibitor [1H-[1,2,4]oxadiazolo[4,3-

a]quinoxalin-1-one] (ODQ); protein kinase G (PKG) inhibitor, KT5823; PD98059 (PD), a specific inhibitor of ERK1/2, Wortman-nin (WT), a potent phosphatidylinositol 3-kinase (PI3K) inhibitor, 5-hydroxydecanoate (5HD), a mitoKchannels blocker, were purchased from Sigma Chemical Co. (St. Louis, MO). All drug-containing solutions were freshly prepared before experimentation.

2.2.1. Chr stimulated preparations

Preliminary experiments (data not shown) obtained by repetitive exposure of each heart to a single concentration of Chr (65 nM) revealed absence of desensitization. Thus, concentration response curves were obtained by perfusing cardiac preparations with KHs enriched with increasing concentrations of Chr (1–165 nM) for 10 min. To evaluate the possible effects of Chr on chronotropism, in this set of experiments hearts were unpaced.

2.2.2. Chr-dependent mechanism of action

To investigate the involvement of the NO pathway in the mechanism of action of Chr, hearts were stabilized for 20 min with KHs and perfused for 10 min with Chr (65 nM); then hearts were washed out with KHs and, after returning to control conditions, perfused with KHs containing Wortmannin (WT) (100 nM) or L-NIO (10 μM) or ODQ (10 μM) or KT5823 (0.1 μM). Subsequently, cardiac preparations were exposed to KHs enriched with Chr plus each of the above inhibitors (n= 6 for each group).

2.3. Myocardial protective effects

After anaesthesia with ethyl carbamate (2 g/Kg rat, i.p.), the hearts were excised, connected to a perfusion apparatus, perfused at constant flow with oxygenated Krebs-

Henseleit buffer, paced at 280 b.p.m and kept at 37°C. Left ventricular pressure (LVP) and aortic pressure (AP) were measured. In the control AP was about 80 mmHg for a coronary flow of 12 mL/min. Developed LVP was taken as an index of contractility. Infarct size was determined with nitro-blue tetrazolium technique. The release of Lactic-dehydrogenase (LDH) was determined on samples of effluent fluid taken at regular intervals during reperfusion.

2.3.1. Ischemia/reperfusion

Each heart was allowed to stabilize for 40 min; at this time, baseline parameters were recorded. After stabilization, hearts were randomly assigned to one of the groups described below and then subjected to 30 min of global, no-flow ischemia followed by 120 min of reperfusion (I/R). Although under basal conditions Chr did not modify HR, to avoid interference by HR during I/R maneuvers, hearts were paced according to Pagliaro et al. 2003.

2.3.2. Cardiac function and infarct size

The hearts were divided in four groups. Group 1 was used as control (Sham, n= 6), hearts were stabilized and perfused for 120 min. In Group 2 (I/R group, n= 6), hearts were stabilized and subjected to I/R protocol only. In Group 3 (postC-Chr group, n= 6) Chr (65 nM) was infused for 20 min at the beginning of 120 min reperfusion. In Group 4 (postC Chr+inhibitors group, n= 6 for each group), hearts were perfused with Chr plus one of the following inhibitors: WT (100 nM; Chr + WT), or PD (10 nM; Chr+PD), or ODQ (0.1 μM; Chr+ODQ), or 5HD (10 μM; Chr+5HD); perfusion with inhibitors started 5 min before ischemia and continued during the early 20 min of reperfusion in the presence of Chr (65 nM). Chr concentration was chosen on the basis of preliminary dose-response curves as the dose that induced the highest infarct size reduction (data not shown). Cardiac

performance before and after ischemia was evaluated by analyzing LVP recovery, as an index of contractile activity, and LVEDP as an index of contracture, defined as an increase in LVEDP of 4 mmHg above the baseline level (Pagliaro et al., 2003).

2.4. Cyclic guanosine monophosphate (cGMP)

At the end of perfusion for each groups, to obtain cGMP determination frozen ventricles (200–300 mg) were treated with 6% (m/V) trichloroaceticacid at 0°C and centrifuged at 1000×g for 10 min. Supernatants were extracted three times with 3 ml of diethyl ether saturated with water, and the aqueous phases were collected and stored at −80°C. The cGMP determination was obtained by using cGMP Bio-track Enzyme Immunoassay (EIA) System, (GE Healthcare, Milan, Italy).

2.5. RNA preparation and quantitative real-time polymerase chain reaction for miRNA expression

Hearts were homogenized prior to RNA extraction. Total RNA was extracted with Trizol, according to the manufacturer. RNA purity and integrity were confirmed by spectroscopy and gel electrophoresis before use. The single tube TaqMan miRNA assays (Applied Biosystems, Life Technologies) was used to detect and quantify mature miRNA-(21) according to the manufacturer, by theuse of iQ5 multicolor detection system (Bio-Rad, Berkeley, CA, USA). miRNA expression was normalized on RNU6.

2.6. Lactate dehydrogenase

Since in isolated rat hearts, ischemic PostC is known to reducethe production of lactate dehydrogenase (LDH) during reperfusion (Penna et al., 2006), the release of this enzyme was examined in each experimental group. Samples of coronary effluent were with drawn with a catheter inserted into the right ventricle via the pulmonary artery. Samples were taken during reperfusion. LDH release was measuredas as described in Penna et al. 2006. Data were expressed as cumulative values for the entire reperfusion period.

3. Antibacterial characterization of Cateslytin derived-peptide

*3.1. Preparation and characterization of the Cateslytin derived-peptides (DOPA*T*bCtl and T*bCtl)*

T*bCtl (forms L and D) and D*T*bCtl (**Figure 9**) were provided from PepMic (Suzhou, China). The purity of these peptides was tested by HPLC with a Dionex HPLC system (Ultimate 3000; Sunnyvale, USA) on a Vydac 208TP C8 column (2.1x150 mm) equipped with a pre-column Vydac 208TP (7.5x2.1 mm). The solvent system consisted of 0.1% (vol/vol) trifluoroacetic acid (TFA) in water (solvent A) and 0.1% (vol/vol) TFA in 70% acetonitrile-water (solvent B) with a flow rate of 0.2 mL/min. Gradient of elution was indicated on chromatograms and each peak was manually collected.

Each peak corresponding to the purified material was analysed by Edman sequencing on an Applied Sequencing System Procise (Applied Biosystems, Foster City, USA) (Metz-Boutigue et al., 1993a) and identified by Matrix Assisted Laser Desorption-Time Of Flight (MALDI-TOF) at the Laboratoire de Spectrométrie de Masse Bio-Organique, UMR7178 (CNRS-UDS) Strasbourg, France. The mass measurements were carried out on a Bruker

BIFLEX MALDI-TOF spectrometer (Bruker Daltonics, USA) according to the procedure previously reported (Goumon et al., 1998).

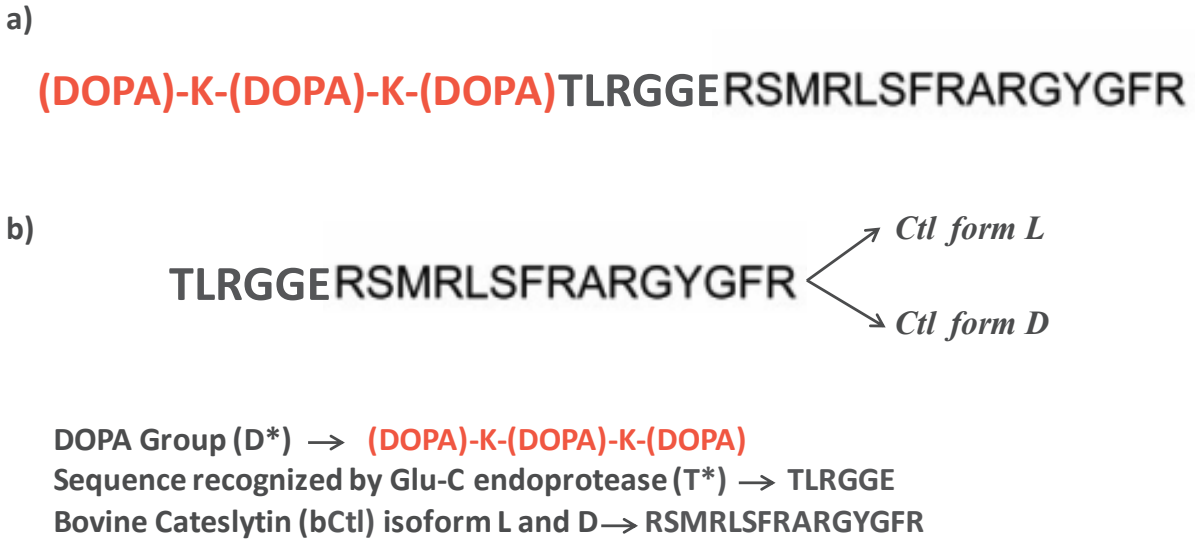

Figure 9: Sequence of Cateslytin-derived peptides: a) D*T*bCtl and b) T*bCtl.

3.2. Antibacterial assays against S. aureus

Different *S. aureus* strains provided by the Institute of Bacteriology of Strasbourg were assessed for their susceptibility to various antibiotics using the agar disc diffusion method (Goumon et al., 1998). Two methicillin sensitive *S. aureus* (MSSA), corresponding to ATCC 25923 and 49775, a methicillin resistant *S. aureus* (MRSA), corresponding to S1 isolated from the blood of an 83 y.o. patient, and a *S. aureus* V8 (strain in which was identified and characterized the endoprotease Glu-C) were tested. They were precultured aerobically at 37°C in Mueller-Hinton Broth (MHB) Medium (Becton-Dickinson Microbiology Company, Sparks, USA) pH 7.4 as previously reported (Aslam et al., 2013). Then, bacteria were suspended and diluted with MHB medium to obtain a bacterial solution in the first phase of bacterial growth with OD620 nm of 0.001. Finally, for each bacteria strain of *S. aureus*, we tested in 96-well plate (Sarstedt AG and Co., Nümbrecht,

Germany) 10 µL of peptide solutions (10-100 µM) in 90 µL of diluted bacterial solution. As positive control (100% of inhibition), it has been used a mixture of 10 µL of Tetracycline (10 µg/mL) and Cefotaxime (0.1 µg/mL) and as negative control (0% of inhibition) bacterial cultures growing without peptide. Microbial growth was assessed by the increased absorbance at OD620 nm after 24 h of incubation at 37°C. Each assay was tested in triplicates.

*3.3. Purification of the fragments resulting from Ctl derived-peptides (T*bCtl and D*T*bCtl) digestion by the endoprotease Glu-C*

Endoprotease Glu-C from *S. aureus* V8 was provided from Sigma Aldrich (Saint Louis, USA). T*bCtl and D*T*bCtl (L and D forms; 12.5 µg) were digested for 18 h at 37°C by endoprotease Glu-C (3.5 µg) in 50 mM Tris-HCl (for T*bCtl) or PBS (for D*T*bCtl) pH 8.2. Enzyme (1.75 µg) was firstly added after 20 min of incubation of the peptides at 37°C and, secondly, the same amount was added 4 h after. After 18 h the enzymatic digestion was stopped by addition of 25 µL of 0.1% (vol/vol) TFA in milliQ water. The fragments resulting from enzymatic digestion were chromatographied with a RP-HPLC with a Dionex HPLC system on a Vydac 208TP C8 column and identified by MALDI-TOF as previously reported.

*3.4. Antibacterial assays of D*T*bCtl against S. aureus after the digestion by the endoprotease Glu-C*

To have a complete study of the antibacterial action of D*T*bCtl we tested the antibacterial assays after incubation of D*T*bCtl (MIC concentration) with Glu-C. This protocol included an incubation of D*T*bCtl (75µM) in 50 µL of PBS pH8.2, at 37°C for 18 h with a ratio E/S (m/m) of 1/3.57. At the end of incubation, it has been tested the antibacterial activity against *S. aureus* V8; 50 µL of bacterial solution in the first phase of bacterial growth with OD620 nm of 0.001 were tested with digested D*T*Ctl (75 µM) in 50 µL of PBS by using a 96-well plate (Sarstedt AG and Co., Nümbrecht, Germany). As positive control (100% of inhibition) it has been used a mixture of 10 µL of Tetracycline (10 µg/mL) and Cefotaxime (0.1 µg/mL) with 40 µL of PBS pH 8.2 and 50 µL of diluted bacterial solution. As negative control (0% of inhibition), which corresponds to bacterial cultures growing without peptide, it has been used a solution with 50 µL of PBS pH 8.2 and 50 µL of diluted bacterial solution. Microbial growth was assessed by the increased absorbance at OD620 nm after 24 h of incubation at 37°C. Each assay was tested in triplicates.

3.5. Prediction of secondary structure of Ctl-derived-peptides

It has been analysed the secondary structure of the peptides by using algorithms of Expasy (http://www.expasy.org/) for GOR 4 and of PBIL Network Protein Sequence Analysis IBCP (http://npsa-prabi.ibcp.fr/) for PHD. We have selected two softwares: GOR (expasy.org) and PHD (npsa-prabi.ibcp.fr).

*3.6. Oxidation of D*T*bCtl: structural analysis and antibacterial activity*

We have oxidized the peptide D*T*bCtl (12.5 µg) in 50 µl of PBS (50 mM) pH 8.2 by Sodium Periodate ($NaIO_4$) in a 5:1 ratio of $NaIO_4$: D*T*bCtl. Furthermore, in order to evaluate the ability of oxidized D*T*bCtl to be cleaved by Glu-C it has been performed the digestion assay as previously described. The resulting product was analyzed by using the HPLC system as previously reported (paragraph 3.1).

For each collected peak the MALDI-TOF analysis was used to identify the resulting fragments. Finally, it has been evaluated the antibacterial action of the isolated oxidized form against *S. aureus* 25923 (ATCC) (MSSA), 49775 (ATCC) (MSSA), S1 (MRSA) and V8. As control, it has been analysed the properties of the oxidized Ctl.

*3.7. Stability analysis of D*T*bCtl in S. aureus supernatant and MHB medium*

S. aureus 25923 (ATCC) (MSSA) was precultured and plated on the agar plates and cultivated for 24 h at 37°C. After incubation, one colony was transferred into 10 mL of MHB medium and incubated at 37°C for about 24 h to late stationary growth phase. After incubation, cultures were centrifuged at 10,000 x g for 15 min and the supernatants were filtered using a 0.22 µM Millex-GV (Millipore, Carrigtwohill, Ireland) to eliminate bacteria. The supernatants were stored at -20°C until further use. In order to check sterility, 1 mL of supernatant was incubated at 37°C for 48 h. Absence of colony formation was interpreted as lack of viable bacteria.

In order to evaluate the stability of the peptide in the bacterial supernatant, D*T*bCtl was incubated at 37°C for 24 h with this supernatant (100 µL) at a concentration corresponding to the MIC value. Furthermore, to verify the supernatant oxidation 5 µL of β-Mercaptoethanol (redox agent) was added in the supernatant plus peptide. At the end of incubation, the samples were analyzed by Nano RP-HPLC. Under the same experimental conditions, the stability of the peptide in MHB medium has been also evaluated.

4. *In vivo treatment with CgA derived-peptides in infected rat model*

4.1 Animals

Male Wistar rats (Harlan Laboratories, Udine, Italy S.r.l.) weighting 250-350 g were housed, three per cage, in a ventilated cage rack system under standard conditions. Animals had food and water access *ad libitum*. The investigation conforms with the *Guide for the Care and Use of Laboratory Animals* published by US National Institutes of Health (NIH Publication No. 85-23, revised 1996) and to the Italian law (DL 116/92 and DL 26/14).

4.2 S. aureus infected rat models

S. aureus (Institute of Bacteriology of Strasbourg France) was frozen at -80°C in Tryptic Soy Broth with 10% glycerol (pH 7.3). Bacteria were precultured aerobically at 37°C in Mueller-Hinton Broth (MHB) Medium (Becton-Dickinson Microbiology Company, Sparks, USA) pH 7.4 as previously reported (Aslam et al., 2013). Bacterial pellets were washed with pyrogen-free phosphate-buffered saline (Invitrogen) and resuspended in a

concentration of 5 to 25x10^8 colony forming units (CFU)/mL. Bacterial counts were determined by serial-dilution plating (Knuefermann et al., 2004) and by spectrophotometric analysis (Szermer-Olearnik et al., 2014).

Rats were inoculated intraperitoneally with 1 to 5x10^8 CFU/mL of *S. aureus* (Knuefermann et al., 2004). The effects of *S. aureus* were compared with vehicle administration and subsequent studies were performed in rats treated with *S. aureus* alone (negative control), *S. aureus* plus Ctl (1.5 mg/kg, intraperitoneally) and Ctl alone (Rabbi et al., 2014).

The positive control was represented by the treatment with *S. aureus* plus Penicillin-Streptomycin (35,000 units/Kg of aqueous Penicillin plus 18 mg/Kg of Streptomycin) (Sigma-Aldrich Produktions GmbH, Steinheim, Germany) (Steigbigel et al., 1975).

All rats were anaesthetized with ethyl carbamate (2 g/Kg rat, i.p.) and killed after 12 h of *S. aureus* challenge (Knuefermann et al., 2004); plasma and hearts were harvested for both microbiological and molecular biology analysis.

4.3 Microbiological analysis

After 12 h of *S. aureus* challenge the rats were killed and blood samples were collected from the abdominal aorta with heparinized syringe. Plasma was then separated by centrifugation at 3000 *g* (15 minutes, 4°C). Immediatelly, 0.5 mL of plasma of each Group (*S. aureus, S. aureus* + antibiotics, *S. Aureus* + Ctl, and Ctl alone) was plated in agar MH Petri and the growth of bacteria was observed after 24 h of incubation at 37°C. At the same time, 50 µL of plasma was incubated with 50 µL of fresh MH broth and incubated for 24 h at 37°C in 96-well plate (Sarstedt AG and Co., Nümbrecht, Germany).

Hearts of each group were isolated in order to evaluate the cardiac infection. The cardiac tissue was homogenized in PBS and 0.5 mL of homogenate was plated in agar MH Petri. The growth of bacteria was observed after 24 h of incubation at 37°C. At the same time, 50 µL of cardiac homogenate was incubated with 50 µL of fresh broth and incubated for 24 h at 37°C in 96-well plate (Sarstedt AG and Co., Nümbrecht, Germany).

Microbial growth was assessedd by the increased absorbance at OD620 nm after 24 h of incubation at 37°C. The positive control (100% of bacterial growth) was represented by the group treated with *S. aureus* and the negative control (0% of bacterial growth) was represented by the group treated with *S. aureus* plus antibiotics after 24 h of incubation at 37°C.

4.4 Plasma analysis of proinflammatory cytokines and damage marker

Blood samples were collected as previously described and stored at -80°C until assays. Blood samples were used to measure plasma levels of TNF-α, IL-1β and LDH, as described below.

4.4.1 Enzyme-linked immunosorbent assay (ELISA)

TNF-α and IL-1β determinations were performed by using ELISA system according to manufacturer's instructions (Thermo Scientific, Rockford, USA). Plasma samples of each group were incubated with antibodies against TNF-α or IL-1β that were pre-coated on well microplates. After discarding samples, biotinylated antibodies were added and the incubation was continued. Biotinylated antibody solution was discarded and incubation

with streptavidin-HRP was continued. Finally, TMB (3,3′,5,5′-tetramethylbenzidine) solution was added and the absorbance was measured at 450 nm immediately after stopping the reaction by adding 2 M H_2SO_4.

4.4.2 Lactate dehydrogenase (LDH) determinations

LDH activity was measured in plasma samples of each group. LDH activity was determined by spectrophotometric analysis at 340 nm and expressed as IU/L (Penna et al., 2006).

The reaction was monitored spectrophotometrically by measuring the decrease in NADH at 340 nm produced in the pyruvate to lactate reaction (Vanderlinde, 1985). It was carried out in 3 mL of buffer solution (23.3 mg K_2HPO_4, 3.0 mg KH_2PO_4 and 0.21 mg Na-Pyruvate) plus 50 µL NADH (0.47 mg NADH-Na_2 and 0.50 mg $NaHCO_3$) plus 100 µL plasma samples (Penna et al., 2006).

4.5 Western blotting analysis

The hearts of each group were homogenized in ice-cold radioimmunoprecipitation assay buffer (Sigma-Aldrich, Saint Louis, USA) containing a mixture of protease inhibitors (1 mmol/L aprotinin, 20 mmol/L phenylmethylsulfonyl fluoride, and 200 mmol/L sodium orthovanadate). Then, homogenates were centrifuged at 200xg for 10 min at 4°C for debris removal. Protein concentration was determined using the Bradford reagent according to the manufacturer (Sigma-Aldrich, Saint Louis, USA). Equal amounts of proteins (40 µg) were separated on 8% SDS-PAGE gel for iNOS or on 10% SDS-PAGE gel for COX2. The gels were transferred to polyvinyl difluoride membrane, blocked with non fat dried

milk, and incubated overnight at 4°C with a polyclonal rabbit anti-iNOS antibody or a polyclonal goat anti-COX2 antibody (Santa Cruz Biotechnology, Santa Cruz, California USA) diluted 1:1000 in Tris-buffered saline and 0.2% Tween 20 containing 5% non fat dry milk. Anti-rabbit and anti-goat peroxidase-linked secondary antibodies (Santa Cruz Biotechnology, Santa Cruz, California USA) were diluted 1:2000 in Tris-buffered saline and 0.2% Tween 20 containing 5% non fat dry milk. Polyclonal rabbit anti-GAPDH antibody was used as loading controls (Santa Cruz Biotechnology, Santa Cruz, California USA) (n=2 for each group). Immunodetection was performed using an enhanced chemiluminescence kit (ECL PLUS; Amersham, Buckinghamshire, UK). Autoradiographs were obtained by exposure to X-ray films (Hyperfilm ECL; Amersham, Buckinghamshire, UK). Immunoblots were digitalized and the densitometric analysis of the bands was carried out using NIH IMAGE 1.6 (National Institutes of Health, Bethesda, Maryland) for a Macintosh computer based on 256 Gy values (0 = white; 256 = black).

5. Statistical analysis

Analysis was performed by using the Graph Pad PrismSoftware® (version 5.0; Graph Pad Software, San Diego, CA, USA) on absolute values. Data were expressed as the means ± SEM. Since each heart represents its own control, the statistical significance of differences within-group was assessed using the ANOVA test ($p<0.05$). Comparison between groups was made by using a one-way analysis of variance (ANOVA) followed by the Dunnett's Multiple Comparison test for post-hoc *t*-tests. Differences were considered to be statistically significant for $p<0.05$. The sigmoid concentration–response curves of Chr was fitted using Graph Pad PrismSoftware® (version 5.0; Graph Pad Software, San Diego, CA,

USA), and this provided, for the concentration–response curve, the log of the concentration (M) producing 50% effect (EC_{50}) of Chr.

The MIC values were reported as means ± SEM of three independent experiments. To determine significance, between different experimental tests and their respective controls, one-way ANOVA was used. Overall significance and correlation was evaluated by 4x4 factorial ANOVA for independent samples. Significance was accepted at $p<0.05$

Results

1. Basal cardiac effects and Postconditioning cardioprotective action of Chromofungin

1.1. Basal cardiac parameters

Cardiac parameters, obtained after 20 min equilibration, are 81±4 mmHg for LVP, 271±8 beats/min for HR, 5-8 mmHg for EDVP, 2502±131 mmHg/s for $+(LVdp/dt)_{max}$, -1641±66 mmHg/s for $-(LVdp/dt)_{max}$, 59±3 mm Hg for CP and Pressure perfusion is 100 mmHg. Endurance and stability of the preparations were analyzed by measuring the performance variables every 10 min, revealing that each heart was stable up to 180 minutes.

1.2. Chr effects on myocardial contractility and relaxation

A preliminary work on the frog heart bioassay revealed that the peptide CgA_{47-66}, corresponding to Chr is able to negatively modulate myocardial contractility in frog (Tota et al. 2003). Here we evaluated whether exogenous Chr directly affects the basal performance of the mammalian heart. By exposing Langendorff perfused rat cardiacpreparations to increasing concentrations (1–165 nM) of Chr for 10 min, we found that the peptide depressed myocardial contractility and relaxation. From 11 nM, the negative inotropic (decreaseof LVP and $+(LVdP/dt)_{max}$) and lusitropic (reduction of $-(LVdP/dt)_{max}$ and increased T/−t) effects were significant and were elicited without influencing CP and HR (**Figure 10**).

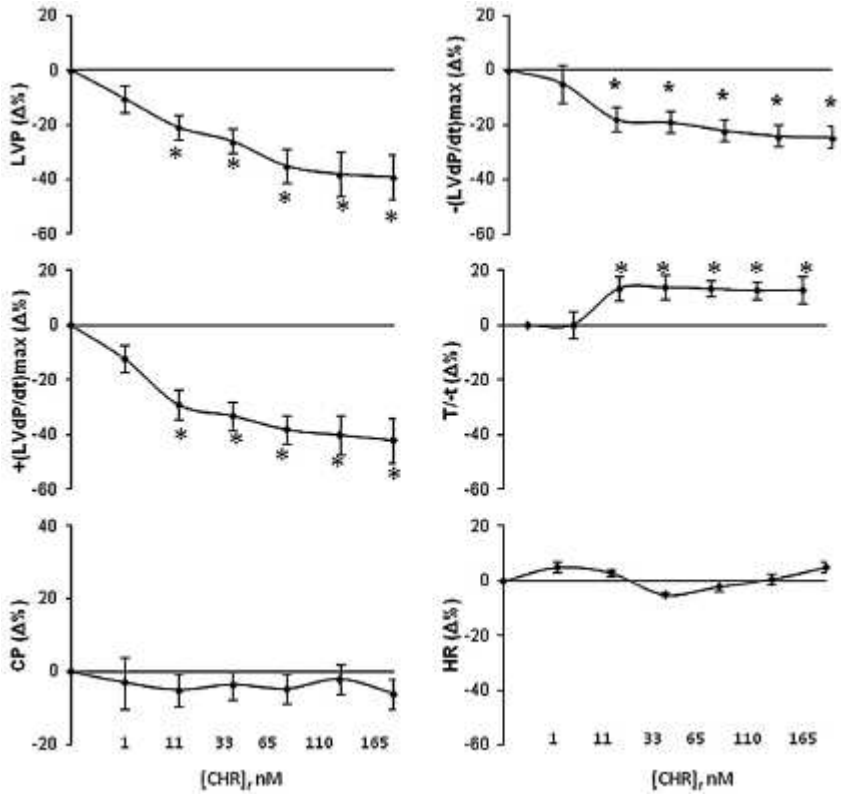

Figure 10: Concentration–response curves of increasing concentrations (1–165 nM) of Chr on LVP, $+(LVdP/dt)_{max}$, $-(LVdP/dt)_{max}$, T/−t, HR, and CP on the isolated and Langendorff perfused rat heart. Percentage changes were evaluated as means ± SEM of 8 experiments for each group. Significance of difference from control values (one-way ANOVA): *$p < 0.05$.

1.3. Mechanisms of action elicited by Chr

In mammals, nitric oxide (NO) is crucially involved in the beat-to-beat, medium- and long-term modulation of the cardiac function (Casadei and Sears, 2003). To evaluate whether the cardiac effects elicited by Chr involve NO generation, Chr-dependent negative inotropism and lusitropism were analysed in the presence of specific inhibitors of the NO pathway. Exposure to the peptide induced a decrease of LVP, $+(LVdP/dt)_{max}$ and $-(LVdP/dt)_{max}$ which was abolished by co-treatment with WT, a specific inhibitors of PI3K, or L-NIO, an selective inhibitor of eNOS, or ODQ, a specific inhibitor of CG, or KT5823, a specific inhibitor of PKG (**Figure 11a**). By ELISA assay, the increased cGMP levels were observed in cardiac extracts after exposure to Chr (65 nM) (**Figure 11b**).

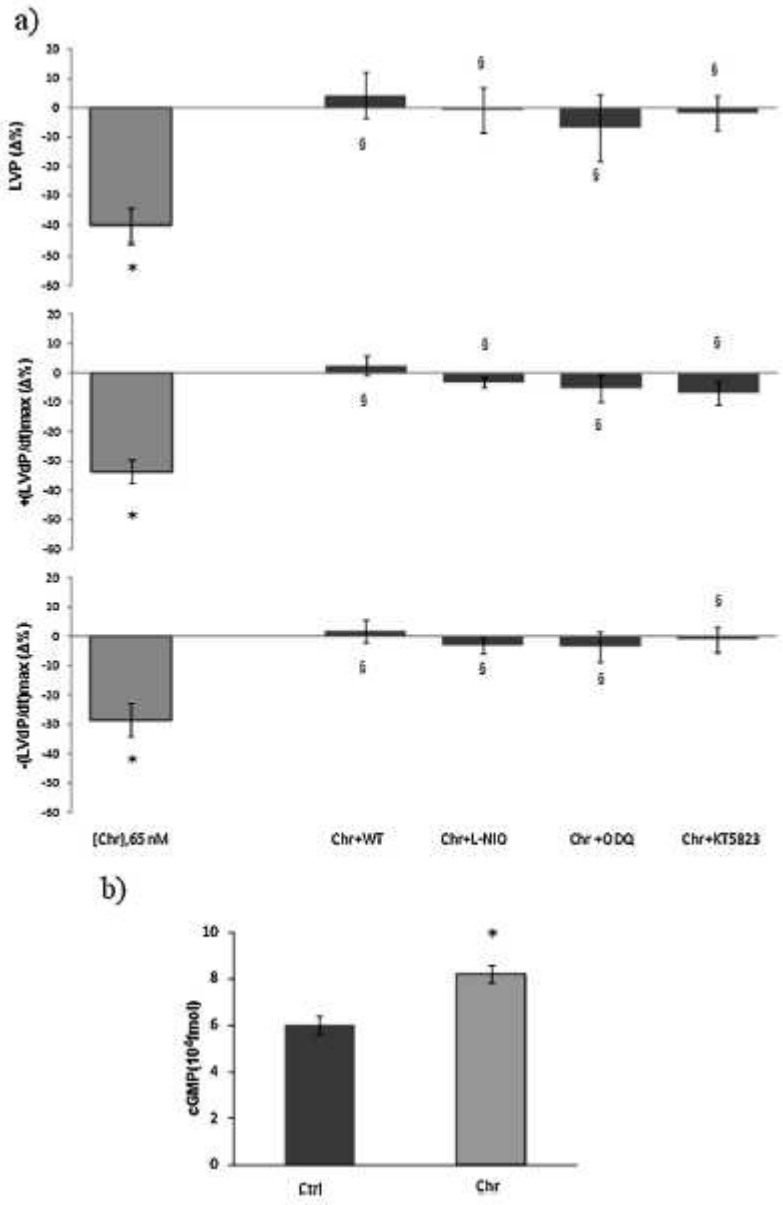

Figure 11: (a) Effects of Chr alone and in the presence of WT (100 nM), l-NIO (10 μM), ODQ (10 μM), and KT5823 (0.1 μM) on LVP, $+(LVdP/dt)_{max}$, and $-(LVdP/dt)_{max}$ on theisolated and Langendorff perfused rat heart. (b) cGMP concentrations in heart extracts. Percentage changes were evaluated as means ± SEM of 6 experiments for each group. Significance of difference (one-way ANOVA) from control values: *$p < 0.05$.

1.4. Chr effects on post-ischemic cardiac function

The possibility that Chr elicits cardioprotection was investigated by comparing the effects induced by I/R manoeuvres with those elicited by the peptide administered after I/R (PostC) (**Figure 12a**). Both systolic and diastolic functions were analysed. Although underbasal condition, Chr did not change HR, hearts undergoing I/R protocols were paced to avoid

chronotropic influences. Systolic function is represented by the level of inotropic activity (i.e., LVP recovery). Hearts of the I/R group presented a limited LVP recovery; in fact, at the end of reperfusion, LVP was 11±1.7 mm Hg (baseline values: 87.75±9.3 mmHg). Chr markedly improved LVP recovery during reperfusion, being LVP at the end of reperfusion 51±4 mm Hg (baseline values, 87.75±9.3 mm Hg) (**Figure 12b**), obtaining a recovery of performance of ~73% with respect to the control. Diastolic function is represented by the level of contracture (i.e., LVEDP 4 mmHg or more above baseline level) (Angelone et al., 2013). I/R markedly increased LVEDP (from 7.1±0.7 mmHg in the baseline to 38±10 mmHg at the end of reperfusion). During reperfusion, Chr abolished contracture development; in fact, LVEDP at the end of reperfusion was 5±0.5 mmHg (**Figures 12a and b**). Total infarct size was expressed as a percentage of LV mass. LV mass was similar in all groups (LV weight was 930±9 mg; range 500–1200 mg). Infarct size was 65±5% in I/R and 35±3% in the heart perfused with Chr (**Figure 12c**). LDH release in the I/R group was 1320±170 U/g (units per g of wet heart), while it was significantly reduced after reperfusion with Chr (820±140 U/g) (**Figure 12d**).

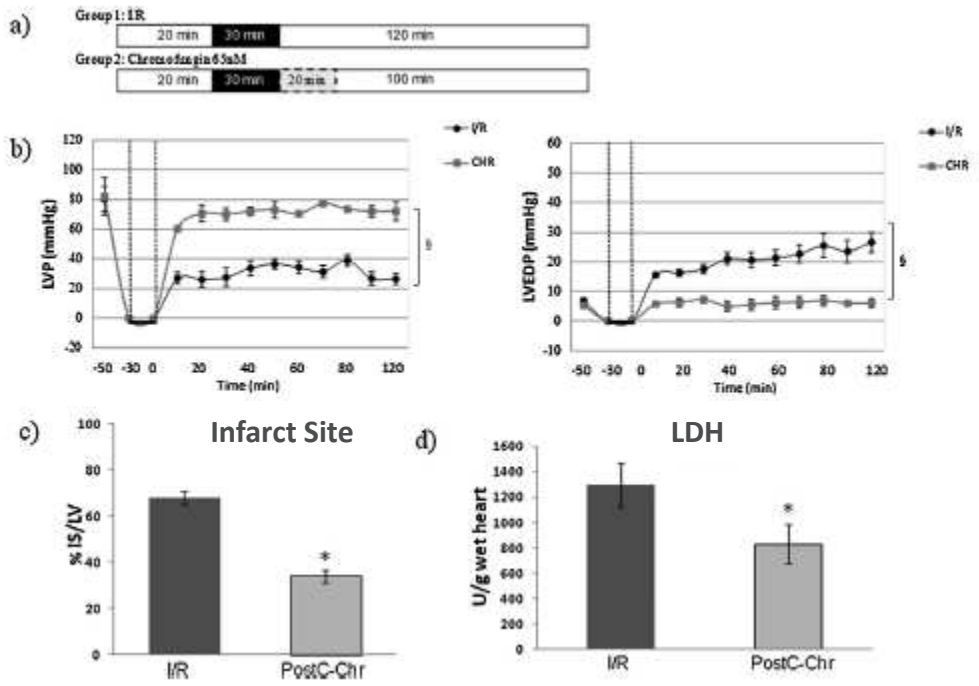

Figure 12: (a) Protocol groups. (b) LVP and LVEDP variations. Data are expressed as changes of LVP and LVEDP values (mmHg) from the stabilization to the end of the 120 min of reperfusion with respect to the baseline values for each group. Vertical lines indicate ischemic administration. Comparison between groups followed by Dunnett's MultipleComparison test: § < 0.05; (c) Infarct size. The amount of necrotic tissue measured after 30 min global ischaemia and 120 min reperfusion is expressed as percentage of left ventricle (% IS/LV): *p < 0.05 with respect to I/R. Significance of differences from control values of Chr vs I/R (one-way ANOVA): *p < 0.05; (d) Effects of Chr on LDH release. Values are expressed as means±SEM of absolute data (U/wet wt, units per g of wet heart). Significance of difference from control values (one-way ANOVA): *p < 0.05; Changes were evaluated as means ± SEM of 8 experiments for each group.

1.5. Chr influence on cardioprotective pathways

The Chr-dependent improvement of post-ischemic LVP was abolished when hearts were co-treated with Chr plus the inhibitor of PI3K (WT), or of CG (ODQ), ERK1/2 (PD), or mitoKATP channels (5HD). Also the improvement induced by Chr on contracture (LVEDP) and on infarct size were abolished by co-treatment with the above inhibitors (**Figure 13**). In hearts perfused only with inhibitors, the recovery of systolic function, the development of contracture and the infarct size were similar to those in I/R group (data not shown).

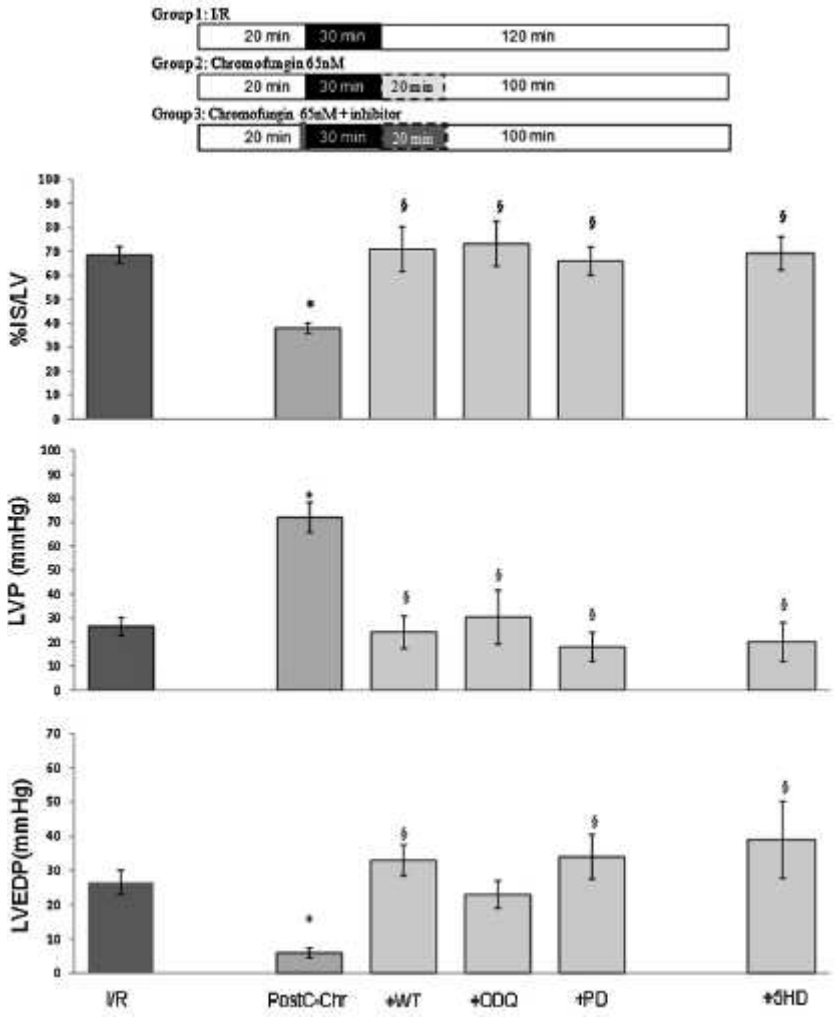

Figure 13: Infarct size, LVP and LVEDP variations of I/R, post-Chr and post-Chr plus inhibitors groups (WT; ODQ; PD; 5HD). Data are expressed as changes of IS/LV (%), of LVP and LVEDP values (mmHg) from the stabilization to the end of the 120-min of reperfusion with respect to the baseline values for each group. Percentage changes were evaluatedas means ± SEM of 6 experiments for each group. Significance of difference (one-way ANOVA): *p < 0.05. Comparison between I/R groups vs PostC-Chr; §p < 0.05. Comparison between groups followed by Dunnett's multiple comparison test.

The cardioprotection determines also an increase of cGMP intracardiac level (**Figure 14a**). miRNA-21 is an interesting candidateto inhibit apoptosis in the heart and to induce cardioprotection (Kukreja et al., 2011). To verify the involvement of miRNA-21 in Chr-dependent cardioprotection, we measured the level in I/R and PostC-Chr hearts. Results showed that, in PostC-Chr, miRNA-21 levels were statistically increased with respect to the I/R and Sham groups (**Figure 14b**), while I/R levels were not significantly different compared to the Sham group.

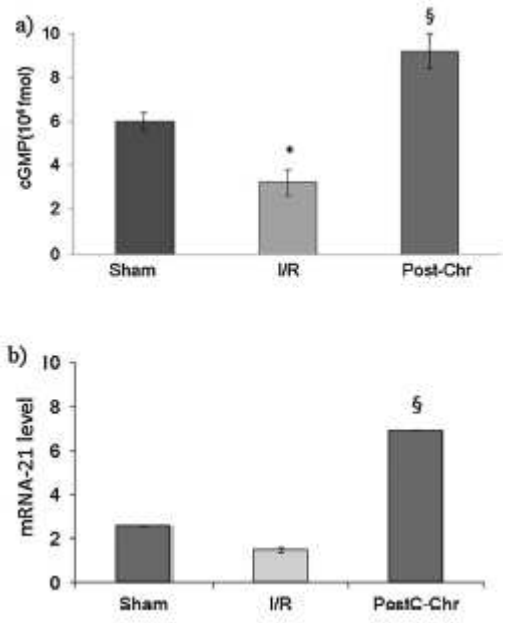

Figure 14: (a) cGMP concentrations in sham, I/R and PostC Chr heart extracts. (b) Real-Time PCR of miRNA-21 expression in Sham, I/R, and PostC Chr-treated hearts. Percentage changes were evaluated as means ± SEM of 7 experiments for each group. Significance of difference (one-way ANOVA) from control values of I/R vs Sham: *p < 0.05. Comparison between I/R groups vs PostC-Chr; §p < 0.05. Comparis onbetween groups followed by Dunnett's multiple comparison test.

2. Antimicrobial action of Cateslytin-derived peptides: coating of prosthetic heart valves to prevent infection by S. aureus

The experimental strategy used to analyse the dynamic of the interaction between D*T*bCtl and *S. aureus* includes: (1) the characterization of the antimicrobial activity of D*T*bCtl against MSSA and MRSA strains, (2) the analytical study of the D*T*bCtl proteolysis by the Glu-C protease from *S. aureus* V8 and (3) the role of oxidative conditions for the antibacterial properties of D*T*bCtl against *S. aureus* (**Figure 15**).

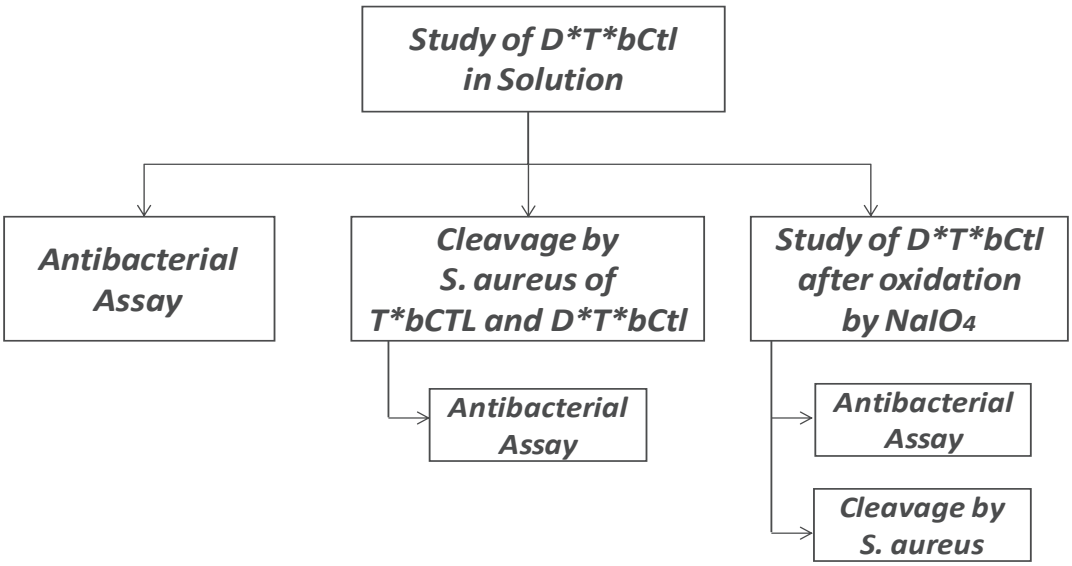

Figure 15: Experimental strategy used to characterize the interaction between D*T*bCtl and *S. aureus*.

*2.1. Antibacterial activity of D*T*bCtl against S. aureus*

Firstly, it has been examined if D*T*bCtl displayed a direct antibacterial action against *S. aureus* (MSSA and MRSA strains). bCtl is a cationic AMP with a positive charge (+5) and D*T*bCtl sequence contains two additional charges corresponding to the two additional K residues of the D* part. Thus, the presence of the residue (E) in the T* sequence, the net charge +6 may improve the interaction of this peptide with the negative charges of the phospholipids present in the bacterial membrane. It has been tested the antimicrobial action of D*T*bCtl (5 µM to 100 µM) against different strains of *S. aureus* including MRSA strain (**Figure 16**). After incubation with 50 µM of D*T*bCtl a stronger antibacterial effect for the MSSA strains 25923 and 49775 than for the MRSA strains S1 and V8 (88±1% and 94±2% *vs* 32±5% and 15±3% of inhibition) was found. However, at 70 µM, all the strains displayed strong antibacterial activity, with an inhibition of 96±1% and 100±1% for MSSA strains and 90±5% for S1 and 100±1% for V8 (**Figure 16**). All these data showed statistical significance (p<0.05).

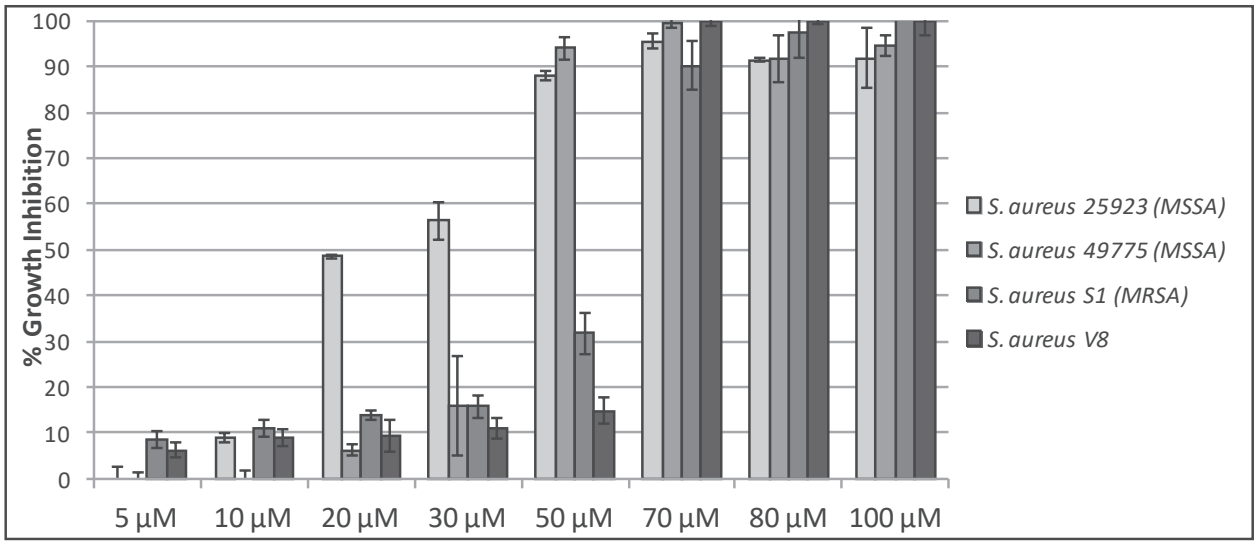

Figure 16: Antibacterial Assays of Cateslytin Derived-peptides (D*T*bCtl) against different *S. aureus* strains

*2.2. Digestion of T*bCtl (L, D) by Glu-C protease from S. aureus V8*

In order to define the experimental conditions for the enzymatic digestion we have treated 12.5 µg of T*bCtl (L) (**Figure 9**) with 3.5 µg of Glu-C protease in 50 mM Tris-HCl pH 8.2 for 18 h at 37°C. After digestion, the resulting peptides were isolated by using reverse HPLC (**Figure 17a**). 3 peaks at 18.0 min, 19.9 min and 21.9 min were isolated and by MALDI-TOF analysis it has been found, respectively, the sequence ARGYGFR (826.457 Da) for peak 1, TLRGG (501.067 Da) for peak 2 and RSMRLSFR (1052.655 Da) for peak 3. The fragment TLRGG resulted from the lost of the C-terminal E residue during MALDI-TOF analysis. The identification of the fragment RSMRLSFR demonstrated the clivage between E and R. From these results, we can conclude that the enzyme acts at the expected site (E-R), but that an additional clivage site (R-A) was obtained at the middle of the bCtl (L) sequence, preventing the release of the complete active bCtl (L).

To prevent this secondary clivage it has been studied the digestion by Glu-C protease of the most stable isoform T*bCtl (D). After separation by HPLC, two peaks eluted at 24.4 and 24.6 min, respectively, were found. MALDI-TOF analysis indicated that peak 1 corresponds

to bCtl (D) (1860.08 Da), and peak 2 to a mixture of T*bCtl (2473.48 Da). Adsorbance monitored at 214 nm revealed a release of bCtl (D) isoform (50-60%) from T*bCtl (D) (**Figure 17b**).

*2.3. Digestion of D*T*bCtl by Glu-C protease from S. aureus V8*

Glu-C digestion of D*T*bCtl was performed for 4 h, 6 h, and 18 h. The resulting peptides were isolated by using HPLC and a similar profile was obtained after the three times of incubation. Nine peaks, eluted respectively at 18.2 min, 18.8 min, 20.0 min, 21.0 min, 21.5 min, 22.0 min, 23.2 min, 24.3 min, and 25.2 min (**Figure 17c),** were identified by the MALDI-TOF analysis.

Peak 1 (826.42 Da) corresponds to D* (812 Da) with addition of 1 oxidation. Peak 2 (1425.76 Da) corresponds to D*T*. Peak 3 was characterized as a complex mixture including D*T* (1426.03 Da and 1449.99 Da with addition of 1 sodium ion) and different oxidized forms of D* (861.31 Da, 877.24 Da, 893.25 Da, 909.21 Da). Peak 4 corresponds to D*TL with addition of 1 oxidation and 1 sodium ion (1068.60 Da). The minor peak 5 was not identified and peak 6 corresponds to a mixture of D*TL with addition of 1 sodium ion (1052.63 Da) and D*TL with addition of 1 oxidation and 1 sodium ion (1068.52 Da). The peak 7 corresponds to bCtl with addition of 1 oxidation (1875.97 Da) and the peak 8 corresponds to bCtl with addition of a sodium ion (1881.36 Da). The complete D*T*bCtl with addition of 1 oxidation (3282.83 Da) was eluted as peak 9. By using the OD214nm, we evaluated a release of bCtl to 90% from D*T*bCtl. This data suggests that for D*T*bCtl the cleavage site is more accessible to the enzyme than for T*bCtl.

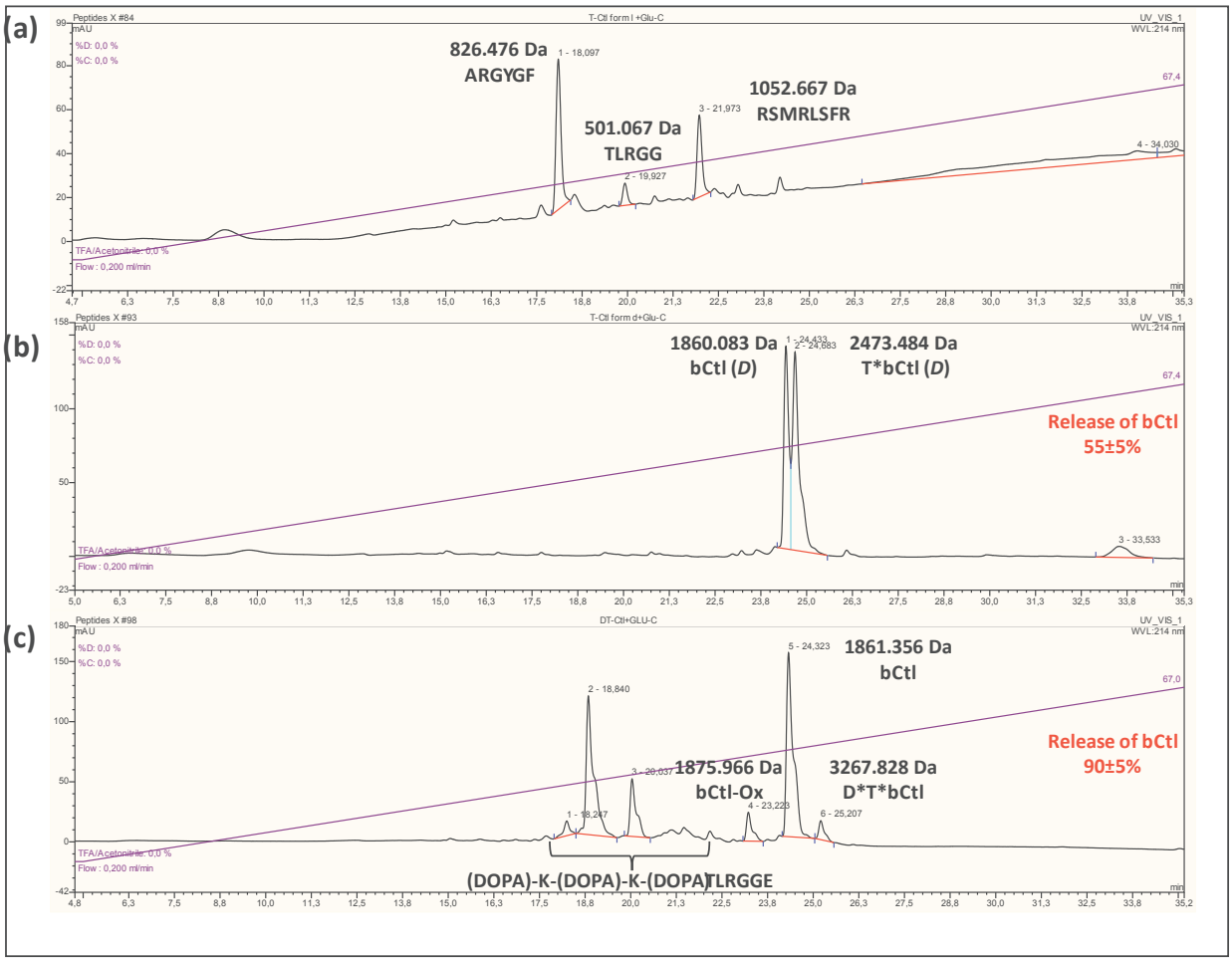

Figure 17: *In vitro* Glu-C cleavage assays of Cateslytin derived-peptides**:** (a) T*Ctl *form L;* (b) T*Ctl *form D;* (c) D*T*Ctl.

2.4. Released Ctl from Glu-C cleavage and antibacterial effect against S. aureus

Finally, we tested the D*T*Ctl antibacterial activity against *S. aureus* V8 strain (able to produce the Glu-C protease) after Glu-C digestion for both 6 h and 18 h.

D*T*bCtl digested at 75 µM (MIC) after 18 h (total time of the *in vitro* protocol) was able to kill *S. aureus* V8 with an inhibitory effect of 99±5%, (**Figure 18**), but, interestingly, after 6 h of incubation with Glu-C it has been obtained an inhibitory effect of 96±2% (**Figure 18**). All these data showed statistical significance (p<0.05).

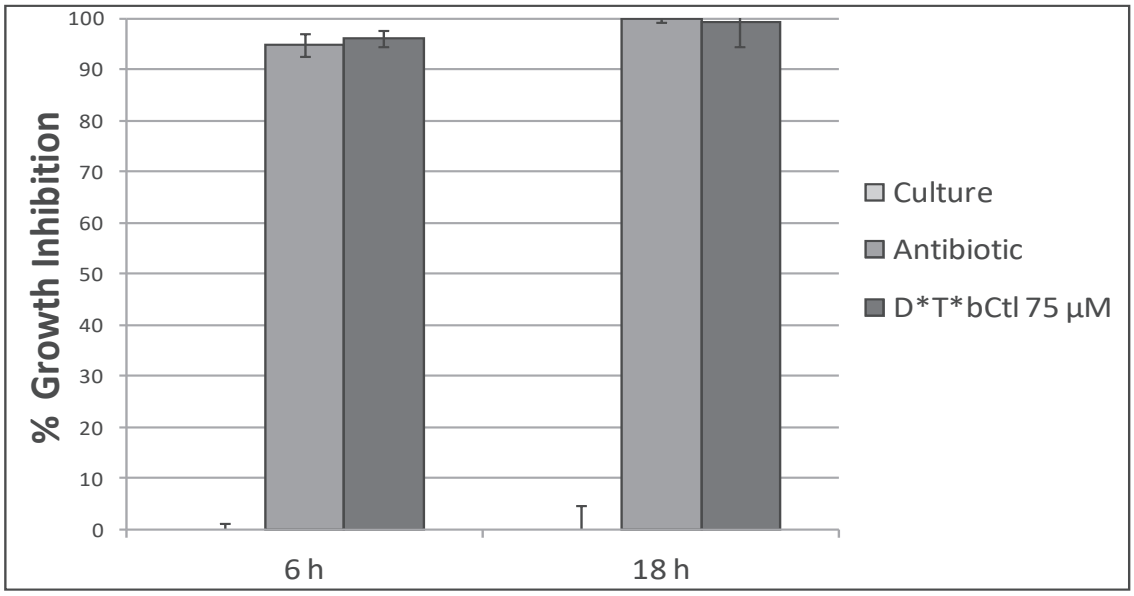

Figure 18: Antibacterial assays of D*T*bCtl after incubation with Glu-C against *S. aureus* V8.

2.5. Different secondary structure/different cleavage of Ctl-derived peptides

In order to understand because the addition of Dopa group improved the stability of the Ctl and allowed a better accessibility to the expected cleavage site, we have analysed predictions of secondary structures. We found that D*T*Ctl possesses in the central structure a longer α helix form (10 aa: RSMRLSFRAR, i.e. 38.46% of the entire sequence by GOR, and 9 aa: RSMRLSFRA, i.e. 34.62% of the entire sequence by PHD) than T*Ctl form *L* (8 aa: MRLSFRA, i.e. 38.10% of the entire sequence by GOR, and 0 aa, i.e. 0% of the entire sequence by PHD) (**Figure 19**). For T*Ctl form *D*, the possible secondary structure is the same of form *L*, but the *D* form resists to the enzymatic proteolysis.

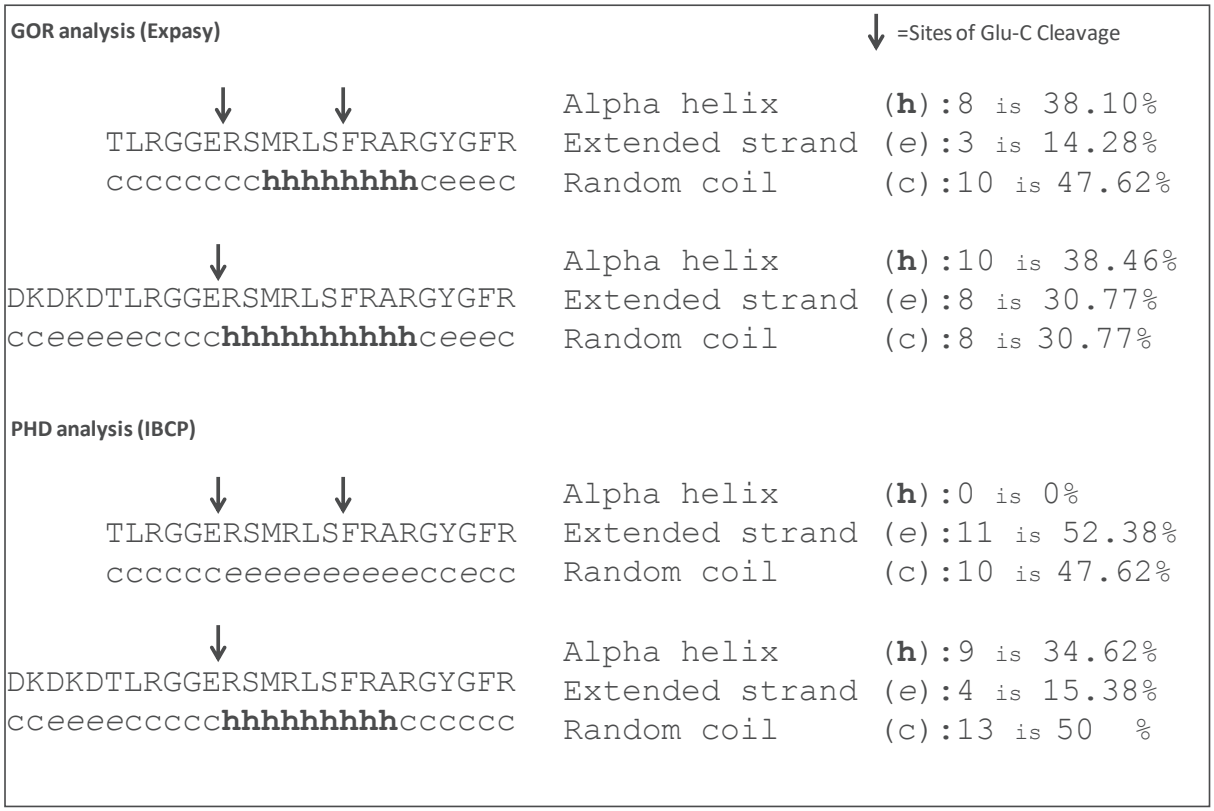

Figure 19: Prediction of secondary structure of Ctl-derived-peptides by GOR and PHD.

*2.6. The oxidation of D*T*Ctl induces the formation of inactive aggregates*

A very important step to cover a biomaterial surface with Dopamine is its oxidation (Ponzio et al., 2014). In our synthetic peptide, this oxidation activates the DOPA group allowing the linkage of peptide with all materials. In order to complete the experiments previously realized in solution, it has been tested the oxidized form of D*T*Ctl for antibacterial and Glu-C cleavage assays to clarify the effect of oxidation on the production of bCtl by digestion of D*T*bCtl by Glu-C protease. Oxidation was performed according to the procedure reported in Materials and Methods.

The oxidation process of D*T*bCtl (3.3 mg) was obtained by using sodium periodate ($NaIO_4$; 1.1mg). After a rapid incubation for 1 min in 50 mM Tris-HCl, it has been analysed

the oxidized material by using HPLC and MALDI TOF. While in the non-oxidized D*T*bCtl only 1 peak at 44 min was eluted, in the oxidized D*T*bCtl 3 peaks were detected **(Figure 20a**). Peak 1 corresponds to a mixture of D*T*bCtl (L) (with addition of 1 oxidation and 1 sodium ion) (3308.91 Da) and a dimeric form of D*T*bCtl (L) (with addition of 2 oxidations; 6567.91 Da). Peak 2 corresponds to a mixture of D*T*bCtl (L) (with addition of 1 oxidation; 3282.63 Da), a dimeric form of D*T*bCtl (L) (with addition of 1 sodium ion; 6559.52 Da), a trimeric form of D*T*bCtl (L) (with addition of 1 sodium ion; 9871.27 Da) and a tetrameric form of D*T*bCtl (L) (with addition of 1 oxidation; 13136.29). Peak 3 corresponds to a mixture of D*T*bCtl (L) (with addition of 1 oxidation; 3281.10 Da), a dimeric form of D*T*bCtl (L) (with addition of 2 oxidations and 1 sodium ion; 6588.43 Da), and a trimeric form of D*T*bCtl (L) (with addition of 3 oxidations; 9844.57 Da).

Then, we have incubated the oxidized form of D*T*bCtl with Glu-C endoprotease and analyzed the resulting fragments by HPLC. No fragments were detected, suggesting that the aggregation blocked the proteolytic digestion. This may indicate that accessibility of the peptide by the enzyme is prevented in the aggregated forms **(Figure 20b)**.

Finally, we have also tested the antibacterial action of D*T*bCtl (L) against *S. aureus* 25923 (ATCC) (SSA), *S. aureus* 49775 (ATCC) (SSA), *S. aureus* S1 (MRSA) and *S. aureus*. Of note, $NaIO_4$ used for oxidation, was unable do display antibacterial action.

The aggregated oxidized forms of D*T*bCtl (L) were unable to display complete antibacterial activity at a concentration lower than 200 μM (**Figure 20c**).

The comparison with non oxidized D*T*bCtl (L) is reported in **Figure 16.** At 70 μM for the strains 25923 (SSA), 49775 (SSA) and V8 it has been obtained, respectively, an inhibitory action of 38±4%, 5±2% and 6±2%, and no inhibition for S1 (MRSA). In contrast, at 70 μM non oxidized D*T*bCtl (L) inhibited the different strains.

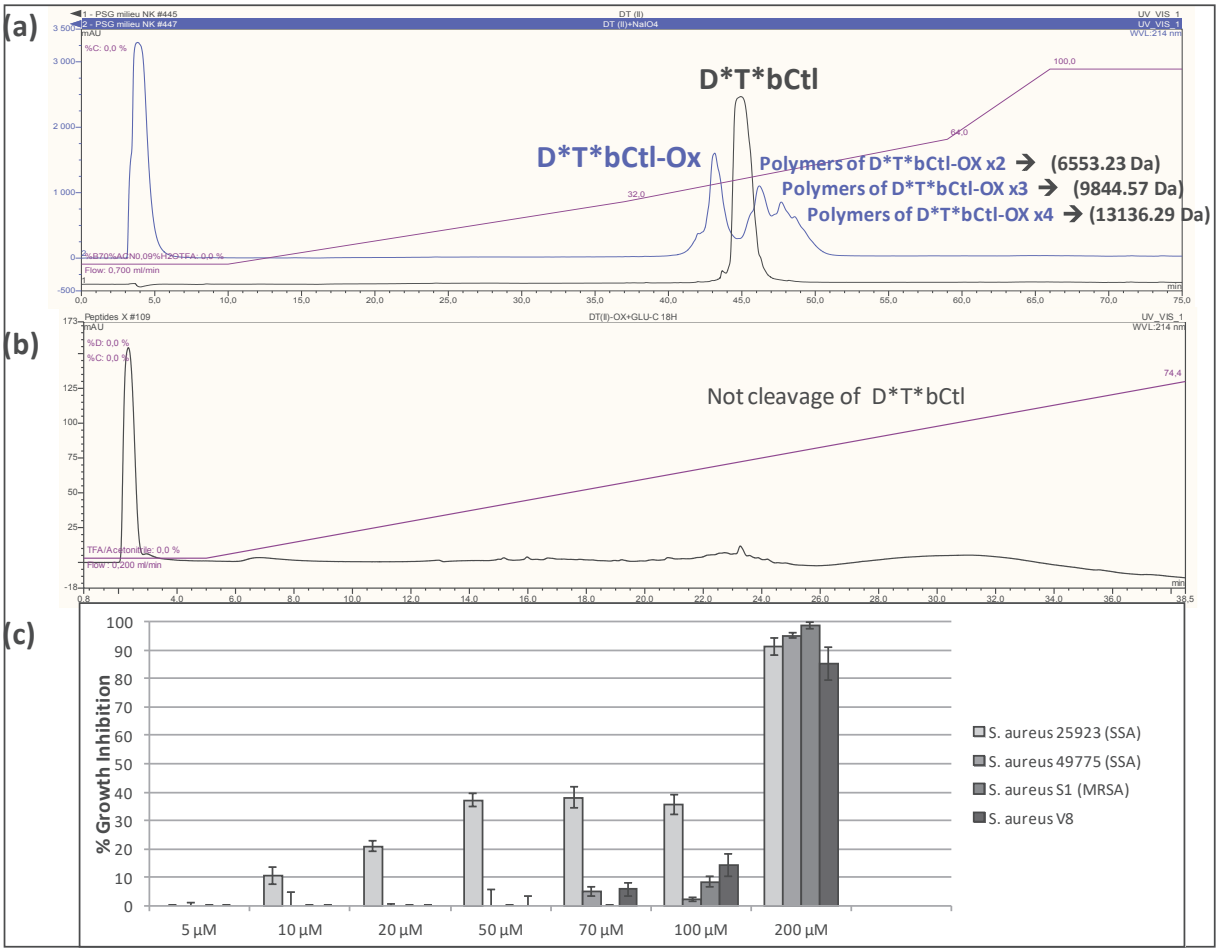

Figure 20: Characterization of D*T*bCtl in oxidizing condition: (a) HPLC profile D*T*bCtl/D*T*bCtl-Ox; (b) Glu-C Cleavage Assay D*T*bCtl-Ox; (c) Antibacterial Assay of D*T*bCtl-Ox against *S. aureus*.

The oxidized form of D*T*bCtl was also analyzed in presence of Muller-Hinton Broth medium and *S. aureus* 25923 supernatant. It has been found that, in the HPLC profile of the oxidized D*T*bCtl, in presence of supernantant, the normal peak of D*T*Ctl HPLC disappeared (**Figure 21a**), but when β-Mercaptoethanol (a strong anti-oxidation agent) was added in supernatant, low amounts of D*T*bCtl peaks (normal and oxidized form) were detected (**Figure 21b**). The aggregated was identified in the first big peak of supernatant HPLC profile (around 4 min). The same data were obtained for the incubation of oxidized D*T*bCtl in MHB medium analysis (data not shown). Furthermore, interestingly, the oxidized form of Ctl maintained its antimicrobial properties.

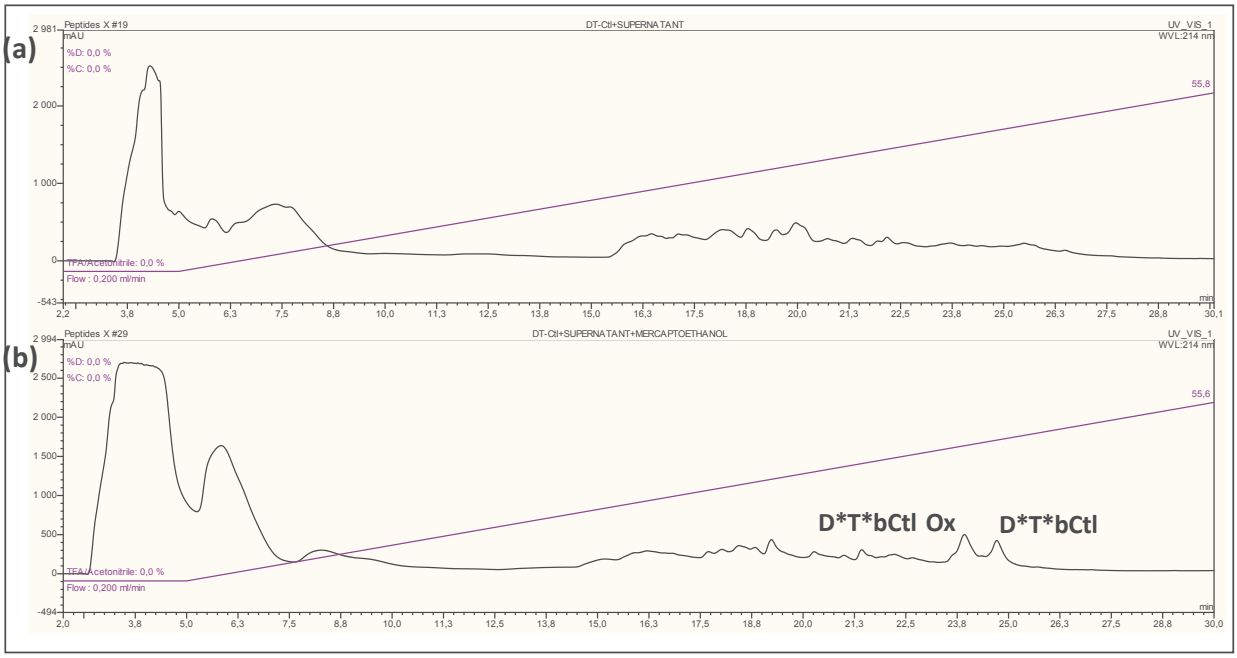

Figure 21: Stability analysis of D*T*bCtl in *S. aureus* supernatant: (a) D*T*bCtl+Supernatant; (b) D*T*bCtl+Supernatant+Mercaptoethanol.

3. In vivo antimicrobial activity of Cateslytin against S. aureus

3.1. In vivo antibacterial action of Ctl against S. aureus in infected rat model

In the present study it has been examined the antibacterial activity of bovine Ctl against *S. aureus* in an infected rat model (Knuefermann et al., 2004). In *in vitro* studies, Ctl was found to be most active against differents *S. aureus* strains in comparison with the other CgA derived-peptides with a MIC value between 37–45 μg/mL (21 μM) (Aslam et al., 2013).

The effects of *S. aureus* were compared with vehicle administration and subsequent studies were performed in rats intraperitoneally treated with *S. aureus* alone (negative control), *S. aureus* plus Ctl (1.5 mg/kg) and Ctl (1.5 mg/kg) alone (Rabbi et al., 2014). The positive control was represented by animals treated with *S. aureus* plus Penicillin-Streptomycin

(35,000 units/Kg of aqueous Penicillin plus 18 mg/Kg of Streptomycin) (Sigma-Aldrich Produktions GmbH, Steinheim, Germany) (Steigbigel et al., 1975). For each group 4 rats were treated.

For each animal, 0.5 mL of plasma was plated in agar MH Petri and the growth of bacteria was observed after 24 h of incubation at 37°C. At the same time, 50 µL of plasma was incubated with 50 µL of fresh MH broth and incubated for 24 h at 37°C in 96-well plate (Sarstedt AG and Co., Nümbrecht, Germany).

In addition, the hearts of each group were isolated to evaluate the cardiac infection. The cardiac tissue was homogenized in PBS and bacterial growth was analyzed as previously described for plasma.

As shown in **Figure 22**, Ctl 1.5 mg/Kg was able to act against *S. aureus* inducing *in vivo* antibacterial effect. It was demonstrated that co-treatment with Ctl reduced the bacterial growth in MH agar petri. No bacterial growth was observed in the plasma of group treated with peptide alone (**Figure 22a**). The same results have been observed in microbiological analysis of the cardiac homogenates (**Figure 22b**).

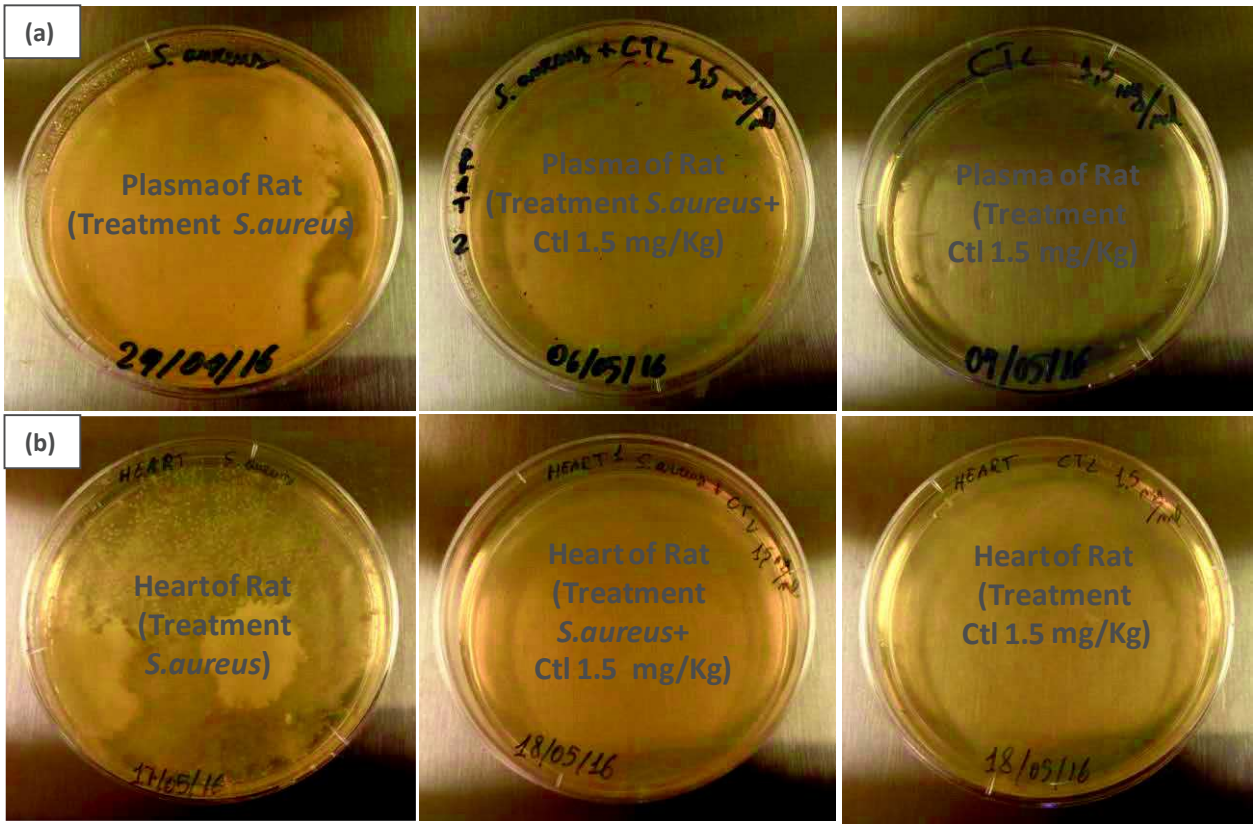

Figure 22: Microbiological Analysis: (a) Plasma and (b) Hearts Homogenates after incubation in Petri at 37°C for 24h of group treated with *S. aureus, S. aureus*+Ctl and Ctl alone.

Quantitative analysis of antibacterial action was made by adding fresh MH medium and incubating plasma and heart homogenates for 24 h at 37 °C. The spectrophotometric analysis at 620 nm showed a percentage of bacterial growth of 95±1% in plasma of rats treated with *S. aureus*. In contrast, in the *S. aureus*+Ctl group we observed a bacterial growth of 9±1% and in the group treated with Ctl alone no growth was observed (**Figure 23a**).

Similarly, the analysis showed a bacterial growth of 87±8% in heart homogenates of rats treated with *S. aureus*, a bacterial growth of 9±7% in the *S. aureus*+Ctl group and a growth of 10±8% in the Ctl alone group (**Figure 23b**).

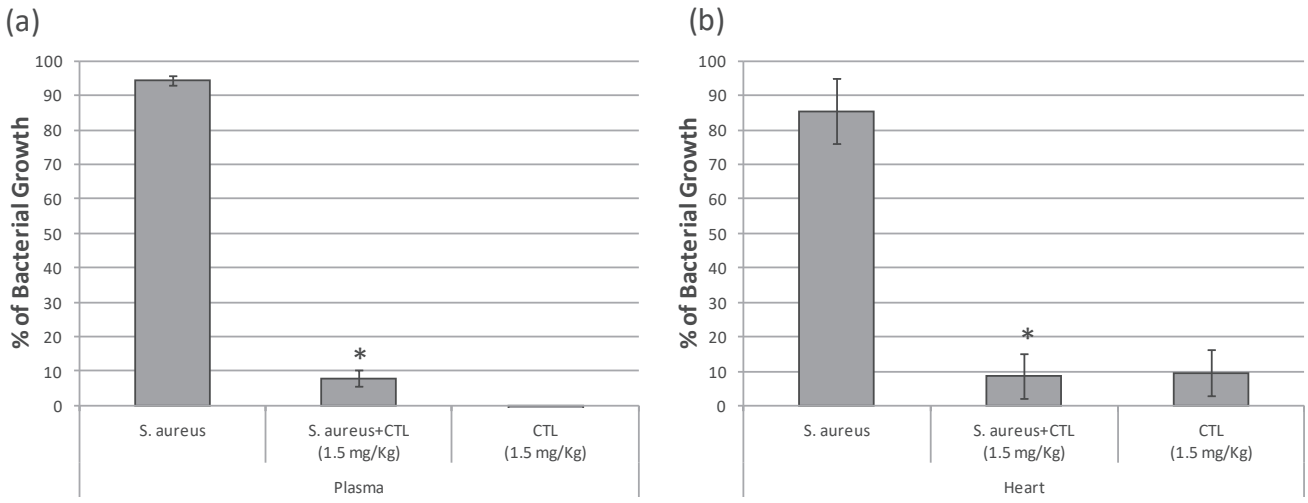

Figure 23: Antibacterial analysis (% of Bacterial Growth): (a) Plasma and (b) Hearts Homogenates after incubation in MH medium at 37°C for 24h of group treated with *S. aureus*, *S. aureus*+Ctl and Ctl alone (Optical Density 620 nm). Comparison between *S. aureus* groups vs *S. aureus*+Ctl was made by Newman-Keuls Multiple Comparison Test (*p< 0.05); n=4.

3.2. In vivo anti-inflammatory action of Ctl in S. aureus infected rat model

Increased expression of tumor necrosis factor (TNF) and interleukin-1β (IL-1β) occurs in experimental sepsis (Knuefermann et al., 2004; Haziotet al., 1999). Several data show that the clearance of *S. aureus* and the plasmatic levels of TNF-α and IL-1β levels are high in both CD14-deficient and wild-type mice after a challenge with *S. aureus*, indicating that these cytokines are markers of inflammation induced by these gram-positive bacteria (Haziot et al., 1999). Based on the anti-inflammatory action and modulation of intestinal inflammation of Cts during colitis (Rabbi et al., 2014) it has been evaluated in each group the state of systemic inflammation by monitoring the levels of plasma TNF-α and IL-1β, two of the main pro-inflammatory cytokines (Knuefermann et al., 2004) (**Figures 24b,c**). The level of plasma LDH as systemic damage index (Cofiell et al., 2015) has been also evaluated (**Figure 24a**).

In the Control group (Saline Solution), LDH plasma level was 121±69 UI/L. The treatment with *S. aureus* induced a significant increase of LDH up to 1041±66 UI/L, while co-treatment *S. aureus* plus Ctl showed a significant reduction (555±200 UI/L). In the group treated with Ctl alone, LDH plasma level was 425±132 UI/L (**Figure 24a**). For TNF-α, in the Control group (Saline Solution), plasma level was 7.8±3.2 pg/mL. The treatment with *S. aureus* induced a significant increase of TNF-α (55.6±17.9 pg/mL), while co-treatment *S. aureus* plus Ctl showed a significant reduction reaching 10.4±3.4 pg/mL. In the group treated with Ctl alone, TNF-α plasma level was 9.8±7.1 pg/mL (**Figure 24b**). The same trend was observed for IL-1β, in fact in the Control group (Saline Solution), plasma level was 11.8±3.4 pg/mL. The treatment with *S. aureus* induced a significant increase of IL-1β and the value measured was 121.5±32.3 pg/mL, while co-treatment *S. aureus* plus Ctl showed a significant reduction of IL-1β (32.4±19.5 pg/mL). In the group treated with Ctl alone IL-1β plasma level was 20.4±10.5 pg/mL (**Figure 24c**). On the whole, these results have demonstrated that, in rat, Ctl (1.5 mg/Kg) during *S. aureus* infection reduces systemic inflammation decreasing the production of pro-inflammatory cytokines such as TNF-α and IL-1β; in addition, LDH plasma levels were also reduced by Ctl treatment.

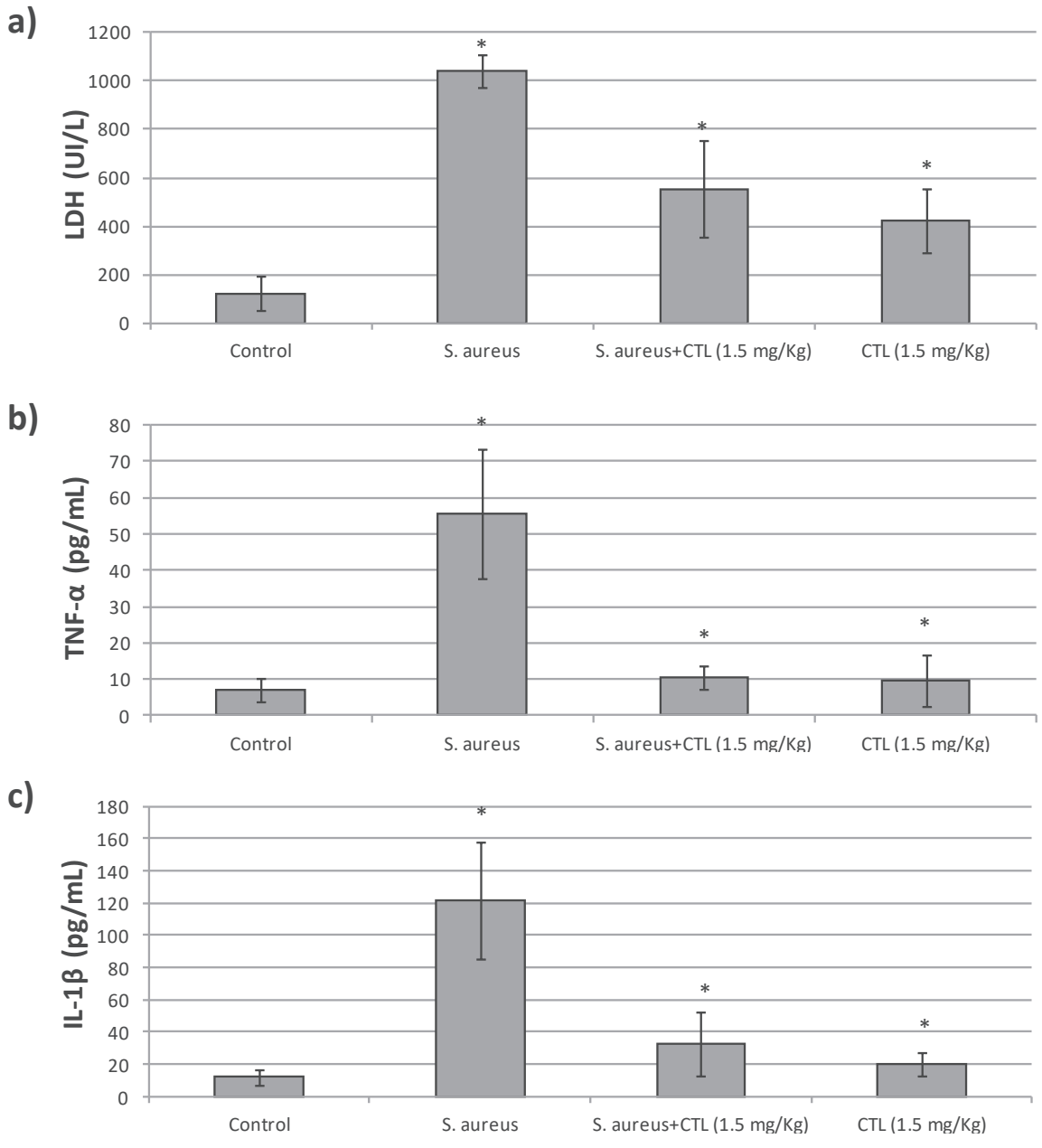

Figure 24: Plasma Level of LDH (a), TNF-α (b) and IL-1β (c) of rat treated with Saline Solution (Control), *S. aureus*, *S. aureus* +Ctl and Ctl only. Newman-Keuls Multiple Comparison Test: (n=4) (*p< 0.05) Control vs *S. aureus*; *S. aureus*+Ctl vs *S. aureus*; *S. aureus* vs Ctl.

3.3. Mechanisms of action elicited by Ctl against S. aureus-induced cardiac inflammation

There is a large consensus that cytokines contribute to cardiac decompensation in human sepsis by the activation of tissue inflammatory pathways (Kumar et al., 1996; Cain et al., 1999). During cardiac infection the major mediators of inflammation are iNOS and COX-2 (Aoki and Narumiya, 2012). To verify the involvement of inflammatory mediators in *S. aureus*-induced cardiac infection, the cardiac homogenates of rats treated with vehicle (Control), *S. aureus* alone, *S. aureus* plus Ctl, and Ctl alone were subjected to Western blotting to evaluate the expression of iNOS and COX-2.

An increased expression of both iNOS and COX-2 was reported in the rat hearts treated with *S. aureus* compared to Control (**Figure 25**). Moreover, their expression appeared significantly lower in the hearts co-treated with *S. aureus* plus Ctl than those treated with *S. aureus* alone. In addition, a significant decreased expression of COX-2 was observed in the Ctl-treated group respect to the control (**Figure 25**).

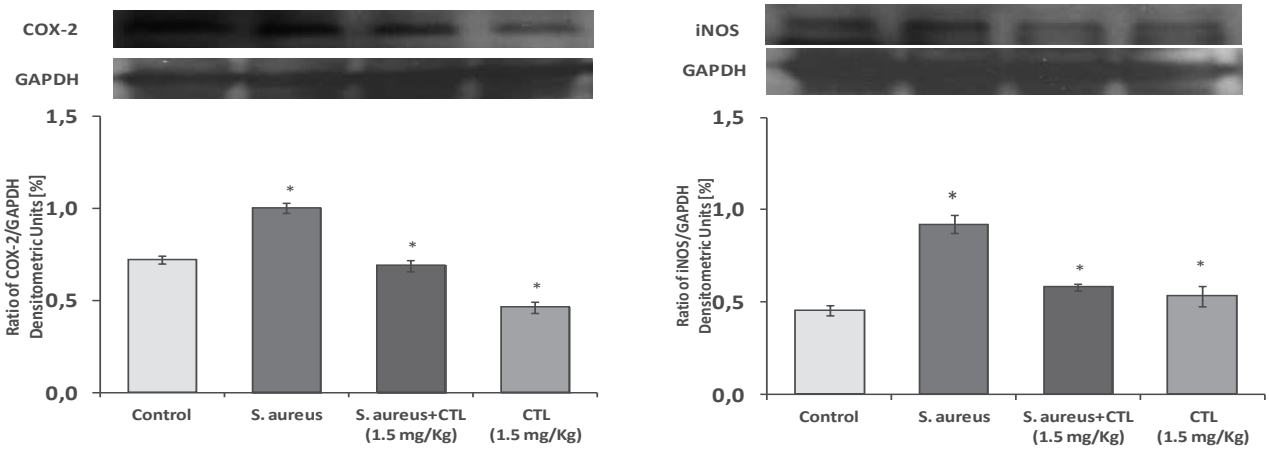

Figure 25: Western Blots and relative densitometric analysis of iNOS and COX-2 in Not Perfused Heart extracts. Newman-Keuls Multiple Comparison Test: (n=2) (*p< 0.05): Control vs *S. aureus*; *S. aureus*+Ctl vs *S. aureus*; *S. aureus* vs Ctl.

Discussion

In this doctoral thesis it has been report that two CgA derived-peptides, Chr (CgA_{47-66}) and Ctl ($CgA_{344-358}$) play important roles in the response to stress stimuli in both immune and cardiovascular system.

Our research has shown, for the first time, the role of antimicrobial Chr in the cardiac system. This peptide, through a PI3K-Akt-NO-cGMP-PKG pathway affects the basal cardiac parameters inducing negative inotropic and lusitropic effects without changing HR and CP. Furthermore, Chr acts as a Post-conditioning-like cardioprotective molecule with an involvement of the RISK pathway and an increased production of miRNA-21.

In a second step we have designed and characterized a new Ctl-derived peptide (D*T*bCtl) to cover artificial heart valves and prevent infection by *S. aureus*. *In vitro,* this synthetic peptide displays antibacterial action against different strains of *S. aureus*, and it is able to be cleaved by a specific protease of *S. aureus* (Glu-C) releasing active Ctl in presence of *S. aureus*.

In a third part, it has been demonstrated, *in vivo,* the antimicrobial action of Ctl against *S. aureus*. This peptide completely blocked the systemic and cardiac infection induced by *S. aureus*, killing the bacteria at plasma and cardiac level. The same treatment reduced the systemic inflammatory state decreasing TNF-α, IL-1β, and LDH plasma levels in infected rats treated with Ctl. Furthermore, in cardiac extracts Ctl treatment reduced expression of pro-inflammatory markers such as iNOS and COX-2.

1. Cardioinhibitory and cardioprotective effects of Chr

We have demonstrated that Chr (CgA_{47-66}) directly affects the performance of the isolated and Langendorff perfused rat heart by dose-dependently inducing negative inotropism and lusitropism and involving the AKT/NOS/cGMP/PKG pathway. Chr also protected against

I/R injury, acting as a post conditioning agent through activation of RISK pathways and mito KATP channels. On the isolated and Langendorff perfused rat heart, we observed that exogenous Chr elicited negative inotropism and lusitropism starting from 11 nM. Under un stimulated conditions, it significantly reduced LVP, and $+(LVdP/dt)_{max}$ (indexes of inotropism), and $(LVdP/dt)_{max}$ and T/−t (indexes of lusitropism), without affecting HR and CP. These effects were obtained at Chr concentrations close to the physiological range of its precursor, CgA, in human serum (normal levels: 0.5–4 nM; neuroendocrine tumors and last stages of chronic heart failure: 100 nM) (Helle et al., 2007). In our study, we reported for the first time the direct effects induced by Chr on the mammalian heart. With respect to the data reported on the frog heart (Tota et al, 2003), we demonstrated in the rat that Chr reduced not only contractility (~40% rat vs ~18% in frog), but also relaxation without changing heart rate. The negative inotropic and lusitropic effects induced by Chr (~40%) resemble the cardiodepression elicited on the rat heart by human recombinant (hrVs-I) (~20%) which includes the vasostatin-1 domain and Chr sequence (Cerra et al., 2006). This highlights the contractile properties of the CgA N-terminal domain. Cerra et al. reported that the negative inotropism and lusitropism of the N-terminal domain are confined to the CgA_{1-64} region, since rat CgA_{65-76} failed to modify the basal inotropism (Cerra et al., 2008). A previous study reported that by endogenous proteolytic degradation of Vs-I, the two fragments CgA_{1-64} and CgA_{65-76} are produced and secreted with catecholamines during stress situations (Lugardon et al., 2001). At the same time, it was reported that rat CgA_{1-64} induces coronary vasodilatation (Cerra et al., 2008). This effect is in contrast with the increase of coronary activity induced on the rat heart by human recombinant Vs-I, containing Chr (Cerra et al., 2006). Here we found that Chr did not change rat coronary reactivity. Accordingly, although Vs-I and Chr elicit similar effects on myocardial contractility and relaxation, sequence specific vascular activities may account for the observed differences in coronary responses.

Of note, a strong structure-function relationship has been demonstrated for CgA-derived peptides suggesting that different fragments may display different cardioactive potency. In addition, Chr is not completely included in CgA_{1-64} and we have previously shown by using the helical wheel prediction of secondary structure that sequence CgA_{53-66} presents a longer hydrophobic domain than CgA_{53-64} (Helle et al., 2007). The presence of classic receptor-ligand interaction which mediate the cardiac effects of Chromogranin-derived peptides remains elusive. At the moment, only the presence of binding sites for both vasostatins and their fragments (i.e., CgA_{1-40} and CgA_{47-66}) in calf aorta vascular smooth muscle and bovine parathyroid cell was suggested (Cerra et al., 2006). In addition, Metz-Boutigue et al. in 2003 reported that these peptides exert antibacterial and antifungal effects by penetrating into, or interacting with, the cell membrane through hydrophobic interactions between specific domains of the peptides and spatially localized regions of the lipid bilayer with consequent modulation of cellular effectors (Metz-Boutigue et al., 2003). In particular, an increase of peptide penetration is observed for the presence of ergosterol, the main sterol in yeast and fungus plasma membrane (Metz-Boutigue et al., 2003). Our study revealed that, as for full length CgA (Pasqua et al., 2013) and other CgA-derived inhibitory fragments, Vs-I and Cts (Cerra et al., 2006; Cappello et al., 2007; Anglone et al., 2008), the effects induced by Chr involve the AKT/NOS-NO/cGMP signal transduction pathway. In fact, Chr exposure increased AKT and eNOS phosphorylation, thus activating the NO-generating cascade. This promotes cGMP production by soluble guanylate cyclase (sGC), with final depressant effects on contractility and relaxation. As demonstrated on the mammalian heart, activation of this pathway decreased L-type Ca^{2+} currents (Abi-Gerges et al., 2001) and troponin I phosphorylation (Hove-Madsen et al., 1996), thus contributing to myocardial contractile performance inhibition. It also attenuates sarcoplasmic reticulum Ca^{2+} reuptake by inhibiting phospholamban phosphorylation (Frank et al., 2003).

In recent years, great attention has been focused on cardiac relaxation (lusitropism), being this a crucial component ofthe cardiac cycle. A proper relaxation (i.e., restoring the diastolic ventricular pressure after each contraction) allows the ventricle to be adequately filled with blood, with impact on the subsequent contraction. Notably, we observed that Chr negatively influenced lusitropism. This is particularly important since an impaired relaxation contributes to cardiac dysfunction, such as in heart failure with normal ejection fraction (Leite-Moreir, 2006). The results on the Chr-induced modulation of the cardiac performance extend the knowledge on the regulatory influence elicited by circulating CgA and its fragments (Vs-I, Cts and Serpinin) on the mammalian cardio-circulatory system (Tota et al., 2010 and 2012). Nothing is known on how these actions, as well as the proteolytic events which generate CgA fragments, are spatio-temporally coordinated. However, it is conceivable that CgA systemic influence, and the effects induced by CgA-derived peptides at organ/tissue (heart and vessels) level may synergically contribute to circulatory homeostasis, playing a role in coordinating and counteracting hyperactivity under normal and diseased conditions. According to the "zero steady-state error" homeostasis realized by counter-regulatory hormones (Koeslag et al.,1999), we suggest that these substances operate as "integral" controllers, so that the controlled variable returns to set "point", at any steady-state disturbance. We found that Chr, given in the early reperfusion, limited the I/R-dependent myocardial damage. This protection, similar to that obtained by ischemic PostC maneuvers (Vinten-Johansen et al., 2005), was indicated by a significant reduction of both infarct size and LDH release, and by a marked improvement of the post-ischemic contractile function expressed as a decrease of contracture development. A reduced contracture is the goal of cardioprotective protocols, due to its inverse relation with the I/R-dependent myocardial damage (Penna et al., 2008). Our results extended to Chr the cardioprotective properties of other CgA fragments, such as Vs-I and Cts (Cappello et al., 2007), paving the

way for analyzing the applicative potential of this peptide as pharmacological PostC agent. Like pre- and post-conditioning maneuvers, many substances protect the heart by recruiting pro-survival intrinsic signalling cascades involving PI3K/Akt, PKC and ERK1/2, which may converge on GSK-3β, a substrate of multiple pro-survival protein kinases that in rodents include the RISK pathway (Hausenloy et al., 2004; Penna at al., 2008), and require the opening of mitoKATP channels (Penna et al. 2007, 2008). Here, we observed that this cascade is activated in hearts exposed to Chr in the early reperfusion. In fact, inhibition of the RISK upstream kinases (PI3K and ERK1/2) abolished the recovery of the systolic performance induced by Chr.

Our results agree with previous data obtained by our and other laboratory showing that these kinases are recruited by pharmacological PostC elicited by many protective substances, including different CgA derived-peptides (Angelone et al. 2013; Perrelli et al., 2013). During reperfusion, both PI3K-Akt and ERK1/2 are activated and converge on GSK3β, inducing its phosphorylation/inactivation with a final control on mitoKATP channels, one of the terminal elements of PostC protection (Gomez et al., 2008). Our results suggest that, in addition to RISK, the efficacy of Chr PostC can be attributed to the control of mitochondria function. We also observed that Chr-dependent cardioprotection is accompanied by increase of intracellular cGMP, an effect which disappears in hearts co-treated with specific inhibitor of Guanylate Cyclase. The importance of cGMP in cardioprotection is well known (Penna et al., 2006b). In fact, PostC depends on GC activation via either NOS-dependent or NOS-independent pathways (Penna et al., 2006b and 2008). Of note, Chr-dependent cardioprotection is accompanied by an increased miRNA-21 expression. miRNA are small noncoding RNAs that mediate post-transcriptional gene silencing (Zhang, 2008). They are involved in cardiac physiopathology and their deregulated expression is linked to the developement of cardiovascular disorders (Da Costa Martins et al., 2012). In particular, it

was demonstrated that miRNA-21 overexpression reduces infarct size, and this is associated with pro-apoptotic genes inhibition and anti-apoptotic genes increase (Dong et al., 2009; Cheng et al., 2009).

*2. Antibacterial effect of D*T*bCtl against S. aureus*

For this application we have used a synthetic peptide added with a Levo-3,4-dihydroxyphenylalanine (DOPA) group, to cover in non-specific manner all the typologies of biomaterials (Lynge et al., 2011; Ponzio et al., 2014), In the past few years, the polydopamine films have become an efficient and versatile system to functionalize biomaterials because it is possible to coat almost all known materials by immerging them in oxygenated and slightly basic dopamine containing solutions (Lynge et al., 2011; Ponzio et al., 2014). The deposition method of polydopamine, also for the analogous L-DOPA7, is based on the use of oxidants, other than O_2 dissolved in water, like metal cations (Bernsmann et al., 2011), sodium periodate and peroxodisulfate (Wei et al., 2010). Once dopamine is oxidized by the oxygen of air and starts to oligomerize, amphiphilic species are created which migrate at the air/water interface forming a film (Ponzio et al., 2014).

Limitations of this approach are represented by formation of aggregates which strongly reduce antibacterial activity. Thus, further studies are needed to develop different strategies which allow to reduce the formation of aggregates preserving the antibacterial action of our peptide also on biomaterials. In fact, until now the problem of the aggregation of D*T*bCtl after oxidation was not resolved and it will be crucial to obtain a new method to reduce or block the formation of D*T*bCtl (L) aggregates on the surface.

Here it has been shown that, *in vitro,* our synthetic peptide D*T*bCtl (L) has an antibacterial action against different strains of *S. aureus*. In presence of Glu-C, a specific endoprotease from *S. aureus,* the synthetic peptide is able to be cleaved and release active bCtl.

D*T*bCtl (L) is lower active than Ctl (L). For bCtl the MIC value was around 20 μM (Aslam et al., 2013), while in our study we showed that in solution D*T*bCtl had a MIC value around 75 μM against different *S. aureus* strains. This data is not concordant with the addition of the two positive charges in DOPA group (the antibacterial action depends on positive charge).

In fact, our study has shown that in oxidizing condition the peptide loses its antibacterial power, generating aggregates (**Figure 26**). Concerning DOPA group, the addition of this sequence to the peptide bCtl (L) gives major stability during digestion by Glu-C. In fact, the Glu-C digestion of bCtl (L) has produced the cleavage in two sites generating the release of fragments that do not have antimicrobial action (**Figure 26**). The presence of DOPA group in D*T*bCtl (L) induces a modification of the secondary structure, generating the formation of alpha helix in the central part of the bCtl (L). This modification improves the stability of the peptide allowing the cleavage at the specific cleavage site by the protease (**Figure 26**). It can be also considered that this approach generates a correct cleavage by Glu-C and increases the antibacterial properties of our synthetic peptides. Based on these data, we have validated a synthetic peptide (D*T*bCtl) for the biomaterials that, during the first phase of *S. aureus* infection, can induce the lysis of bacteria and the release of the endoprotease Glu-C. This enzyme is able to cleave the peptide after the Glu residue releasing the active form of bCtl (L) (**Figure 27**). In fact, we have showed that D*T*bCtl (L) was cleaved by Glu-C with the specific release of bCtl. This cleavage occurs after 4 h of incubation and at 18 h the yield of D*T*bCtl (L) cleaved was 85-95%.

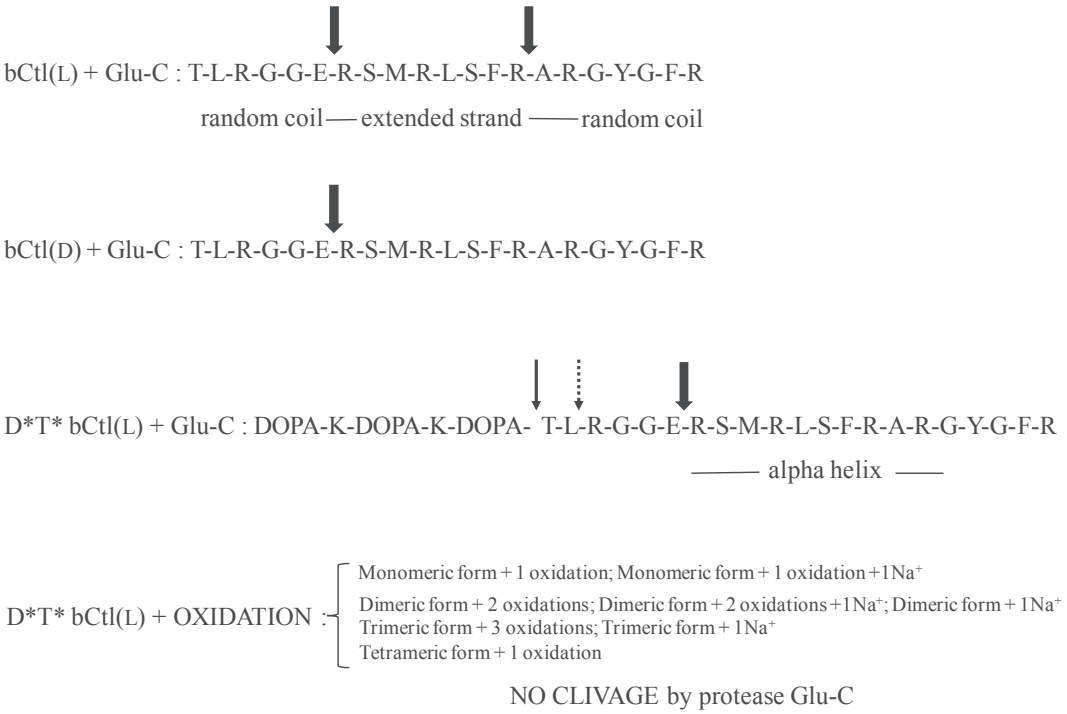

Figure 26: Schematic summary of the results obtained by digestion of synthetic Cateslytin-derived peptides by Glu-C protease of *S. aureus* V8.

Nosocomial infections are often caused by biofilm colonization of medical implants. Many strategies to avoid biofilm-associated infections have been proposed focusing on preventing biofilm biogenesis as well as disrupting formed biofilms (Ribeiro et al., 2016). For biofilm prevention several strategies are adopted. For instance, agents able to blocking bacterial adhesion to medical implants or to inhibit the production of extracellular matrix have been widely used. At the same time, molecules that may induce the disruption and destabilization of biofilms or extracellular matrix are desirable. The cationic AMPs are able to have many of these effects, including killing bacteria, stopping extracellular matrix production and stability of biofilm (Melvin et al., 2016).

On the basis of our results, the D*T*bCtl appears to be a perfect cationic AMP to prevent biofilm biogenesis as well as to disrupt formed biofilms. In fact, when *S. aureus* interacts on the biomaterial covered with D*T*bCtl, this peptide firstly kills bacteria with a direct antibacterial action inducing pathogen lysis (**Figure 27a**). Furthermore, as result of this

event, an increase of protease released by the bacterium is observed (Ribeiro et al., 2016) and so the level of Glu-C will be higher in the medium (**Figure 27b**). At this point, in addition to the direct antibacterial activity, D*T*bCtl may be processed by the endoprotease Glu-C produced by *S. aureus* to generate free Ctl, which appears more active against *S. aureus* than our synthetic D*T*bCtl (**Figure 27c-d**).

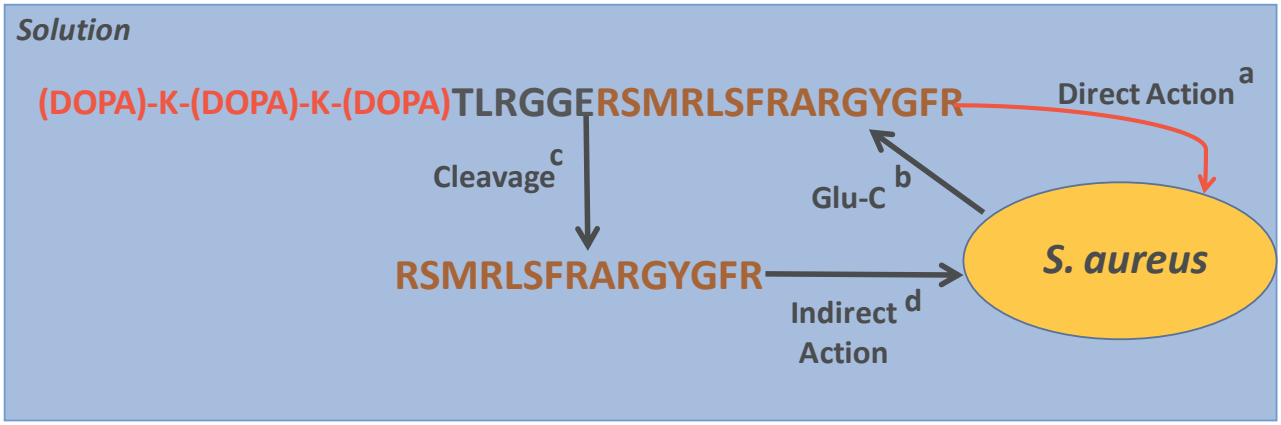

Figure 27: Schematic diagram showing the putative mechanism of action of D*T*bCtl against *S. aureus*.

This indirect antibacterial action of D*T*bCtl, depending on the presence of Glu-C, gives to our peptide an exponential antibacterial action against *S. aureus*.

3. *In vivo antibacterial and anti-inflammatory effect of Ctl in S. aureus infected rat model*

S. aureus is an opportunistic pathogen which causes a wide range of severe clinical infections (Frieri et al., 2016) and hospital-acquired infections (Klein et al., 2007; Moran et al., 2006). Furthermore, this pathogen is the main cause of lower respiratory tract infections and surgical infections (Klein et al., 2007) and the most frequently isolated pathogen in Gram-positive sepsis, often involved in blood clotting disorders and destruction of endocardial

tissue (Ohbayashi et al., 2011). *S. aureus* is able to resist to the antibiotics and to develop various multidrug-resistant mechanisms, thus limiting therapeutic strategies for *S. aureus* infection (Frieri et al., 2016). The diffusion of methicillin-resistant *S. aureus* (MRSA) has become one of the most common causes of bacterial nosocomial infections (Frieri et al., 2016; Klein et al., 2007; Moran et al., 2006). This evidence, together with the increase in resistance to classical antibiotics, have made of Vancomycin the first choice in the treatment of infections induced by *S. aureus* (Holubar et al., 2016). In this context, the interest for natural AMPs is increasing as some of them display potent antibacterial activity (Riberio et al., 2016).

In vitro studies have shown that Ctl has antibacterial activity against different strains of *S. aureus* with a MIC value of 37–45 mg/mL (Aslam et al., 2013). In the present study, by using an *in vivo* approach, we have confirmed that Ctl is able to counteract *S. aureus* infection in rat. Treatment with Ctl (1.5 mg/Kg) during *S. aureus* infection showed an antibacterial effect with a total inhibition of plasmatic and cardiac bacterial growth. For the first time, these results show that the treatment with a CgA-derived peptide (Ctl) has the same effects of an antibiotic treatment against a *S. aureus* infection.

In the specific field of inflammation, increased expression of tumor necrosis factor (TNF) and interleukin-1β (IL-1β) occurs in experimental sepsis and this expression is the major index of infection induced by pathogens (Knuefermann et al., 2004; Haziotet al., 1999). Several data show that the clearance of *S. aureus* and the plasmatic levels of TNF-α and IL-1β levels are high both in CD14-deficient that in wild-type mice after a challenge with *S. aureus*, indicating that these cytokines are markers of inflammation induced by these gram-positive bacteria (Haziot et al., 1999). Rabbi et al. (2014) showed that a lower amount of TNF-α and IL-1β was released in the culture supernatant of macrophages isolated from the peritoneal cavity of colitic mice treated *in vivo* with the three different fragments of hCts

(hCgA$_{352–372}$: SSMKLSFRARAYGFRGPGPQL; proximal sequence that corresponds to hCtl (hCgA$_{352–366}$: SSMKLSFRARAYGFR, and the distal sequence hCgA$_{360–372}$: ARAYGFRGPGPQL). These findings suggest that hCts and hCtl have an important role in the pathogenesis of colitis by regulating the infiltration of inflammatory cells and production of pro-inflammatory mediators in the colon (Rabbi et al., 2014). Based on these results, we have demonstrated that in rat the treatment with bCtl (1.5 mg/Kg) (Rabbi et al., 2014) during *S. aureus* infection reduces systemic inflammation with a decreased production of pro-inflammatory cytokines such as TNF-α and IL-1β. We have also evaluated the level of plasma LDH as systemic damage index (Cofiell et al., 2015) showing that treatment with bCtl reduces also the plasma levels of this marker.

During the infection, the expression of cytokines in cardiac tissue induces the activation of inflammatory pathway but also the recruitment of inflammatory cells (Kumar et al., 1996; Cain et al., 1999; Aoki and Narumiya, 2012). Under this condition, the major mediators of inflammation are iNOS and COX-2 (Aoki and Narumiya, 2012). Their increased expression also contributes to tissue remodeling like angiogenesis and fibrosis and can induce organ dysfunction. The roles of prostaglandins were verified in human cardiovascular diseases, suggesting that prostaglandin signaling is a promising therapeutic target for chronic inflammatory diseases. In fact, while in the group treated with *S. aureus* the cardiac expression iNOS and COX-2 increased, the co-treatment with Ctl reduced their production. These data show how the treatment with Ctl (1.5 mg/Kg) (Rabbi et al., 2014) during *S. aureus* infection in rat can switch off systemic and cardiac inflammation.

Taken together these data support the hypothesis that CgA-derived peptides play an important role in antimicrobial response against pathogens and, at the same time, have anti-inflammatory property, expressed during the remission phase, able to reduce the inflammation.

Conclusions

This study has demonstrated, for the first time, that the antibacterial and antifungal Chr modulates the cardiac function through a NO-dependent negative inotropism and lusitropism. This peptide elicits post-conditioning protection of the myocardium against I/R injury by activating RISK pathway and by modulating miRNA-21 expression. These data are of physiological relevance since they contribute to clarify the role of naturally occurring CgA-derived peptides in cardiac stabilization against stress responses. They are also of interest in an applicative context since left ventricular functional alterations, consequent to I/R, are major determinants of mortality and prognosis. Accordingly, in the search of novel endocrine modulators that can target and attenuate reperfusion-induced cell death, these results on Chr-induced cardioprotection deserve further attention.

The results obtained with D*T*bCtl allow to establish it as a new AMP that might be used to cover biomaterial surfaces. In solution, its antibacterial mechanism has been explained by two mechanisms: *a direct action* (shown by the entire peptide) where the positive charges of D*T*bCtl confer to this synthetic peptide a non-specific antimicrobial activity against various micro-organisms, and *an indirect action,* related to the cleavage of Glu-C protease. Of note, for the first time in the present study, an indirect action of D*T*bCtl, specifically related to *S. aureus,* has been demonstrated. In fact, the endoprotease Glu-C, produced by *S. aureus*, induces the release of Ctl exclusively in the presence of this pathogen. New experiments are currently in process in our laboratory to show that this strategy may be extended to others microorganisms.

A next step will be to test its action on the Dacron artificial cardiac valves hoping to confirm the data obtained in solution. This coating application might be extended to any type of biomaterial thus accounting Ctl as a possible candidate for biomedical applications (prosthetic heart valves). Until now, the problem of the aggregation of D*T*bCtl after

oxidation has not been resolved, thus it will be crucial to obtain a new method to reduce or block the formation of D*T*bCtl aggregates on the surface.

In parallel, future studies will be of interest to evaluate the effects of Ctl and D*T*bCtl on the isolated and perfused Langendorff rat hearts in order to compare their cardiac actions with those induced by Chr. The cardiac effects of Ctl and D*T*bCtl will be evaluate on basal cardiac performance, i.e. contractility, relaxation and coronary modulation, and on cardioprotection by administering these molecules before and after ischemia.

Results from *in vivo* studies have suggested that in rat Ctl is able to counteract *S. aureus* infection and its cardiac deleterious effects. The treatment with Ctl during *S. aureus* infection induces: i) antibacterial effects with total inhibition of plasmatic and cardiac bacterial growth; ii) reduction of inflammatory effectors in cardiac tissue (iNOS and COX-2); iii) reduction of both pro-inflammatory cytokines (TNF-α and IL-1β) and marker of sistemic damage (LDH). The next goal will be to evaluate the *in vivo* cardioprotective activity of Ctl in a rat model of *S. aureus* sepsis. This will allow the cardioprotective action of this molecule as a preconditioning agent in chronic treatments during *S. aureus* infection.

Other important aspect will be to evaluate if the stress condition of *S. aureus* infection can affect the tissue production of Ctl and the plasma half time of this peptide. In particular, the intracardiac CgA expression could be stimulated by infection conditions, but also the processing of this antistress pro-hormone and the production of smaller active peptides, such as Ctl, could be promoted. In order to evaluate how the *S. aureus* infection can modulate the production of this antimicrobial peptide an ELISA assay specific for Ctl will be developed.

In conclusion, these experimental data show that the antimicrobial CgA derived-peptides play an important role both in cardiac homeostasis and cardioprotection as well as in innate immunity, suggesting that these systems are strongly linked under stressful conditions such as infections.

References

Aardal S. and Helle K.B. (1992). The vasoinhibitory activity of bovine chromogranin A fragment (vasostatin) and its independence of extracellular calcium in isolated segments of human blood vessels. Regul. Pept. 41(1):9-18.

Abi-Gerges N., Fischmeister R., Meiry P.F. (2001). G protein-mediated inhibitoryeffect of a nitric oxide donor on the L-type Ca2+ current in rat ventricularmyocytes. J. Physiol. 531:117–130.

Angeletti R.H., Aardal S., Serck-Hanssen G., Gee P., Helle K.B. (1994). Vasoinhibitory activity of synthetic peptides from the amino terminus of chromogranin A. Acta Physiol. Scand. 152(1):11-19.

Angelone T. and Tota B. (2012). Editorial: chromogranin A at the crossroads of health and disease. Curr. Med. Chem. 19(24):4039-4041.

Angelone T., Filice E., Quintieri A.M., Imbrogno S., Recchia A., Pulerà E., Mannarino C., Pellegrino D., Cerra M.C. (2008). Beta3-adrenoceptors modulate left ventricular relaxation in the rat heart via the NO-cGMP-PKG pathway. Acta Physiol. (Oxf). 193(3):229-239.

Angelone T., Mazza R., Cerra M.C. (2012a). Chromogranin-A: a multifaceted cardiovascular role in health and disease. Curr. Med. Chem. 19(24):4042-4050.

Angelone T., Quintieri A.M., Brar B.K., Limchaiyawat P.T., Tota B., Mahata S.K., Cerra M.C. (2008). The antihypertensive chromogranin a peptide catestatin acts as a novel endocrine/paracrine modulator of cardiac inotropism and lusitropism. Endocrinology. 149(10):4780-4793.

Angelone T., Quintieri A.M., Pasqua T., Gentile S., Tota B., Mahata S.K., Cerra M.C. (2012b). Phosphodiesterase type-2 and NO-dependent S-nitrosylation mediate the cardioinhibition of the antihypertensive catestatin. Am. J. Physiol. Heart Circ. Physiol. 302(2):H431-442.

Angelone T., Filice E., Pasqua T., Amodio N., Galluccio M., Montesanti G., Quintieri A.M., Cerra M.C. (2013). Nesfatin-1 as a novel cardiac peptide: identification, functional characterization, and protection against ischemia/reperfusioninjury. Cell. Mol. Life Sci. 70(3):495–509.

Aoki T. and Narumiya S. (2012). Prostaglandins and chronic inflammation. Trends Pharmacol. Sci. 33(6):304-311.

Aslam R., Atindehou M., Lavaux T., Haïkel Y., Schneider F., Metz-Boutigue M.H. (2012). Chromogranin A-derived peptides are involved in innate immunity. Curr. Med. Chem.19(24):4115-4123.

Aslam R., Marban C., Corazzol C., Jehl F., Delalande F., Van Dorsselaer A., Prévost G., Haïkel Y., Taddei C., Schneider F., Metz-Boutigue M.H. (2013). Cateslytin, a chromogranin A derived peptide is active against Staphylococcus aureus and resistant to degradation by its proteases. PLoS One. 8(7):e68993.

Attaran S., Chukwuemeka A., Punjabi P.P., Anderson J. (2012). Do all patients with prosthetic valve endocarditis need surgery? Interact. Cardiovasc. Thorac. Surg. 15(6):1057-1061.

Auvynet C. and Rosenstein Y. (2009). Multifunctional host defense peptides: antimicrobial peptides, the small yet big players in innate and adaptive immunity. FEBS J. 276(22):6497-6508.

Banks P. and Helle K.B. (1965) The release of protein from the stimulated adrenal medulla. Biochem. J. 97, 40C-41C.

Bar-Or D., Carrick M.M., Mains C.W., Rael L.T., Slone D., Brody E.N. (2015). Sepsis, oxidative stress, and hypoxia: Are there clues to better treatment? Redox Rep. 20(5):193-7.

Bauer S.H., Zhang X.Y., Van Dongen W., Claeys M., Przybylski M. Chromogranin A from bovine adrenal medulla: molecular characterization of glycosylations, phosphorylations, and sequence heterogeneities by mass spectrometry. (1999). Anal. Biochem. 274(1):69-80.

Benedum U.M., Baeuerle P.A., Konecki D.S., Frank R., Powell J., Mallet J., Huttner W.B. (1986) The primary structure of bovine chromogranin A: a representative for a class of acidic secretory proteins common to a variety of peptidergig cells. EMBO J. 5:1495-1502.

Bernsmann F., Ball V., Addiego F., Ponche A., Michel M., Gracio J., Toniazzo V., Ruch D. (2011). Dopamine-Melanin Film Deposition Depends on the Used Oxidant and Buffer Solution. Langmuir. 27: 2819−2825.

Biswas N., Rodriguez-Flores J.L., Courel M., Gayen J.R., Vaingankar S.M., Mahata M., Torpey J.W., Taupenot L., O'Connor D.T., Mahata S.K. (2009). Cathepsin L colocalizes with chromogranin a in chromaffin vesicles to generate active peptides. Endocrinology 150:3547–3557.

Briolat J., Wu S.D., Mahata S.K., Gonthier B., Bagnard D., Chasserot-Golaz S., Helle K.B., Aunis D., Metz-Boutigue M.H. (2005). New antimicrobial activity for the catecholamine release-inhibitory peptide from chromogranin. Cell. Mol. Life Sci. 62:377-385.

Brogden K.A. (2005). Antimicrobial peptides: pore formers or metabolic inhibitors in bacteria? Nat. Rev. Microbiol. 238-250.

Burley D.S., Hamid S.A., Baxter G.F. (2007). Cardioprotective actions of peptide hormones in myocardial ischemia. Heart Fail. Rev. 12(3-4):279-91.

Cain B.S., Meldrum D.R., Dinarello C.A., Meng X., Joo K.S., Banerjee A., Harken A.H. (1999). Tumor necrosis factor-α and interleukin-1β synergistically depress human myocardial function. Crit. Care Med.; 27:1309-1318.

Calvin J.E., Driedger A.A., Sibbald W.J. (1981). Assessment of myocardial function in human sepsis utilizing ECG gated cardiac scintigraphy. Chest. 80:579–586.

Cappello S., Angelone T., Tota B., Pagliaro P., Penna C., Rastaldo R., Corti A., Losano G., Cerra M.C. (2007). Human recombinant chromogranin A-derived vasostatin-1 mimics preconditioning via an adenosine/nitric oxide signaling mechanism. Am. J. Physiol. Heart Circ. Physiol. 293(1):H719-727.

Carleton H.A., Diep B.A., Charlebois E.D., Sensabaugh G.F., Perdreau-Remington F. (2004). Community-adapted methicillin-resistant Staphylococcus aureus (MRSA): population dynamics of an expanding community reservoir of MRSA. J. Infect. Dis. 190:1730–1738.

Carroll R.K., Robison T.M., Rivera F.E., Davenport J.E., Jonsson I.M., Florczyk D., Tarkowski A., Potempa J., Koziel J., Shaw L.N. (2012) Identification of an intracellular M17 family leucine aminopeptidase that is required for virulence in Staphylococcus aureus. Microbes Infect. 14(11): 989-999.

Casadei B. and Sears C.E. (2003). Nitric-oxide-mediated regulation of cardiac contractility and stretch responses. Prog. Biophys. Mol. Biol. 82(1–3):67–80.

Ceconi C., Ferrari R., Bachetti T., Opasich C., Volterrani M., Colombo B., Parrinello G., Corti A. (2002). Chromogranin A in heart failure; a novel neurohumoral factor and a predictor for mortality. Eur. Heart J. 23(12):967-974.

Cerra M.C., Gallo M.P., Angelone T., Quintieri A.M., Pulerà E., Filice E., Guérold B., Shooshtarizadeh P., Levi R., Ramella R., Brero A., Boero O., Metz-Boutigue M.H., Tota B., Alloatti G. (2008). The homologous rat chromogranin A1-64 (rCGA1-64) modulates myocardial and coronary function in rat heart to counteract adrenergic stimulation indirectly via endothelium-derived nitric oxide. FASEB J. 22(11):3992-4004.

Cerra, M.C., De Iuri, L., Angelone, T., Corti A and Tota, B. (2006) Recombinant N-terminal fragments of chromogranin-A modulate cardiac function of the Langendorff-perfused rat heart. Basic Res. Cardiol. 101:43–52.

Cheng Y., Liu X., Zhang S., Lin Y., Yang J., Zhang C. (2009). MicroRNA-21 protects against the H2O2-induced injury on cardiac myocytes via its target gene PDCD4. J. Mol. Cell. Cardiol. 47:5–14.

Chu V.H., Park L.P., Athan E., Delahaye F., Freiberger T., Lamas C., Miro J.M., Mudrick D.W., Strahilevitz J., Tribouilloy C., Durante-Mangoni E., Pericas J.M., Fernández-Hidalgo N., Nacinovich F., Rizk H., Krajinovic V., Giannitsioti E., Hurley J.P., Hannan M.M., Wang A. (2015). Association between surgical indications, operative risk, and clinical outcome in infective endocarditis: a prospective study from the International Collaboration on Endocarditis. Circulation. 131(2):131-140.

Cofiell R., Kukreja A., Bedard K., Yan Y., Mickle A.P., Ogawa M., Bedrosian C.L., Faas S.J. (2015). Eculizumab reduces complement activation, inflammation, endothelial damage, thrombosis, and renal injury markers in aHUS. Blood. 21;125(21):3253-3262.

Corti A. and Ferrero E. (2012). Chromogranin A and the endothelial barrier function. Curr. Med. Chem. 19(24):4051-4058.

Corti A., Sanchez L.P., Gasparri A., Curnis F., Longhi R., Brandazza A., Siccardi A.G., Sidoli A. (1997). Production and structure characterization of recombinant chromogranin A N-terminal fragments (vasostatins)-evidence of dimer-monomer equilibria. Eur. J. Biochem. 15, 248(3):692–699.

Da Costa Martins P.A., De Windt L.J. (2012). MicroRNAs in control of cardiachypertrophy, Cardiovasc. Res. 93:563–572.

Díaz I. and Smani T. (2013). New insights into the mechanisms underlying vascular and cardiac effects of urocortin. Curr. Vasc. Pharmacol. 11(4):457-64.

Dong S., Cheng Y., Yang J., Li J., Liu X., Wang X., Wang D., Krall T.J., Delphin E.S., Zhang C. (2009). MicroRNA expression signature and the role of microRNA-21 in theearly phase of acute myocardial infarction. J. Biol. Chem. 284:29514–29525.

Drapeau G.R. (1976). Protease from Staphyloccus aureus. Methods Enzymol. 45:469-475.

Drapeau G.R. (1977). Cleavage at glutamic acid with staphylococcal protease. Methods Enzymol. 47: 189-191.

Edfeldt K., Agerberth B., Rottenberg M.E., Gudmundsson G.H., Wang X.B., Mandal K., Xu Q., Yan Z.Q. (2006). Involvement of the antimicrobial peptide LL-37 in human atherosclerosis. Arterioscler. Thromb. Vasc. Biol. 26(7):1551-1557.

Eiden L. (1987). Is chromogranin A a prohormone? Nature. 325(6102):301.

Egger M., Beer A.G., Theurl M., Schgoer W., Hotter B., Tatarczyk T. (2008). Monocyte migration: a novel effect and signaling pathways of catestatin. Eur. J. Pharmacol. 598:104–11.

Fasciotto B.H., Trauss C.A., Greeley G.H., Cohn D.V. (1993). Parastatin (porcine chromogranin A347 – 419), a novel chromogranin A-derived peptide, inhibits parathyroid cell secretion. Endocrinology. 133:461-466.

Frank K.F., Bölck B., Erdmann E., Schwinger R.H. (2003). Sarcoplasmic reticulum Ca2+-ATPase modulates cardiac contraction and relaxation, Cardiovasc. Res.57(1):20–27.

Frieri M, Kumar K, Boutin A. (2016) Antibiotic resistance. J. Infect. Public Health. pii: S1876-0341(16)30127-7.

Gadroy P., Stridsberg M., Capon C., Michalski J.C., Strub J.M., Van Dorsselaer A., Aunis D., Metz-Boutigue M.H. (1998). Phosphorylation and O-glycosylation sites of human chromogranin A (CGA79-439) from urine of patients with carcinoid tumors. J. Biol. Chem. 273(51):34087-34097.

Gallo M.P., Levi R.C., Ramella R., Brero A., Boero O., Tota B., Alloatti G. (2007). Endothelium-derived nitric oxide mediates the antiadrenergic effect of human vasostatin-1 (CgA1–76) in rat ventricular myocardium. Am. J. Physiol. Heart Circ. Physiol. 292(6):H2906-2912.

Ganz T. (2003). The role of antimicrobial peptides in innate immunity. Integr. Comp. Biol. 43(2):300-304.

Georget M., Mateo P., Vandecasteele G., Lipskaia L., Defer N., Hanoune J., Hoerter J., Lugnier C., Fischmeister R. (2003). Cyclic AMP compartmentation due to increased cAMP-phosphodiesterase activity in transgenic mice with a cardiac-directed expression of the human adenylyl cyclase type 8 (AC8). Faseb J. 17(11): 1380-1391.

Glattard E., Angelone T., Strub J.M., Corti A., Aunis D., Tota B., Metz-Boutigue M.H., Goumon Y. (2006). Characterization of natural vasostatin-containing peptides in rat heart. FEBS J. 273:3311-3321.

Golzio P.G., Gabbarini F., Anselmino M., Vinci M., Gaita F., Bongiorni M.G. (2010). Gram-positive occult bacteremia in patients with pacemaker and mechanical valve prosthesis: a difficult therapeutic challenge. Europace. 12(7):999-1002.

Gomez L., Paillard M., Thibault H., Derumeaux G., Ovize M. (2008). Inhibition ofGSK3beta by postconditioning is required to prevent opening of themitochondrial permeability transition pore during reperfusion. Circulation 117:2761–2768.

Goumon Y., Lugardon K., Kieffer B., Lefèvre J.F., Van Dorsselaer A., Aunis D., Metz-Boutigue M.H. (1998). Characterization of antibacterial COOH-terminal proenkephalin-A-derived peptides (PEAP) in infectious fluids. Importance of enkelytin, the antibacterial PEAP209-237 secreted by stimulated chromaffin cells. J. Biol. Chem. 6;273(45): 29847-29856.

Hausenloy D.J., Barrabes J.A., Bøtker H.E., Davidson S.M., Di Lisa F., Downey J., Engstrom T., Ferdinandy P., Carbrera-Fuentes H.A., Heusch G., Ibanez B., Iliodromitis E.K., Inserte J., Jennings R., Kalia N., Kharbanda R., Lecour S., Marber M., Miura T., Ovize M., Perez-Pinzon M.A., Piper H.M., Przyklenk K., Schmidt M.R., Redington A., Ruiz-Meana M., Vilahur G., Vinten-Johansen J., Yellon D.M., Garcia-Dorado D. (2016). Ischaemic conditioning and targeting reperfusion injury: a 30 year voyage of discovery. Basic Res Cardiol. 111(6):70.

Hausenloy D.J., Yellon D.M. (2004). New directions for protecting the heart against ischaemia-reperfusion injury: targeting the reperfusion injury salvage kinase (RISK)-pathway, Cardiovasc. Res. 61:448–460.

Hausenloy D.J., Tsang A., Yellon D.M. (2005). The reperfusion injury salvage kinase pathway: a common target for both ischemic preconditioning and postconditioning. Trends Cardiovasc. Med. 15(2):69-75.

Haziot A.N. Hijiya K., Schultz F., Zhang S.C., Gangloff and S. M. Goyert. (1999). CD14 plays no major role in shock induced by Staphylococcus aureus but down-regulates TNF-alpha production. J. Immunol. 162:4801–4805.

Helle K.B. (2004). The granin family of uniquely acidic proteins of the diffuse neuroendocrine system: comparative and functional aspects. Biol. Rev. Camb. Philos. Soc. 79:769 –794.

Helle K.B. and Aunis D. (2000). A physiological role for the granins as prohormones for homeostatically important regulatory peptides? A working hypothesis for future research. Adv. Exp. Med. Biol.482:389-397.

Helle K.B., Corti A., Metz-Boutigue M.H., Tota B. (2007). The endocrine role for chromogranin A: a prohormone for peptides with regulatory properties. Cell. Mol. Life Sci- 64:2863–2886

Hetem D.J., de Ruiter S.C., Buiting A.G., Kluytmans J.A., Thijsen S.F., Vlaminckx B.J., Wintermans R.G., Bonten M.J., Ekkelenkamp M.B. (2011). Preventing Staphylococcus aureus bacteremia and sepsis in patients with Staphylococcus aureus colonization of intravascular catheters: a retrospective multicenter study and meta-analysis. Medicine (Baltimore). 90(4):284-288.

Holubar M., Meng L., Deresinski S. (2016). Bacteremia due to Methicillin-Resistant Staphylococcus aureus: New Therapeutic Approaches. Infect. Dis. Clin. North Am. 30(2): 491-507.

Hove-Madsen L., Mery P.F., Jurevicius J., Skeberdis A.V., Fischmeister R. (1996). Regulation of myocardial calcium channels by cyclic AMP metabolism. Basic. Res. Cardiol. 91:1–8.

Iacangelo A., Okayama H., Eiden L.E. (1988). Primary structure of rat chromogranin A and distribution of its mRNA. FEBS Lett. 227:115-121.

Ikeda Y., Young L.H., Scalia R., Ross C.R., Lefer A.M. (2001). PR-39, a proline/arginine-rich antimicrobial peptide, exerts cardioprotective effects in myocardial ischemia-reperfusion. Cardiovasc. Res. 49(1):69-77.

Jan Danser A.H. and Saris J.J. (2002). Prorenin uptake in the heart: a prerequisite for local angiotensin generation?. J. Mol. Cell. Cardiol. 34:1463–1472.

Javadov S.A., Lim K.H., Kerr P.M., Suleiman M.S., Angelini G.D., Halestrap A.P. (2000). Protection of hearts from reperfusion injury by propofol is associated with inhibition of the mitochondrial permeability transition. Cardiovasc. Res. 45: 360-369.

Jean-François F., Khemtémourian L., Odaert B., Castano S., Grélard A., Manigand C., Bathany K., Metz-Boutigue M.H., Dufourc E.J. (2007). Variability in secondary structure of the antimicrobial peptide Cateslytin in powder, solution, DPC micelles and at the air-water interface. Eur. Biophys. J.36(8):1019-1027.

Jean-François F., Castano S., Desbat B., Odaert B., Roux M., Metz-Boutigue M.H., Dufourc E.J. (2008a). Aggregation of cateslytin beta-sheets on negatively charged lipids promotes rigid membrane domains. A new mode of action for antimicrobial peptides? Biochemistry. 47(24):6394-6402.

Jean-François F., Elezgaray J., Berson P., Vacher P., Dufourc E.J. (2008b). Pore formation induced by an antimicrobial peptide: electrostatic effects. Biophys. J. 95(12):5748-5756.

Jenssen H., Hamill P., Hancock R.E. (2006). Peptide antimicrobial agents. Clin. Microbiol. Rev. 19:491-511.

Jeroudi M.O., Hartley C.J., Bolli R. (1994). Myocardial reperfusion injury: role of oxygen radicals and potential therapy with antioxidants. Am. J. Cardiol. 73:2B–7B.

John M.D., Hibberd P.L., Karchmer A.W., Sleeper L.A., Calderwood S.B. (1998). Staphylococcus aureus prosthetic valve endocarditis: optimal management and risk factors for death. Clin. Infect. Dis. 26(6):1302-1309.

Johnson J.K., Khoie T., Shurland S., Kreisel K., Stine O.C., Roghmann M.C. (2007). Skin and soft tissue infections caused by methicillinresistant Staphylococcus aureus USA300 clone. Emerg. Infect. Dis. 13:1195–1200.

Kennedy B.P., Mahata S.K., O'Connor D.T., Ziegler M.G. (1998). Mechanism of cardiovascular actions of the chromogranin A fragment catestatin in vivo. Peptides. 19:1241-1248.

King M.D., Humphrey B.J., Wang Y.F., Kourbatova E.V., Ray S.M., Blumberg H.M. (2006). Emergence of community-acquired methicillin-resistant Staphylococcus aureus USA 300 clone as the predominant cause of skin and soft-tissue infections. Ann. Intern. Med. 144:309–317.

Klein E., Smith D.L., Laxminarayan R. (2007). Hospitalizations and deaths caused by methicillin-resistant Staphylococcus aureus, United States, 1999-2005. Emerg. Infect. Dis. 13(12):1840-1846.

Klevens R.M., Edwards J.R., Tenover F.C., McDonald L.C., Horan T., Gaynes R. (2006). Changes in the epidemiology of methicillin-resistant Staphylococcus aureus in intensive care units in US hospitals, 1992–2003. Clin. Infect. Dis. 42:389–391

Knuefermann P., Sakata Y., Baker J.S., Huang C.H., Sekiguchi K., Hardarson H.S., Takeuchi O., Akira S., Vallejo J.G. (2004). Toll-like receptor 2 mediates Staphylococcus aureus-induced myocardial dysfunction and cytokine production in the heart. Circulation. 110(24):3693-3698.

Koeslag J.H., Saunders P.T., Wessels J.A. (1999). The chromogranins and thecounter-regulatory hormones: do they make homeostatic sense? J. Physiol. 517:643–649.

Koshimizu H., Cawley N.X., Kim T., Yergey A.L., Loh Y.P. (2011). Serpinin: a novel chromogranin A-derived, secreted peptide up-regulates protease nexin-1 expression and granule biogenesis in endocrine cells. Mol. Endocrinol. 25(5):732-744.

Kukreja R.C., Yin C., Salloum F.N. (2011). MicroRNAs new players in cardiac injuryand protection. Mol. Pharmacol. 80(4):558-564.

Kumar A., Thota V., Dee L., Olson J., Uretz E., Parrillo J.E. (1996). Tumor necrosis factor-α and interleukin1β are responsible for in vitro myocardial cell depression induced by human shock serum. J. Exp. Med.; 183:949–958.

Kwiecinski J., Josefsson E., Mitchell J., Higgins J., Magnusson M., Foster T., Jin T., Bokarewa M. (2010). Activation of plasminogen by staphylokinase reduces the severity of Staphylococcus aureus systemic infection. J. Infect. Dis. 202: 1041–1049.

Lai Y., Villaruz A.E., Li M., Cha D.J., Sturdevant D.E., Otto M. (2007). The human anionic antimicrobial peptide dermcidin induces proteolytic defence mechanisms in staphylococci. Mol. Microbiol. 63(2):497-506.

Lee J.C., Taylor C.V., Gaucher S.P., Toneff T., Taupenot L., Yasothornsrikul S., Mahata S.K., Sei C., Parmer R.J., Neveu J.M., Lane W.S., Gibson B.W., O'Connor D.T. (2003). Primary sequence characterization of catestatin intermediates and peptides defines proteolytic cleavage sites utilized for converting chromogranin a into active catestatin secreted from neuroendocrine chromaffin cells. Biochemistry. 42:6938–6946.

Li Y. (2009). The role of antimicrobial peptides in cardiovascular physiology and disease. Biochem. Biophys. Res. Commun. 390(3):363-367.

Leite-Moreira A.F. (2006). Current perspectives in diastolic dysfunction and diastolic heart failure. Heart. 92(5):712-718.

Lynge M.E., van der Westen R., Postma A., Städler B. (2011). Polydopamine-A Nature-Inspired Polymer Coating for Biomedical Science. Nanoscale. 3:4916−4928.

Lugardon K., Chasserot-Golaz S., Kieffer A.E., Maget-Dana R., Nullans G., Kieffer B., Aunis D., Metz-Boutigue M.H. (2001). Structural and biological characterization of chromofungin, the antifungal chromogranin A-(47–66)-derived peptide, J. Biol. Chem. 276(38): 35875–35882.

Lugardon K., Raffner R., Goumon Y., Corti A., Delmas A., Bulet P., Aunis D., Metz-Boutigue M.H. (2000). Antibacterial and antifungal activities of vasostatin-I, the N-terminal fragment of chromogranin A. J. Biol. Chem. 275:10745-10753.

Maget-Dana R., Metz-Boutigue M.H., Helle K.B. (2002). The N-terminal domain of chromogranin A (CgA1–40) interacts with monolayers of membrane lipids of fungal and mammalian compositions. Ann. N. Y. Acad. Sci. 971:352-354.

Mahata S.K., O'Connor D.T., Mahata M., Yoo S.H., Taupenot L., Wu H., Gill B.M., Parmer R.J. (1997). Novel autoendocrine feedback control of catecholamine release. A discrete chromogranin A fragment is a non competitive nicotinic cholinergic antagonist. J. Clin. Invest. 100:1623-1633.

Melvin J.A., Montelaro R.C., Bomberger J.M. (2016). Clinical potential of engineered cationic antimicrobial peptides against drug resistant biofilms. Expert Rev. Anti-Infect. Ther. 14(11): 989-991.

Mermel L.A., Farr B.M., Sherertz R.J., Raad I.I., O'Grady N., Harris J.S., Craven D.E. (2001) Infectious Diseases Society of America, American College of Critical Care Medicine, Society for Healthcare Epidemiology of America. Guidelines for the management of intravascular catheter-related infections. J. Intraven. Nurs. 24(3):180-205.

Metz-Boutigue M.H., Garcia-Sablone P., Hogue-Angeletti R., Aunis D. Intracellular and extracellular processing of chromogranin A. Determination of cleavage sites. (1993a). Eur. J. Biochem. 217(1):247-257.

Metz-Boutigue M.H., Garcia-Sablone P., Hogue-Angeletti R., Aunis D. (1993b). Antibacterial peptides are present in chromaffin cell secretory granules. Cell. Mol. Neurobiol. 18:249-266.

Metz-Boutigue M.H., Goumon Y., Lugardon K., Strub J.M., Aunis D. (1998). Antibacterial peptides are present in chromaffin cell secretory granules. Cell. Mol. Neurobiol. 18(2):249-266.

Metz-Boutigue M.H., Kieffer A.E., Goumon Y., Aunis D. (2003). Innate immunity: involvement of new neuropeptides. Trends Microbiol. 11(12):585-592.

Minicucci M.F., Azevedo P.S., Polegato B.F., Paiva S.A., Zornoff L.A. Heart failure after myocardial infarction: clinical implications and treatment. Clin. Cardiol. 2011 34(7):410-414.
Moran G.J., Krishnadasan A., Gorwitz R.J., Fosheim G.E., McDougal L.K., Carey R.B. Talan D.A., EMERGEncy ID Net Study Group. (2006). Methicillin-resistant S. aureus infections among patients in the emergency department. N. Engl. J. Med. 355: 666–674.

Murphy E., Kohr M., Sun J., Nguyen T., Steenbergen C. (2012). S-nitrosylation: a radical way to protect the heart. J. Mol. Cell. Cardiol. 52:568–577.

Muth E., Driscoll W.J., Smalstig A., Goping G., Mueller G.P. (2004). Proteomic analysis of rat atrial secretory granules: a platform for testable hypotheses. Biochim. Biophys. Acta. 1699:263–275.

Nichols W.W., and Epstein B.J. (2009). Actions of selected cardiovascular hormones on arterial stiffness and wave reflections. Curr. Pharm. Des. 15(3):304-20.

O'Connor D.T., Kailasam M.T., Kennedy B.P., Ziegler M.G., Yanaihara N., Parmer R.J. (2002). Early decline in the catecholamine release-inhibitory peptide catestatin in humans at genetic risk of hypertension. J. Hypertens. 20:1335-1345.

Ohbayashi T., Irie A., Murakami Y., Nowak M., Potempa J., Nishimura Y, Shinohara M., Imamura T. (2011). Degradation of fibrinogen and collagen by staphopains, cysteine proteases released from Staphylococcus aureus. Microbiology 157:786–792.

Packer M.M., Shelhamer J.H., Natason C., Alling D.W., Parillo J.E. (1987). Serial cardiovascular variables in survivor and nonsurvivor of human septic shock heart rate as an early predictor of prognosis. Crit. Care Med. 15:923–929.

Pagliaro P., Mancardi D., Rastaldo R., Penna C., Gattullo D., Miranda K.M., Feelisch M., Wink D.A., Kass D.A., Paolocci N. (2003). Nitroxyl affords thiol-sensitivemyocardial protective effects akin to early preconditioning. Free Radic. Biol. Med. 34(1):33–43.

Parmer R.J., Mahata M., Gong Y., Mahata S.K., Jiang Q., O'Connor D.T., Xi X.P., Miles L. A. (2000). Processing of chromogranin A by plasmin provides a novel mechanism for regulating catecholamine secretion. J. Clin. Invest. 106:907–915.

Pasqua T., Corti A., Gentile S., Pochini L., Bianco M., Metz-Boutigue M.H., Cerra M.C., Tota B., Angelone T. (2013). Full-length human chromogranin-A cardioactivity: myocardial, coronary, and stimulus-induced processing evidence in normotensive and hypertensive male rat hearts. Endocrinology. 154(9):3353-3365.

Penna C., Cappello S., Mancardi D., Raimondo S., Rastaldo R., Gattullo D., Losano G., Pagliaro P. (2006b). Post-conditioning reduces infarct size in the isolated rat heart: role of coronary flow and pressure and the nitric oxide/cGMP pathway. Basic Res. Cardiol. 101(2): 168–179.

Penna C., Rastaldo R., Mancardi D., Raimondo S., Cappello S., Gattullo D., Losano G., Pagliaro P. (2006a). Post-conditioning induced cardioprotection requiressignaling through a redoxsensitive mechanism, mitochondrial ATP-sensitive K+ channel and protein kinase C activation, Basic Res. Cardiol. 101:180–189.

Penna C., Mancardi D., Rastaldo R., Losano G., Pagliaro P. (2007). Intermittent activation of bradykinin B2 receptors and mitochondrial KATP channels trigger cardiac postconditioning through redox signalling. Cardiovasc. Res. 75:168–177.

Penna C., Mognetti B., Tullio F., Gattullo D., Mancardi D., Pagliaro P., Alloatti G. (2008). The platelet activating factor triggers preconditioning-like cardioprotective effect via mitochondrial K-ATP channels and redox-sensible signaling. J. Physiol. Pharmacol. 59:47–54.

Penna C., Alloatti G., Gallo M.P., Cerra M.C., Levi R., Tullio F., Bassino E., Dolgetta S., Mahata S.K., Tota B., Pagliaro P. (2010). Catestatin improves post-ischemic left ventricular function and decreases ischemia/reperfusion injury in heart. Cell. Mol. Neurobiol. 30(8):1171-1179.

Penna C., Pasqua T., Amelio D., Perrelli M.G., Angotti C., Tullio F., Mahata S.K., Tota B., Pagliaro P., Cerra M.C., Angelone T. (2014). Catestatin increases the expression of anti-apoptotic and pro-angiogenetic factors in the post-ischemic hypertrophied heart of SHR. PLoS One. 9(8):e102536.

Perrelli M.G., Tullio F., Angotti C., Cerra M.C., Angelone T., Tota B., Alloatti G., Penna C., Pagliaro P. (2013). Catestatin reduces myocardial ischaemia/reperfusion injury: involvement of PI3K/Akt, PKCs, mitochondrial KATP channels and ROS signalling. Pflugers Arch. 465(7):1031-1040.

Pieroni M., Corti A., Tota B., Curnis F., Angelone T., Colombo B., Cerra M.C., Bellocci F., Crea F., Maseri A. (2007). Myocardial production of chromogranin A in human heart: a new regulatory peptide of cardiac function. Eur. Heart J. 28(9):1117-1127.

Ponzio F., Payamyar P., Schneider A., Winterhalter M., Bour J., Addiego F. Krafft M.P., Hemmerle J., Ball V. (2014). Polydopamine Films from the Forgotten Air/Water Interface. J. Phys. Chem. Lett. 5: 3436−3440.

Potempa J. and Pike R.N. (2009). Corruption of innate immunity by bacterial proteases. J. Innate Immun. 1:70–87.

Preece N.E., Nguyen M., Mahata M., Mahata S.K., Mahapatra N.R., Tsigelny I., O'Connor, D.T. (2004). Conformational preferences and activities of peptides from the catecholamine release-inhibitory (catestatin) region of chromogranin A. Regul. Pept. 118:75–87.

Rabbi M.F., Labis B., Metz-Boutigue M.H., Bernstein C.N., Ghia J.E. (2014). Catestatin decreases macrophage function in two mouse models of experimental colitis. Biochem. Pharmacol. 89(3):386-398

Radek K.A., Lopez-Garcia B., Hupe M., Niesman I.R., Elias P.M., Taupenot L., Mahata S.K., O'Connor D.T., Gallo R.L. (2008). The neuroendocrine peptide catestatin is a cutaneous antimicrobial and induced in the skin after injury. J. Invest. Dermatol. 128(6):1525-1534.

Ribeiro S.M., Felicio M.R., Boas E.V., Goncalves S., Costa F.F., Samy R.P., Santos N.C., Franco O.L. (2016). New frontiers for anti-biofilm drug development. Pharmacol. Ther. 160:133-144.

Rudiger A., Singer M. (2007). Mechanisms of sepsis-induced cardiac dysfunction. Crit. Care Med. 35(6):1599-1608.

Sarzani R., Spannella F., Giulietti F., Balietti P., Cocci G., Bordicchia M. (2017). Cardiac Natriuretic Peptides, Hypertension and Cardiovascular Risk. High Blood Press. Cardiovasc. Prev. doi: 10.1007/s40292-017-0196-1.

Seidah N.G. and Chretien M. (1999). Proprotein and prohormone convertases: a family of subtilases generating diverse bioactive polypeptides. Brain. Res. 848:45–62.

Shooshtarizadeh P., Zhang D., Chich J.F., Gasnier C., Schneider F., Haïkel Y., Aunis D., Metz-Boutigue M.H. (2010). The antimicrobial peptides derived from chromogranin/secretogranin family, new actors of innate immunity. Regul. Peptides. 165(1): 102-110.

Sieradzki K., Roberts R.B., Haber S.W., Tomasz A. (1999). The development of vancomycin resistance in a patient with methicillin-resistant Staphylococcus aureus infection. N. Engl. J. Med. 340:517–523.

Steigbigel R.T., Greenman R.L., Remington J.S. Antibiotic combinations in the treatment of experimental Staphylococcus aureus infection. (1975). J. Infect. Dis. 131(3):245-251.

Steiner H.J., Weiler R., Ludescher C., Schmid K.W., Winkler H. (1990). Chromogranins A and B are co-localized with atrial natriuretic peptides in secretory granules of rat heart. J. Histochem. Cytochem. 38:845–850.

Strub J.M., Hubert P., Nullans G., Aunis D., Metz-Boutigue M.H. (1996a). Antibacterial activity of secretolytin, a chromogranin B-derived peptide (614-626), is correlated with peptide structure. FEBS Lett. 379(3):273-278.

Strub J.M., Goumon Y., Lugardon K., Capon C., Lopez M., Moniatte M., Van Dorsselaer A., Aunis D., Metz-Boutigue M.H. (1996b). Antibacterial activity of glycosylated and phosphorylated chromogranin A derived peptide 173-194 from bovine adrenal medullary chromaffin granules. J. Biol. Chem. 271(45):28533-28540.

Strub J.M., Sorokine O., van Dorsselaer A., Aunis D., Metz-Boutigue M.H. (1997). Phosphorylation and O-glycosylation sites of bovine chromogranin A from adrenal medullary granules and their relationship with biological activities. J. Biol. Chem. 272:11928–11936.

Sugawara M., Resende J.M., Moraes C.M., Marquette A., Chich J.F., Metz-Boutigue M.H., Bechinger B. (2010). Membrane structure and interactions of human catestatin by multidimensional solution and solid-state NMR spectroscopy. FASEB J. 24(6):1737-1746.

Sun J., Picht E., Ginsburg K.S., Bers D.M., Steenbergen C., Murphy E. (2006). Hypercontractile female hearts exhibit increased S-nitrosylation of the L-type Ca2+ channel alpha1 subunit and reduced ischemia/reperfusion injury. Circ. Res. 98:403–411.

Suzuki T., Suzuki Y., Okuda J., Kurazumi T., Suhara T., Ueda T., Nagata H., Morisaki H. (2017). Sepsis-induced cardiac dysfunction and β-adrenergic blockade therapy for sepsis. J. Intensive Care. 5:22.

Szermer-Olearnik B., Sochocka M., Zwolińska K., Ciekot J., Czarny A., Szydzik J., Kowalski K., Boratyński J. (2014). Comparison of microbiological and physicochemical methods for enumeration of microorganisms. Postepy Hig. Med. Dosw. 68:1392-1396.

Tota B., Angelone T., Cerra M.C. (2014). The surging role of Chromogranin A in cardiovascular homeostasis. Front. Chem. 2:64.

Tota B., Cerra M.C., Gattuso A. (2010). Catecholamines, cardiac natriuretic peptides and chromogranin A: evolution and physiopathology of a ‘whip-brake’ system of the endocrine heart, J. Exp. Biol. 213:3081–3103.

Tota B., Gentile S., Pasqua T., Bassino E., Koshimizu H., Cawley N.X., Cerra M.C., Loh Y.P., Angelone T. (2012). The novel chromogranin A-derived serpinin and pyroglutaminated serpinin peptides are positive cardiac β-adrenergic-like inotropes. FASEB J. 26(7):2888-2898.

Tota B., Mazza R., Angelone T., Nullans G., Metz-Boutigue M.H., Aunis D., Helle, K. B. (2003). Peptides from the N-terminal domain of chromograninA (vasostatins) exert negative inotropic effects in the isolated frog heart. Regul. Pept. 114:123–130.

Tota B., Quintieri A.M., Di Felice V., Cerra, M.C. (2007). New biological aspects of chromogranin A-derived peptides: focus on vasostatins. Comp. Biochem. Physiol. A. Mol. Integr. Physiol. 147:11-18.

Vanderlinde R.E. (1985). Measurement of total lactate dehydrogenase activity. Ann. Clin. Lab. Sci. 15(1):13-31.

Vinten-Johansen J., Zhao Z.Q., Jiang R., Zatta A.J. (2005). Myocardial protection inreperfusion with postconditioning, Expert Rev. Cardiovasc. Ther. 3:1035–1045

Vittone L., Mundina-Weilenmann C., Mattiazzi A., Cingolani H. (1994). Physiologic and pharmacologic factors that affect myocardial relaxation. J. Pharmacol. Toxicol. Methods 32(1):7-18.

Wei Q., Zhang F., Li J., Li B., Zhao C. (2010). Oxidant-Induced Dopamine Polymerization for Multifunctional Coatings. Polymer. Chem. 1:1430−1433.

Weiergraber M., Pereverzev A., Vajna R., Henry M., Schramm M., Nastainczyk W., Grabsch H., Schneider T. (2000). Immunodetection of alpha1E voltage-gated Ca(2+) channel in chromogranin-positive muscle cells of rat heart, and in distal tubules of human kidney. J. Histochem. Cytochem. 48:807–819.

Wohlfarter T., Fischer-Colbrie R., Angeletti R.H., Eiden L.E., Winkler H. (1989). Processing of chromogranin A within chromaffin granules starts at C- and N-terminal cleavage sites. FEBS Lett. 231:67–70.

Yanaihara N., Nishikawa Y., Hoshino M., Mochizuki T., Iguchi K., Nagasawa S., et al. (1998). Evaluation of region-specific radioimmunoassays for rat and human chromogranin A: measurement of immunoreactivity in plasma, urine and saliva. In: The Adrenal Cell, pp. 305-313, Kanno, T., Nakazato, Y. and Kumakura, K. (eds.), Hokkaido University Press, Sapporo.

Yeaman M.R. and Yount N.Y. (2003). Mechanisms of antimicrobial peptide action and resistance. Pharmacol. Rev. 55(1): 27-55.

Yusuf S.W., Sharma J., Durand J.B., Banchs J. (2012). Endocarditis and myocarditis: a brief review. Expert Rev. Cardiovasc. Ther. 10(9):1153-1164.

Zhang D., Shooshtarizadeh P., Laventie B.J., Colin D.A., Chich J.F., Vidic J., de Barry J., Chasserot-Golaz S., Delalande F., Van Dorsselaer A., Schneider F., Helle K., Aunis D., Prévost G., Metz-Boutigue M.H. (2009). Two chromogranin a-derived peptides induce calcium entry in human neutrophils by calmodulin-regulated calcium independent phospholipase A2. PLoS One. 4(2):e4501.

Zhang C. (2008). MicroRNAs role in cardiovascular biology and disease. Clin. Sci.(Lond.) 114:699–706.

Zhang X., Dillen L., Bauer S.H., Van Dongen W., Liang F., Przybylski M., Esmans E., De Potter W.P., Claeys M. (1997) Mass spectrometric identification of phosphorylated vasostatin II, a chromogranin A-derived protein fragment (1-113). Biochim. Biophys. Acta. 1343(2):287-298.

Zheng M., Streck R.D., Scott R.E., Seidah N.G. Pintar J.E. (1994). The developmental expression in rat of proteases furin, PC1, PC2, and carboxypeptidase E: implications for early maturation of proteolytic processing capacity. J. Neurosci. 14:4656–4673.

Ziegler A. (2008). Thermodynamic studies and binding mechanisms of cellpenetrating peptides with lipids and glycosaminoglycans. Adv. Drug. Deliv. Rev.60:580–597.

Francesco SCAVELLO

Cateslytine et Chromofungine, deux peptides dérivés de la Chromogranine A qui sont de nouveaux acteurs des systèmes immunitaire et cardiaque

Résumé

La CgA est une pro-hormone stockée dans les granules de sécrétion et elle subit une maturation protéolytique conduisant à la formation d'un très grand nombre de peptides dérivés. La Chromofungine (Chr: CgA_{47-66}) et la Cateslytine (Ctl: $CgA_{344–358}$) possèdent des propriétés antimicrobiennes.

Staphylococcus aureus est un pathogène très virulent qui provoque un très grand nombre de graves infections cliniques et il représente une des causes principales des infections nosocomiales et la destruction du tissu endocardiaque après implantation de valve cardiaque.

La première partie de l'étude nous avons montré que la Chr induise un effet inotropique négatif sans changement de la pression coronarienne. L'activation de la voie de signalisation AKT/eNOS/cGMP/PKG est responsable de cet effet de Chr. Nous avons aussi montré que Chr agit comme un agent de post-conditionnement contre les effets négatifs de l'ischémie/reperfusion, a responsables de cette cardio-protection impliquent les cascades de signalisation PI3K, RISK, MitoKATP et miRNA-21.

Dans le but d'élaborer un nouveau revêtement de valves cardiaques le peptide D*T*Ctl se révèle intéressant dans des conditions non oxydantes car (1) il présente une activité antimicrobienne contre *S. aureus*; (2) en présence de *S. aureus* il permet par clivage protéolytique de libérer le peptide Ctl actif.

Une première expérience réalisée *in vivo* a montré le rôle de Ctl pour combattre l'infection à *S. aureus* au niveau systémique et au niveau cardiaque, mais aussi assurer la protection du myocarde.

Mots-clés: Chromofungine, Cateslytine, *Staphylococcus aureus,* Cardioprotection, Valves Cardiaques, Peptides Antimicrobiens.

Abstract

CgA is a pro-hormone costored in secretory granules and numerous cleavage products of this protein have been identified. Chromofungin (Chr: CgA_{47-66}) and Cateslytin (Ctl: $CgA_{344–358}$) are peptides that display antimicrobial activities.

Staphylococcus aureus is an opportunistic pathogen and the leading cause of a wide range of severe clinical infections and one of the most important cause of hospital-acquired infections and leading infective cause of destruction of endocardial tissue after implantation of prosthetic heart valve.

The first part of the study, we found that Chr induced negative inotropic effects without changing coronary pressure. The AKT/eNOS/cGMP/PKG pathway mediated this action. We also found that Chr acted as a postconditioning agent against ischemia/reperfusion damages. Cardioprotection involved PI3K, RISK pathway, MitoKATPand miRNA-21.

In order to develop a new coating of cardiac valves, the peptide D*T *Ctl proves to be useful under non-oxidizing conditions because (1) it exhibits antimicrobial activity *against S. aureus*; (2) in the presence of *S. aureus*, it allows proteolytic cleavage to release the active Ct1 peptide.

In the last part of this thesis we showed *in vivo* the antibacterial role of Ctl against *S. aureus* infection at the systemic and cardiac levels, but also its cardioprotective action.

Key Words: Chromofungin, Cateslytin, *Staphylococcus aureus,* Cardioprotection, Cardiac Valves, Antimicrobial Peptides.